Instituto Superior de Engenharia do Porto

DEPARTAMENTO DE ENGENHARIA MECÂNICA

ESTABLISHING THE MAIN GUIDELINES FOR CAST STEEL TO PRODUCE TRUCK PARTS

Jorge Filipe Moreira dos Santos

2015

isep Instituto Superior de Engenharia do Porto

POLITÉCNICO DO PORTO

Instituto Superior de Engenharia do Porto
DEPARTAMENTO DE ENGENHARIA MECÂNICA

ESTABLISHING THE MAIN GUIDELINES FOR CAST STEEL TO PRODUCE TRUCK PARTS

Jorge Filipe Moreira dos Santos
1120155

Dissertation presented at the ISEP - School of Engineering, Polytechnic of Porto, Portugal, as partial fulfill of the requirements to obtain the Master Degree in Mechanical Engineering, being supervised by Prof. Dr. Francisco José Gomes da Silva, Auxiliar Professor at the Mechanical Engineering Department, ISEP.

2015

isep Instituto Superior de Engenharia do Porto

POLITÉCNICO
DO PORTO

REFEREE

President	**Doutor Arnaldo Manuel Guedes Pinto** *Professor Adjunto, Instituto Superior de Engenharia do Porto*
Supervisor	**Doutor Francisco José Gomes da Silva** *Professor Adjunto, Instituto Superior de Engenharia do Porto*
Company Supervisors	**Mr. Henrik Sieurin, PhD** *Development Engineer, Materials Technology at Scania CV AB* **Ms. Baohua Zhu, PhD** *Development Engineer, Materials Technology at Scania CV AB*
Vogal	**Doutor José Duarte Ribeiro Marafona** *Professor Auxiliar, Faculdade de Engenharia da Universidade do Porto*

Acknowledgements

There are some people that have been an extra guidance in this project and I want to use this opportunity to express my gratitude.

Firstly, I would like to thank Mimmi Härdeman from the Industrial Engineering and Management (KTH) for the cooperation compiling this master thesis and cast steel guideline. Your strength, organization and work were essential to conduct this work.

I would like to say thank you to my supervisors Henrik Sieurin, at UTMD–chassis, and Baohua Zhu, at UTMB–Engine, both at Scania, for support, great advising and knowledge in all work.

Secondly, I would like to thank my academic supervisor, Francisco Silva at the School of Engineering, Polytechnic of Porto, for advising and helping with the academic process and master thesis.

I would also like to thank the following people for being a great help during the project:

Erik Andersson – RTCB–Basic Chassis Development, Scania
Christina Sunderkötter – Volkswagen
Madeleine Ekström – UTMB–Engine, Scania
Jonas Hagsjö – RTCC–Dynamics and Strength Analysis, Scania
Magnus Brandstedt – NMGV–Exhaust Components, Scania
Johan Parsons – RTCB–Basic Chassis Development, Scania
Jan Kron – UTMY–Hybrid Electronics Testing of Materials
Lennart Persson – UTMY–Hybrid Electronics Testing of Materials
Tomas Hammarlund – UTMY–Hybrid Electronics Testing of Materials
Gustav Makander – UTMN–Axles Transmission
Dan Erhav – SEB–Commodity Castings, Scania
Mathias König – UTMB–Engine, Scania
Jessica Elfsberg – UTMB–Engine, Scania
Henrik Sedig – SEE–Project Purchasing Castings, Scania
Torbjörn Carlsson – SNE–Cost Engineering, Scania
Shaun Berry and Will Wigor – Newby foundry
Anders Eliasson – Material Science, Royal Institute of Technology

Lennart Sibeck – Swerea Swedish research

Scania Foundry for the study visit

The rest of UTM, thanks for the warm welcome at the department.

I am sincerely thankful for your constructive criticism and friendly advice.

Resumo

Este trabalho foi realizado na Scania CV AB e teve como principal objectivo estabelecer uma diretriz sobre a possível utilização de aços vazados.

Existe uma grande necessidade na realização deste trabalho, de forma a apoiar os engenheiros de projecto no seu processo de selecção dos materiais mais adequados, para produzir componentes mais leves e de elevado desempenho.

Esta diretriz apresenta informação relacionada com propriedades mecânicas, processos de fundição, vazabilidade, tipologia de defeitos, tratamentos térmicos, soldabilidade e tratamentos superficiais dos aços vazados.

Este trabalho foi limitado, na seleção de materiais para componentes do camião, a aços vazados que poderiam ser aplicados em dois componentes específicos: um componente estrutural da carroçaria sujeito a esforços de fadiga e a um colector de gases de combustão, sujeito a fluência, oxidação, fadiga por corrosão, fadiga-térmica e fadiga-mecânica. Foi realizado um *benchmark* focado nestes dois componentes de forma a saber que materiais são utilizados de momento por outras empresas concorrentes.

Foi realizada ainda uma análise sobre possíveis materiais que possam ser aplicados em cada componente referido.

Foi conduzida uma caracterização no estado bruto de fundição de um aço inoxidável vazado usado para produzir um protótipo do colector de gases. Esta caracterização consistiu numa análise microestrutural e medição de macro e microdurezas. Além da caracterização inicial, foram aplicados um conjunto de tratamentos térmicos, de forma a estudar a possibilidade de eliminar os carbonetos presentes inicialmente nas fronteiras de grão.

As principais conclusões deste trabalho são que o aço vazado apresenta potencial para ser uma escolha válida em diversas aplicações, devido a um leque alargado de propriedades apresentadas tipicamente por este material. Relativamente a aplicações estruturais, o aço vazado é vantajoso comparativamente ao ferro fundido, quando são requeridos, por exemplo, soldabilidade e elevada resistência, combinada com elevada tenacidade à fractura. Para componentes sujeitos a elevadas temperaturas de serviço, o aço inoxidável vazado é vantajoso quando usado a temperaturas superiores a 750°C, apesar do seu elevado custo.

O tratamento térmico composto por um recozimento de solubilização seguido de envelhecimento, elimina quase na totalidade os carbonetos presentes nas fronteiras de grão e verifica-se um aumento de dureza através de uma precipitação de carbonetos finamente dispersos na matriz, que poderão também aumentar a resistência à fluência.

Palavras-Chave

Aço vazado, Guia de aplicação dos aços vazados, Aço inoxidável vazado, Componentes estruturais, Materiais para altas temperaturas, Tratamentos térmicos, Fundição

Abstract

The present work was conducted at Scania CV AB and has as main goal to produce a cast steel guideline.

There is a great need to conduct a cast steel guideline, in order to help designers in their process to choose suitable materials and methods to produce lightweight components and with higher performance.

This work contains information related to mechanical properties, casting processes, castability, machinability, defect characterization, heat treatments, weldability and surface treatments of cast steels.

This work was limited to cast steels which could be applied on two specific components: bracket, a structural component of chassis subjected to fatigue and turbo manifold, component subjected to creep, oxidation, corrosion, thermal and mechanical- fatigue. A benchmark search was performed focused on these two components.

An analysis of possible material solutions for each component was performed.

A characterization of a cast stainless steel turbo manifold prototype was performed in the as-cast state, which included microstructural analyzes and hardness measurements. Besides this initial characterization, a set of heat treatments were conducted, in order to study the possibility to eliminate the initial grain boundary carbides.

The main conclusions of this work are that cast steel has potential to be a material choice in many applications due to its wide range of properties. For structural parts, cast steel is advantageous compared with cast iron when for instance welding and high strength combined with high fracture toughness are requirements. For high temperature resistance components, cast steel or more precisely cast stainless steel, is advantageous for service at temperatures >750^{o}C, besides its higher price.

The annealing heat treatment followed by an aging treatment eliminated most of the grain boundary carbides and increase the hardness through a fine dispersion of carbides in matrix, which can also increase the creep resistance.

Keywords

Cast steel, Cast steel guideline, Cast stainless steel, Structural components, High temperature materials, Heat treatments, Casting

Abbreviations and Symbols List

A	Elongation %
A5N	Hitachi stainless steel
ADI	Austempered Ductile Iron
AISI	American Iron & Steel Institute
ASTM	American Society for Testing and Materials
AT	Aging Treatment at 760°C
BC	Bond Coat
CFD	Computational fluid dynamics
CT	Cast Tolerances
D5S	Kind of austenitic ductile iron
DFA	Design For Assembly
DFC	Design For Cost
DFM	Design For Manufacturability
DFR	Design For Reliability
DIN	Deutsches Institut für Normung
DM	Detroit Materials
EN	European Norm
EN-GJS-500-7	Ductile cast iron, at Scania Cast iron 0727
FEA	Finite Element Analysis
FMEA	Failure Mode Effect Analysis
GF	Georg Fischer Automotive
GHG	Greenhouse Gas
GMAW	Gas Metal Arc Welding
GTAW	Gas Tungsten Arc Welding
HAZ	Heat Affected Zone
HB	Hardness in Brinell
HBW	Hardness in Brinell tungsten (wolfram) carbide
HC	Grade of Stainless steel
HDV	Heavy-Duty Vehicles
HK	Grade of Stainless steel
HK30	Kind of cast stainless steel alloy
HN	Grade of Stainless steel
HRB	Hardness in Rockwell B
HRC	Hardness in Rockwell C
HV	Hardness in Vickers
IEC	International Electrotechnical Commission
ISO	International Organisation of Standardisation
K_{IC}	Plain-strain fracture toughness parameter
LCC	Life Cycle Cost

LCF	Low Cycle Fatigue
MPa	Mega Pascal
Ms	Martensite start
Ra	Arithmetic average of the unfiltered raw profile, Arithmetic average roughness
Rm	Tensile strength, MPa
RMA	Required Machining Allowance
$Rp_{0.2}$	Yield strength, MPa
RTCB	Department of basic chassis development
SAE	Society of Automotive Engineers
SCC	Stress-Corrosion Cracking
SFA	Swedish Foundry Association
SiboDur®	Ultra high strength ductile iron alloy
SiMo51	Spheroidal graphite iron
SIS	Swedish Standards Institute (formerly Standardiseringskommissionen i Sverige)
SMAW	Shielded Metal arc Welding
SPS	Scania Production System
SS	Swedish Standard
ST	Solution annealing
ST/1.5 + O.C.	ST for 1.5 h at 1200°C followed by oven cooling
ST/1.5 + O.C. + AT	ST for 1.5 h at 1200°C followed by oven cooling and aging at 760°C
ST/1.5 + W.Q.	ST for 1.5 h at 1200°C followed by water quenching
ST/1.5 + W.Q. + AT	ST for 1.5 h at 1200°C followed by water quenching and aging at 760°C
ST/3 + O.C.	ST for 3 h at 1200°C followed by oven cooling
ST/3 + O.C. + AT	ST for 3 h at 1200°C followed by oven cooling and aging at 760°C
ST/3 + W.Q.	ST for 3 h at 1200°C followed by water quenching
ST/3 + W.Q. + AT	ST for 3 h at 1200°C followed by water quenching and aging at 760°C
STD	Scania Standard Document (Internal document)
STR	Scania Technical Report (Internal document)
T	Thickness
TBC	Thermal Barrier Coatings
TGO	Thermal Growth Oxide
TMF	Thermomechanical Fatigue
UTM	Materials Technology
UTMB	Materials Technology for Basic Engine
UTMD	Materials Technology for Chassis
UTMN	Materials Technology for Axle and Transmission
UTMR	Materials Technology for Cabs and Buses
YSZ	Yttrium-Stabilized Zirconia

List of Figures

Figure 2-1. *Fe-C phase diagram* [3]. 4

Figure 2-2. *Illustration of different graphite morphologies of graphitic cast irons, such as grey iron, compacted graphite iron and ductile iron* [4]. 4

Figure 2-3. *Schematic illustration of bainitic and ausferritic microstructures* [13]. 7

Figure 2-4. *To the left: DM cast steel shows the best combination of strength and ductility. To the right: DM cast steel show the highest specific strength. In both charts DM cast steel is compared with common chassis and drivetrain casting materials* [14]. 8

Figure 2-5. *Sand casting process overview* [19]. 12

Figure 2-6. *Croning shells making process* [22]. 13

Figure 2-7. *Investment casting process overview* [19]. 14

Figure 2-8. *Lost Foam process steps* [25]. 15

Figure 2-9. *C-9 microfinish comparator* [26]. 16

Figure 2-10. *Minimum thickness of sections as a function of their largest dimension* [27]. 17

Figure 2-11. *Recommended dimensional relationships for cores to avoid fusion. (a) Cylindrical hole with D less than 2e, Maximum length =D; (b) blind hole with D less than 2e, maximum length = D/2; (c) cylindrical hole with 2e ≤ D ≤ 3e, maximum length = 3D; (d) blind hole with 2e ≤ D ≤ 3e, maximum length = 2D* [29] 18

Figure 2-12. *Predictive shrinkage cavities* [27]. 19

Figure 2-13. *Some examples of sections showing correct design to prevent shrinkage cavities* [27]. 19

Figure 2-14. *Cut section of pressure vessel drawing showing added padding in the rectangles to feed and isolated heavy section* [27]. 20

Figure 2-15. *Chill applied to a boss increase the heat extraction* [30]. 20

Figure 2-16. *Increasing of mass resulting from joining sections shown by inscribed circle* [27]. 21

Figure 2-17. *Rib thickness with several T-junctions thermally neutral* [27]. 21

Figure 2-18. *To the left: Rib addiction to increase rigidity and reduce weight. To the right: Eliminate hot spot in rib using a core* [27]. 22

Figure 2-19. *Design for changing section thickness* [27]. 23

Figure 2-20. *Design rule for section thickness change (T= thickness)* [27]. 23

Figure 2-21. *To the left: Gas cavities. To the right: Inclusions* [32]. 28

Figure 2-22. *To the left: Shrinkage. To the right: Hot tear* [32]. 29

Figure 2-23. *To the left: Primary grain boundary fracture. To the right: Al-N precipitates* [32]. 30

Figure 2-24. *Typical gear tooth hardness profiles, where HRc 60 is a hardness measurement on the Rockwell C scale* [47]. 32

Figure 2-25. *Temperature time transformation (TTT) for 0.55C-1.62Si-0.78Mn-0.77Cr steel. The dashed line represents austempering heat treatment* [53]. 35

Figure 2-26. *Comparative machinability of common metals* [58]. 38

Figure 2-27. *Diagram comparing the hardness and factor for cutting speed* [59]**.** 38

Figure 2-28. *Fatigue strength versus yield point in the weld* [60]**.** 39

Figure 2-29. *A schematic diagram showing the welding process* [61]*.* 40

Figure 2-30. *The diagram shows the different formations in the heat-affected zone; (I) overheated section, (II) grain-refined (normalized) section, (III) partially grain-refined section, (IV) recrystallized section, (V) aging section; (1) weld metal, (2) fusion zone* [62]**.** 40

Figure 2-31. *A Schaeffler diagram shows the limits of the austenitic, ferritic and the martensitic phases in relation to the chromium and nickel equivalent* [64]. 41

Figure 2-32. *Some of the most commonly flaw types that can be found during welding processes* [76]**.** 46

Figure 2-33. C*omponent before (to the left) and after (to the right) shot peening* [81]**.** 47

Figure 2-34. *A heat tinting that shall be removed and the easiest way to do this is by pickling process* [65]. 48

Figure 2-35. *Appearance of different cleaning methods. Grinding to the left, polishing in the middle and pickling to the right* [77]*.* 48

Figure 2-36. *Thermal barrier schematic structure coating and corresponding temperature profile* [89]**.** 50

Figure 3-1. *Turbo Manifold and the assembly view of the exhaust system.* 52

Figure 3-2. *Schematic description showing a turbo manifold attached to a turbo charger and connected to exhaust manifolds* [4]*.* 53

Figure 3-3. B*racket at the assembly line, bracket drawings and bracket's assembly view.* 55

Figure 3-4. *Microstructure effect on ductile iron fracture toughness* [3]. 58

Figure 3-5. *Exhaust turbo manifold casted together with turbo housing* [100]**.** 59

Figure 3-6. *To the left: A single austenite stainless steel casting that integrates the turbo manifold and turbine housing. To the right: A complete manifold assembly* [101]*.* 59

Figure 3-7. *A SiboDur® spring hanger bracket* [103]*.* 60

Figure 3-8. *The current market cost/unit strength position for a forged or cast aluminium process carries an exponential cost burden vs. alternative higher-strength alloys when considering yield strength behaviour* [105].. 61

Figure 3-9. *X-link used on heavy duty MAN TGA truck. It ensures the directional and vehicle stability and damping control.* 62

Figure 3-10. *To the left: Samples removed from the prototype produced in HK30. To the right: Samples removed from the manifold SiMo51.* 67

Figure 3-11. *Vertical sections of ternary equilibrium system for 55% weight in Fe* [111]. 68

Figure 3-12. *To the left: Microstructure obtained in as-cast state for thin part composed of a fully austenitic matrix, grain boundaries chromium rich carbides and massive carbides into the matrix; Objective: 20X; Kallings Etsmedel etch. To the right: Microstructure obtained in the as-cast state for thick part composed of a fully austenitic matrix, grain boundaries chromium rich carbides and massive carbides into the matrix; Objective: 50X; Kallings Etsmedel etch.* 69

Figure 3-13. *Microstructure showing the grain growth from the right to the left (from surface showed in* Figure 3-12 *to middle); Objective: 1.25X; Kallings Etsmedel etch.* 70

Figure 3-14. *To the left: SEM image of grain boundary carbides and unconnected carbide islands in as-cast sample. To the right: SEM image of an unconnected carbide island showing a lamellar structure in as-cast sample.* 71

Figure 3-15. *Thermal cycles applied in heat treatments.* 73

Figure 3-16. C*arbon solubility in austenite for 18Cr-12Ni and 20Cr-25Ni austenitic stainless steels represented by solid line and dashed line, respectively* [115]**.** 74

Figure 3-17. *To the left: Microstructure obtained after solution annealing at 1200°C for 1.5 h followed by water quenching composed of a fully austenitic matrix, very thin grain boundaries chromium rich carbides, massive carbides in the matrix and decomposed carbides; Objective: 20X; Kallings Etsmedel etch. To the right: Microstructure obtained after solution annealing at 1200°C for 3 h followed by water quenching composed of a fully austenitic matrix, massive carbides, decomposed carbides and small traces of grain boundary carbides; Objective: 20X; Kallings Etsmedel etch.* 75

Figure 3-18. *To the left: Microstructure obtained after solution annealing at 1200°C for 1.5 h followed by water quenching composed of a fully austenitic matrix, thin grain boundaries chromium rich carbides and massive carbides, decomposed carbides and spheroidized carbides highlighted by circles; Objective: 50X; Kallings Etsmedel etch. To the right: Microstructure obtained after solution annealing at 1200°C for 3 h followed by water quenching composed of a fully austenitic matrix, grain boundaries chromium rich carbides and massive carbides, decomposed carbides, and spheroidized carbides highlighted by circles; Objective: 50X; Kallings Etsmedel etch.* 75

Figure 3-19. *To the left: Microstructure obtained after solution annealing at 1200°C for 1.5 h followed by oven cooling composed of a fully austenitic matrix, thin grain boundaries chromium rich carbides, massive carbides into the matrix and decomposed/precipitated carbides; Objective: 20X; Kallings Etsmedel etch. To the right: Microstructure obtained after solution annealing at 1200°C for 3 h followed by oven cooling composed of a fully austenitic matrix, thin grain boundaries chromium rich carbides, massive carbides into the matrix and decomposed/precipitated carbides; Objective: 20X; Kallings Etsmedel etch.* 77

Figure 3-20. *To the left: Microstructure obtained after solution annealing at 1200°C for 1.5 h followed by oven cooling composed of a fully austenitic matrix, thin grain boundaries chromium rich carbides, massive carbides into the matrix and decomposed/precipitated carbides; Objective: 50X; Kallings Etsmedel etch. To the right: Microstructure obtained after solution annealing at 1200°C for 3 h followed by oven cooling composed of a fully austenitic matrix, thin grain boundaries chromium rich carbides, massive carbides into the matrix and decomposed/precipitated carbides; Objective: 50X; Kallings Etsmedel etch.* 77

Figure 3-21. *To the left: Microstructure obtained after solution annealing at 1200°C for 1.5 h followed by water quenching and aged at 760°C for 24 h, which contains a fully austenitic matrix, thin grain boundaries chromium rich carbides, massive carbides and fine dispersed carbides into a austenitic matrix; Objective: 20X; Kallings Etsmedel etch. To the right: Microstructure obtained after solution annealing at 1200°C for 3 h followed by water quenching and aged at 760°C for 24 h, which contains massive carbides and fine dispersed carbides into a austenitic matrix; Objective: 20X; Kallings Etsmedel etch.* 79

Figure 3-22. *To the left: SEM micrograph showing fine dispersed carbides into the matrix for the sample solution annealed for 1.5 h water quenching and aged for 24 h; Kallings Etsmedel etch. To the right: SEM micrograph showing fine dispersed carbides into the matrix for the sample solution annealed for 1.5 h water quenching and aged for 24 h; Kallings Etsmedel etch; Higher magnification.* 79

Figure 3-23. *To the left: Microstructure obtained after solution annealing at 1200°C for 1.5 h followed by oven cooling and aging composed of a fully austenitic matrix, grain boundaries chromium rich carbides, massive carbides and decomposed/precipitated carbides; Objective: 20X; Kallings Etsmedel etch. To the right: Microstructure obtained after solution annealing at 1200°C for 3 h followed by oven cooling composed of a fully austenitic matrix, thin grain boundaries chromium rich carbides, massive carbides and fine dispersed carbides; Objective 20X; Kallings Etsmedel etch.* 80

Figure 3-24. *Macrohardness obtained for different heat treatments.* 81

Figure 3-25. *Microhardness measured on matrix obtained for each heat treatment.* 83

Figure 3-26. Cast steels and casting processes selection scheme........ 86

List of Tables

Table 2-1. *Typical Unalloyed Cast Irons and the range of their chemical composition* [5]. 4

Table 2-2 - *Chemical composition of cast iron 0727 and SiMo51* [4] [7]. 5

Table 2-3. *Mechanical properties of DM cast steels* [14] [15]. 8

Table 2-4. *Areas of application and limitations of lost foam process* [24]. 15

Table 2-5. *Surface finish capabilities by process (in RMS, with extreme low values in parentheses)* [26]. 16

Table 2-6. *Typical draft allowances* [31]. 24

Table 2-7. *Steel casting tolerance grades for long-production series, SS EN-ISO 8062-3:2007* [31]. 25

Table 2-8. *Additional operations to be conducted to produce castings with tighter tolerance limits* [31]. 26

Table 2-9. *Comparison of steel casting methods – General* [31]. 27

Table 2-10. *Main defects in steel castings heat treatment* [32][49]. 36

Table 2-11. *Common welding methods* [65]. 42

Table 2-12. *Design considerations for different welding methods on steels* [66]. 42

Table 2-13. *Carbon equivalent levels to compare the weldability* [68]. 43

Table 2-14. *Preferred and maximum weight percent content of some elements* [69]. 43

Table 2-15. *Stainless steels weldability* [68]. 44

Table 2-16. *Improvements that can be achieved through TBC use* [91]. 50

Table 3-1. *SiboDur® 700–10 chemical analysis according to Scania Internal Document* 60

Table 3-2. *Material properties of two SiboDur® grades compared to cast iron 0727* 61

Table 3-3. *Mechanical properties of the ADI alloy used to produce the X-Link and forged steel 42CrMo4 for thickness higher than 20 mm, EN 10083-3:2006* [106]. 62

Table 3-4. *Selection of materials for turbo manifold and bracket* 63

Table 3-5. Price comparison on average material price for some materials 65

Table 3-6. Comparison of weight and price between materials needed to produce bracket. ... 66

Table 3-7. *Chemical compositions of HK30 and SiMo51* 66

Table 3-8. *Variables and experimental parameters* 72

Table 3-9. *Matrix of experiments* 72

Table 3-10. *Calculation of the parameters effect on hardness. Factorial analysis.* 85

Contents

Resumo v

Abstract vii

Abbreviations and Symbols List ix

List of Figures xi

List of Tables xv

1 Introduction 1

1.1 Background 1
1.2 Thesis goals 1
1.3 Delimitations 1
1.4 Choice of methods 2
1.5 Deliveries 2

2 Literature review 3

2.1 Reducing Heavy-Duty Vehicles' fuel consumption and CO_2 emissions 3
2.2 Materials' challenges 3
2.2.1 Ductile Cast Iron 3
2.2.1.1 SiMo51 and 0727 5
2.2.2 Cast steel 5
2.2.2.1 Structural steels 6
2.2.2.2 Austenitic Cast stainless steels 9
2.2.2.3 Ferritic cast stainless steels 9
2.2.3 Alloying elements 10
2.3 Cast steel properties 11
2.3.1 Chemical compositions 11
2.3.2 Cast steels for general structural purpose 11
2.3.3 High-strength cast steels 12
2.3.4 Heat resistant steel castings 12
2.4 Production 12
2.4.1 Cast Processes 12
2.4.1.1 Green Sand Casting 12
2.4.1.2 Nobake Sand Casting 12
2.4.1.3 Croning shell moulding process 13
2.4.1.4 Investment casting 13
2.4.1.5 Lost foam 14
2.4.2 Surface Finishes in Casting Processes 16

2.4.3 Advantage and disadvantage of the casting processes 16
2.5 Castability 16
2.5.1 Minimum section thickness 17
2.5.2 Internal soundness 18
2.5.3 Tapers 19
2.5.4 Padding 20
2.5.5 Chills 20
2.5.6 Joined Sections and Ribs 20
2.5.7 Surface integrity 22
2.5.8 Changes in Section Size 22
2.5.9 External corners 24
2.5.10 Wave construction 24
2.6 Steel Castings tolerances 24
2.6.1 Draft tolerances 24
2.6.2 Machining allowances 25
2.6.3 Dimensional tolerances 25
2.6.4 Moulding process 26
2.6.5 Geometrical casting tolerances 26
2.7 Defect characterization in cast steels 27
2.8 Bulk and surface cast steels heat treatments 30
2.8.1 Surface hardenings 30
2.8.1.1 Carburizing 30
2.8.1.2 Nitriding 31
2.8.1.3 Carbonitriding 31
2.8.1.4 Flame hardening 31
2.8.1.5 Induction hardening 32
2.8.1.6 Laser hardening 32
2.8.1.7 Comparison between hardening processes 32
2.8.2 Bulk heat treatments 33
2.8.2.1 Solution annealing (+AT) 33
2.8.2.2 Normalizing (+N) 33
2.8.2.3 Quenching (+Q) 33
2.8.2.4 Tempering (+T) 34
2.8.2.5 Austempering 34
2.8.3 Main defects caused by heat treatments 35
2.9 Machinability 37
2.9.1 Machinability Index 37
2.9.2 Relative machinability 37

2.10 Welding ... 39
2.10.1 Welding process ... 39
2.10.1.1 Choice of methods ... 40
2.10.1.2 Welding methods ... 41
2.10.1.3 Carbon equivalent ... 42
2.10.1.4 Weldability ... 43
2.10.2 Defects in welds ... 45
2.11 Castings after treatment ... 46
2.11.1 Surface treatment ... 46
2.11.1.1 Sand blasting and shot blasting / Shot peening ... 46
2.11.1.2 Steel degreasing ... 47
2.11.1.3 Pickling ... 47
2.11.1.4 Grinding and polishing ... 48
2.11.1.5 Passivation ... 48
2.11.1.6 Paint coatings ... 49
2.11.1.7 Thermal barrier coating ... 49
3 Practical work ... 51
3.1 Compile a cast steel guideline ... 51
3.2 Introduction to Materials Selection ... 51
3.2.1 Challenges of the components ... 51
3.2.1.1 Heat resistant cast manifolds ... 51
3.2.1.2 High strength brackets ... 55
3.2.2 Benchmarks ... 58
3.2.2.1 Volkswagen ... 58
3.2.2.2 Hitachi ... 59
3.2.2.3 Hyundai ... 59
3.2.2.4 MAN ... 60
3.2.3 Materials from benchmarking ... 60
3.2.3.1 Sibodur® ... 60
3.2.3.2 Austempering ductile iron (ADI) ... 61
3.2.4 Materials selection for turbo manifold and bracket ... 63
3.2.4.1 Turbo manifold ... 64
3.2.4.2 Bracket ... 64
3.3 Materials examination – materials and methods ... 66
3.3.1 Samples characterization in the as-cast state ... 66
3.3.2 Heat treatments ... 67
3.4 Results and discussions ... 68

3.4.1 Ductile cast iron SiMo51 68
3.4.2 Austenitic cast stainless steel - HK30 68
3.4.3 Heat treatments 71
3.4.3.1 Samples source 71
3.4.3.2 Heat treatments design 71
3.4.4 Microstructures 73
3.4.4.1 Solution annealing followed by water quenching 73
3.4.4.2 Solution annealing followed by oven cooling 76
3.4.4.3 Aging heat treatment 78
3.4.5 Hardness measurements 81
3.5 Cast steels/casting process selection 85
4 Conclusions and suggestions 87
Bibliography 89

Appendices

1 Introduction

Scania is one of the world's leaders on trucks and buses manufacturing. Scania has a global production network into which all units around the world are integrated. This provides high flexibility and cost-effective production. Working methods, quality standards and environmental standards are the same at all production units [1].

1.1 Background

One important issue in the automotive field is to reduce CO_2 emissions. Improving fuel economy, enhancing combustion efficiency and reducing weight of heavy duty vehicles are some ways to achieve this goal.

Increasing combustion efficiency will result in a change of the exhaust gas composition and even higher exhaust temperature, which is putting higher demands on both corrosion-resistance and heat-resistance of exhaust manifolds. The ferritic ductile cast iron served as manifold is close to its limiting temperature. For much higher exhaust temperature applications, heat-resistance cast steels have been developed.

Extensive research of materials for higher specific strength has been conducted in order to reduce weight, making components with thinner wall sections. To replace cast iron components by high strength cast steel may be a way to reduce heavy duty vehicles weight.

There is a great need to conduct a guideline for cast steels. This will be a crucial help for designers in their process to choose suitable materials and methods to produce lightweight components with high performance.

1.2 Thesis goals

The overall objective of this work is to find and compare material data of most promising cast steel, casting characteristics and mechanical properties of cast steels to be a guide for Design Engineers in material selection.

Another objective is to analyse a prototype manifold made by cast steel, concerning the microstructure, hardness, cast defects, heat treatment, et cetera.

1.3 Delimitations

The thesis project is limited to two products: a spring bracket (during this work, the component will be referred as bracket) from chassis and a turbo manifold from engine.

1.4 Choice of methods

In this thesis, a detailed literature review was conducted regarding cast steels and its properties. It is a complex work to understand the underlying factors affecting the steels at elevated temperatures and the material requirements to withstand acids from engine emissions. To collect data needed, research has been conducted both in material databases and from papers and books regarding the subject.

By KTH (Royal Institute of Technology) wide database, reports, publications, e-books such as ASM Handbooks has been accessed. Scania and Volkswagen have given full access to technical reports, standards and internal standards and defect characterisations to fulfil the guideline.

Semi-structured and unstructured interviews in form of meetings, e-mail and over telephone have been conducted internally with departments like chassis, engines, purchase and so on, but also with foundries and different suppliers.

Analyses of two turbo manifold, one produced in austenitic cast stainless steel and another in ductile cast iron SiMo51 has been carried out in which the microstructure of the materials and the hardness were analysed to characterize the materials. The effect of heat treatments on the dissolution of grain boundary carbides was also studied.

1.5 Deliveries

A master thesis report and a Scania guideline of cast steel are the final result of this study.

2 Literature review

2.1 Reducing Heavy-Duty Vehicles' fuel consumption and CO_2 emissions

Up to now, the Euro 6 legislation is only limited to NO_x and particles emission. Besides a continue decreasing of NO_x and particles emission, it is expected that the coming Euro 7 will deal with the CO_2 emissions. Improving fuel economy, enhancing combustion efficiency and reducing weight of heavy duty vehicles are some ways to achieve the goal. Scania is developing the new engines generation which will manage the coming Euro 7 emission legislation.

2.2 Materials’ challenges

As an engineering material, ductile cast iron is used in a wide range of applications, for example steering arm knuckles, crankshafts and equalizer beams for large trucks. The good castability, machinability and relatively high strength and toughness of ductile iron may give it an advantage over cast steels.

Cast steel can achieve better mechanical properties than ductile cast iron but presents lower castability, machinability and is more expensive [2].

The manufacturing processes for metal parts and assemblies can be grouped into the following areas, primary shaping (casting), forming (forging), cutting (machining) and joining (welding).

The big difference between forged (or wrought) and cast steels are how the properties of strength and ductility work. Wrought products are anisotropic and have higher strength and ductility in working direction, meanwhile cast products are isotropic and can stand the same loads in all directions [2].

The casting process will be the focus of this work.

2.2.1 Ductile Cast Iron

Cast irons contain higher carbon and silicon contents than cast steel, suffering the eutectic reaction presented in the Fe-C diagram, see Figure 2-1. Depending mainly on composition, cooling rate and melt treatment, cast iron can solidify according to the thermodynamically metastable version $Fe-Fe_3C$ (solid line) or the stable iron-graphite system (dashed line). When the stable solidification path is followed, the rich carbon phase is graphite [3].

These graphite cast irons can be classified by their graphite shape. There are three types, which give the name to cast irons, flake, spheroidal (nodular) and compacted. The Table 2-1 presents the chemical composition of the different cast irons. In this work focus will be on ductile cast iron as a comparison with cast steel [3].

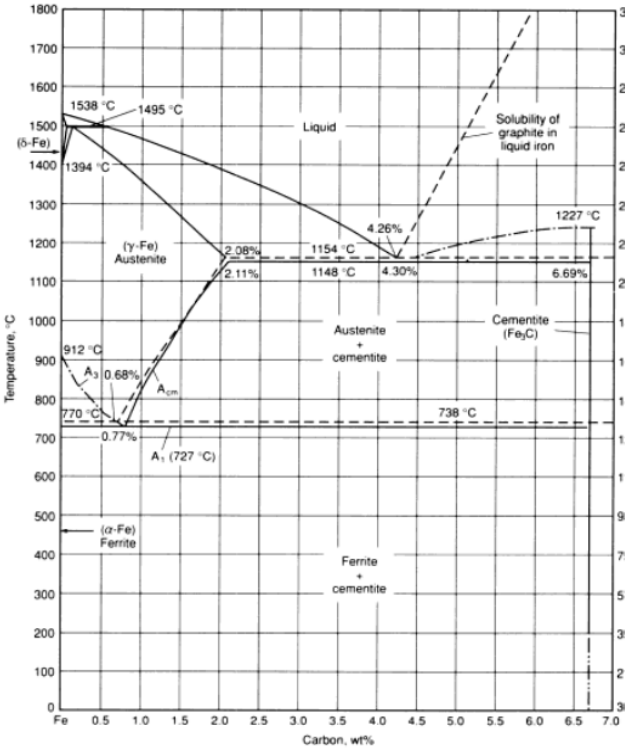

Figure 2-1. *Fe-C phase diagram* [3].

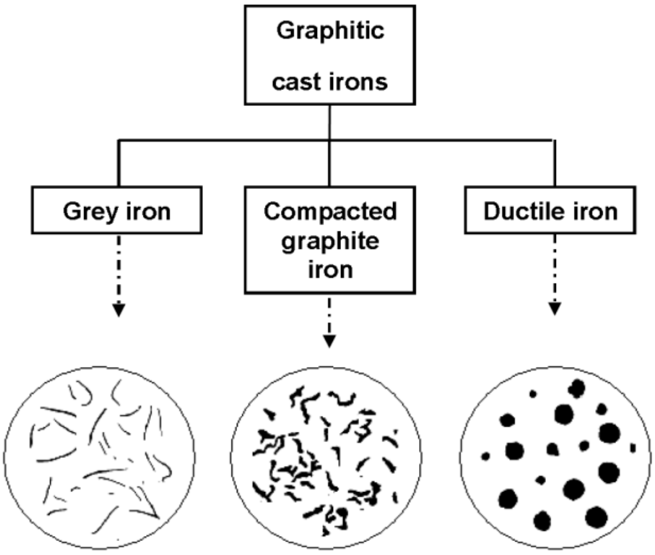

Figure 2-2. *Illustration of different graphite morphologies of graphitic cast irons, such as grey iron, compacted graphite iron and ductile iron* [4].

Table 2-1. *Typical Unalloyed Cast Irons and the range of their chemical composition* [5]**.**

Percent [%]						
Type of Iron	C	Si	Mn	S	P	Fe
Gray	2.5-4.0	1.0-3.0	0.2-1.0	0.02-0.25	0.02-1.0	Balance
Ductile	3.0-4.0	1.8-2.8	0.1-1.0	0.01-0.03	0.01-0.1	Balance
Compacted Graphite	2.5-4.0	1.0-3.0	0.2-1.0	0.01-0.03	0.01-0.1	Balance

Ductile cast iron is produced by a small addition of magnesium to the molten iron (less than 0.05%). This element will interact with sulfur and oxygen present in molten iron and avoid their interference in the nodular graphite formation during eutectic reaction. This cast iron presents good fluidity in the liquid state, allowing produce components with thin sections and complicated shapes. When solidifying, graphite formation (low density) causes an expansion which opposes the metal shrinkage during solidification, letting to produce sound parts with high metal yield. This cast iron has good strength and reasonable ductility. The metallic matrix can be totally ferritic (maximum ductility and machinability), ferritic/pearlitic, totally perlitic or tempered martensitic (highest tensile strength) [6].

It has the capacity to replace steels in many applications. Ductile cast iron is used in many structural applications, mainly those requiring strength and toughness combined with good machinability and low cost [6].

2.2.1.1 SiMo51 and 0727

SiMo51 is usually used in turbo manifolds due to its heat resistance and low price, although it shows limitations regarding corrosion and fatigue resistance above 750°C [4].

This cast iron is alloyed with silicon and molybdenum. The chemical composition is given in the Table 2-2. The microstructure of this material is composed by a ferritic matrix with graphite nodules and stable M_6C carbides in the intercellular regions. The silicon added contributes to oxidation resistance, due to the formation of a SiO_2- layer at the oxide/metal interface [4].

Table 2-2 - *Chemical composition of cast iron 0727 and SiMo51* [4] [7].

	C %	Si %	Mn %	Cr %	Ni %	Mo %	Cu %	Mg %
0727	3.2-4.0	1.5-2.8	0.05-1.0	-	0-2.0	-	-	0.02-0.08
SiMo51	3.0-3.5	4.2-4.8	0.4	0.1	0.1	0.8-.12	0.1	0.02-0.08

Cast iron 0727 (EN-GJS-500-7) is a common structural material used at Scania for brackets and other structural components. It is used when higher tensile strength and yield stress are wanted while toughness is of less importance. It has a ferritic/pearlitic matrix and is usually applied in the as-cast state [7].

2.2.2 Cast steel

Steels are Fe-C alloys, with carbon content up to 2.11% that may or not have additions of other elements.

Cast steel is a very versatile material. It can be welded and processed and has a wide range of applications from high strength to high temperature. Due to its diverse properties cast steels can be used in applications where weldability, abrasion resistance, high strength, toughness, high temperature and corrosion resistance are important [8].

Cast steels used in structural components can be divided in two main groups: low and medium carbon unalloyed steels and alloyed steels with low and medium carbon.

Ausferritic cast steel is a material with high potential to be used in structural components but with low utilization at the moment.

For high temperature applications two groups of cast steels are used: austenitic and ferritic cast stainless steels.

2.2.2.1 Structural steels

Low and medium carbon unalloyed steels

Steels group with carbon content between 0.10 and 0.25% are normally used in the normalized state, due to their low hardenability, because they are not hardened by quenching and tempering. These steels can also be surface hardened essentially by carburizing. Nitriding and carbonitriding are used in steels with higher carbon content [9].

In order to improve the machinability of these steels, a normalizing heat treatment is applied. Steels with a ferritic matrix are too soft, presenting a bad quality surface after machining, caused by ferrite deformation during the cutting. One way to decrease this effect is to conduct a normalizing heat treatment, which increase pearlite fraction and steel becomes less likely to deform during machining. There is also a possibility to improve the machinability, through addition of lead or manganese sulphide replacing the normalizing heat treatment [9].

The steels with carbon content between 0.25 and 0.60%, is the group of steels for heat treatment. These steels present enough hardenability to improve their mechanical properties by quenching and tempering. This group of steels can be ferritic or pearlitic, martensitic and less usual bainitic [9].

These steels require severe cooling rates during quenching, being used water or at least oil (for thin sections) due to their low hardenability. Just thin sections up to 12 mm can be quenched in oil and present a martensitic structure through the whole part. These severe quenching requirements, can lead to dimensional variations that may be unacceptable. In order to avoid these dimensional variations, alloyed steels may be required with higher hardenability [9].

One of the unalloyed structural steels limitations is the tensile strength, which hardly overcome 700 MPa [9].

The increase of thickness in components requires the use of alloyed steels, to obtain a quenched and tempered microstructure and higher tensile strengths [9].

Alloyed steels with low and medium carbon

As referred before, to achieve better mechanical properties in thick sections, alloyed steels are necessary. The most used is the group with 1.6 to 1.9% of manganese. This group of steels have better hardenability, allowing products with 20 mm in diameter to be quenched in oil [10].

The steels with chromium are also frequently used as high strength materials. Some molybdenum addition to these steels is usual. Nickel and vanadium are other elements used, together with the others referred, that increase the mechanical strength after quenching and tempering [10].

The standard EN 10293:2005 presents a list of cast steels used for general purposes, showing the increasing of mechanical strength which is accomplished by adding elements like Mn-Cr-Mo-Ni-V, alone or combined, achieving variations of $R_{p0.2}$ from 300 to 1000 MPa [10].

The standard also shows chemical compositions range, mechanical properties and guidance data for welding. The steel hardness is not commonly shown in SS-EN Standards. Thus, a conversion table from SS-EN ISO 18265:2013 Annex A, can be used.

Ausferritic cast steel

The ausferritic steels have gained importance for automobile industries. These steels have demonstrated very interesting mechanical properties in respect to strength, ductility, fatigue strength, fracture toughness and impact strength. The material contains additions of silicon or aluminium, exceeding 2%, allowing the steel to be austempered with no carbide phase formation during the process, unlike the bainitic structure [11][12]. The microstructure obtained is similar to bainite and the difference is the carbide absence. As the term bainite is used for a microstructure containing carbides, ausferrite is the term used to name the microstructure composed by fine plates of acicular ferrite separated by carbon-enriched region of austenite. Figure 2-3 shows a microstructure scheme found in these steels. The austempering heat treatment will be referred further in this work [13].

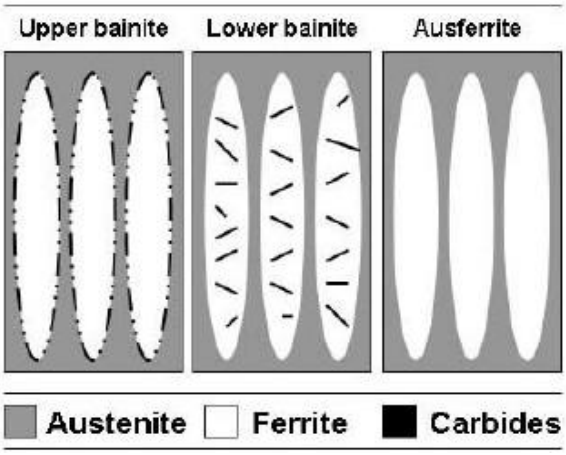

Figure 2-3. *Schematic illustration of bainitic and ausferritic microstructures* [13].

This material has shown great potential to be used as structural material at low cost. Detroit Materials (DM) is a company focused on the development and commercialization of ultra-high performance materials, possessing patent for high-strength low-alloy structural steels and cast irons used for applications, among others, in the automotive industries. To accomplish automotive light-weighting requirements, mainly for drivetrain and suspension components, the company delivery a series of thin wall castable steels which provides unmatched cost and competitive weight saving solutions. Figure 2-4 shows the benefits of DM steel [14].

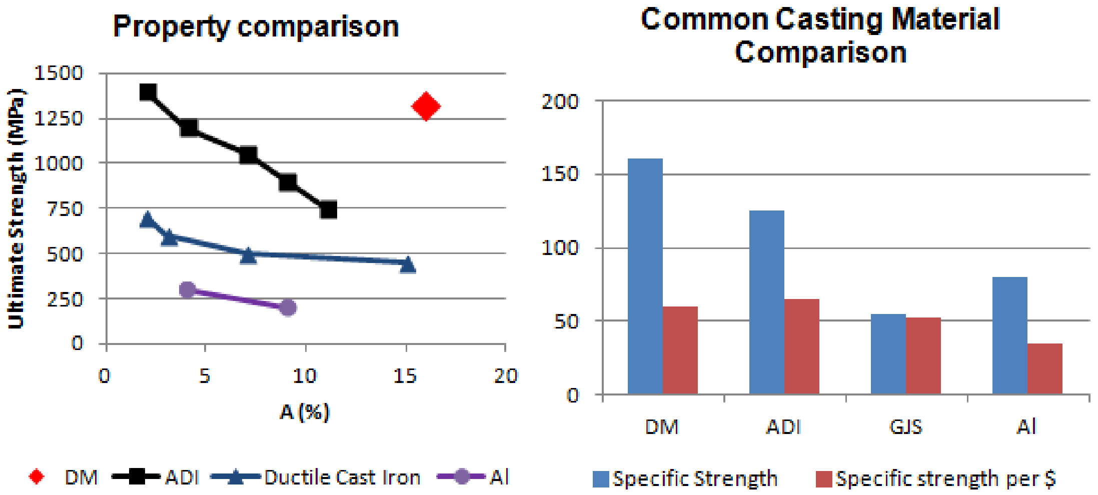

Figure 2-4. *To the left: DM cast steel shows the best combination of strength and ductility. To the right: DM cast steel show the highest specific strength. In both charts DM cast steel is compared with common chassis and drivetrain casting materials* [14].

DM steel also allows cast thin wall sections and complex geometries. The company refers the possibility to cast 3 mm wall section with tensile strength over 1300 MPa and 16% elongation. The material type is not referred, just enunciated as a cast steel. Through the information given, we can assume that the material may be an ausferritic cast steel. The high castability referred can be achieved by the high silicon content present in ausferritic steels and high strength with good ductility are also carbide free bainitic steel characteristics. Table 2-3 shows the properties of two steel grades supplied by DM [14].

Table 2-3. *Mechanical properties of DM cast steels* [14] [15].

	R_m [MPa]	$R_{p0.2}$ [MPa]	A [%]	E Modulus [MPa]	Fatigue limit [MPa]
DM 800-15	809	469	15	228	--
DM1300-16	1302	1049	16.4	229	>400

2.2.2.2 Austenitic Cast stainless steels

Stainless steels are essentially iron-carbon-chromium alloys that may have other alloying elements, like nickel and molybdenum. These materials are used in applications requiring high corrosion and/or temperature resistance. To be considered stainless the steel should have at least 12% chromium dissolved in the matrix. Chromium reacts with oxygen and forms a thin oxide layer, very adherent, which protect the metal [16].

Austenitic cast stainless steels are usually found in the most demanding conditions where ferritic alloys show limitations. Besides chromium, they present high amount of nickel in their compositions [4].

The austenitic alloy HK30 (ASTM A351) is a 25Cr/20Ni alloy commonly found in turbo manifolds of high power gasoline engines, where the gas temperatures may reach 1000°C [4].

The microstructure is composed of austenite with massive carbides. When the cooling is slow, precipitation of carbides at the grain boundaries can occur, depleting the matrix of chromium and the steel becomes sensitive to intergranular corrosion. This precipitation occurs when in service at temperatures between 400 and 850°C or after welding, where the cooling can be slow enough to allow the steel sensitization [17].

Austenitic cast stainless steels present higher strength at high temperatures and better castability than ferritic cast stainless steels [4].

2.2.2.3 Ferritic cast stainless steels

Ferritic cast stainless steels are iron-chromium alloys. The chromium content is usually in the range of 10.5 to 30%. Some grades may contain other alloying elements like molybdenum, silicon, aluminum, titanium or niobium. Sulfur can be added to improve machinability [17].

Their advantages (comparing with austenitic alloys) relies on the high oxidation and corrosion resistance (heat resistance materials) due to their chromium content, better thermal fatigue resistance due to their lower thermal expansion coefficient and higher thermal conductivity, at relatively low cost [4].

These alloys present a relatively low high temperature strength compared with austenitic alloys [17][4]. The relatively low carbon content of these alloys may result in some disadvantages besides low high temperature strength, poor castability and a microstructure containing large grains, with the last one result in decreased ductility and fatigue life. So, these alloys are found in turbo manifolds made of sheet metal, which present a grain size reduction due to metal forming process [4].

It is possible to increase the castability and reducing the grain size of ferritic cast stainless steels increasing the carbon content and adding ferrite stabilizing elements like niobium or tungsten. These elements are added in order to compensate the austenite stabilizing effect of the additional carbon keeping a ferritic structure [4].

2.2.3 Alloying elements

The steel is a complex alloy composed with various elements and each of them has its role in the steels' properties. The influence of each element will be summarized next.

Carbon is the main steels' element. The progressive content growth of this element cause the increase of mechanical strength and hardness with the consequently decrease of ductility and weldability. It improves the steels hardenability and acts as austenite stabilizer. This element is the source of the great steel properties versatility [10].

Aluminium does not have any affinity to carbon and does not improve the hardenability. Main effects are thin dispersions formation with the nitrogen and oxygen, limiting the austenitic grain growth. Aluminium also creates a hardening layer by reaction with nitrogen in the ferritic domain (nitruration of aluminium alloyed steels). It is a powerful deoxidizer and effective to control austenite grain growth in reheated steels [10].

Chromium is a ferrite stabilizer, having tendency to associate with carbon forming carbides and improving the hardenability when dissolved. Chromium is the stainless steels main element, improving the corrosion, oxidation resistance and high temperature strength, as well as wear resistance for steels with high carbon content [10].

Cobalts´ main effect is to improve the strength at high temperatures, but decreases the hardenability [10].

Copper improves resistance to atmospheric corrosion through additions within the range of 0.2-0.5% [10].

Manganese has an equal partition ratio between the matrix and carbides, improving the hardenability, stabilizing the austenite, decreasing the M_S (Martensite start) temperature and decreasing the weldability. It increases the ferrite strength and improves the machinability forming manganese sulphides [10].

Molybdenum is a strong carbide former and improves the hardenability. Molybdenum has as main effect controlling the austenitic grain size, improving the high temperature resistance and improving the pitting corrosion resistance [10].

Nickel does not have affinity to carbon. However, it improves the hardenability, also allowing the austenitic steels production with high chromium content (austenitic stainless steels) and improves the impact resistance. In stainless steels, it improves the strength at high temperatures [10].

Nitrogen adds yield strength to austenitic stainless steels. It also improves the corrosion resistance and increases the high temperature tensile strength [10].

Phosphorous does not have any affinity with carbon. It improves the hardenability and has as main effect increasing the low carbon steels hardness, improving their resistance to corrosion. It also decreases the ductility, contributing to the embrittlement after quenching and tempering and increases the tendency to crack during welding [10].

Silicon improves castability and does not present carbon affinity, increases the ferrite hardness, improves refractory steels oxidation resistance, being also a strong deoxidizer agent and helping to increase the toughness [10].

Tungsten, *Niobium, Titanium and Vanadium* are strong carbide formers and have a great contribution for hardenability improvement when dissolved. They have as main effects controlling the austenitic grain size growth, improving the high temperature resistance, preventing the stainless steels sensitization (grain boundary carbides) and increasing the ferrite strength by precipitation [10].

2.3 Cast steel properties

2.3.1 Chemical compositions

The chemical composition refers to the type and amount of elements added.

The materials used by Scania and other materials commonly applied in the automotive industry are collected and described considering chemical composition, physical and mechanical properties. The alloys and their composition for the *Cast steel Guideline* are compiled in APPENDIX A.

When selecting materials for a new design it is important to understand the key properties. A material's property is often quantitative and the benefits are to compare different materials properties to match the design requirement. Alloy steels are broken down into smaller groups depending on their mechanical properties. A wide range of ultimate tensile strength, yield strength and hardness depends on different heat treatment conditions.

2.3.2 Cast steels for general structural purpose

The compiled list of steels for general structural purpose can be found in APPENDIX B *Steel castings for general engineering SS-EN 10293:2005.*

2.3.3 High-strength cast steels

The compiled list of steels for high-strength purpose (yield strength > 500 MPa to typically 700 MPa) can be found in APPENDIX C *High-strength cast steels SS-EN 10293:2005*

2.3.4 Heat resistant steel castings

The compiled list of steels for heat resistant purpose can be found in APPENDIX D *Heat resistant steel castings SS-EN10295:2002, SS-EN10095.*

2.4 Production

2.4.1 Cast Processes

2.4.1.1 Green Sand Casting

Green sand is the most widely used casting process. It has many advantages such as allowing complex shapes, large parts, low tooling and equipment cost. The mould is not baked or dried and contains silica sand, clay, water and sometimes other additives, therefore the process got the term *green*, although the sand is black. A metal, or sometimes a wooden frame is used to place the pattern to produce a cavity in the flask halves. A hollow section needs a core consisting of baked hardened sand [18].

The process contain six main steps: mould-making, clamping where the mould halves are closed and clamped together, pouring the molten metal into the mould, casting cooling, casting removal from the sand mould and lastly casting trimming and machining [19].

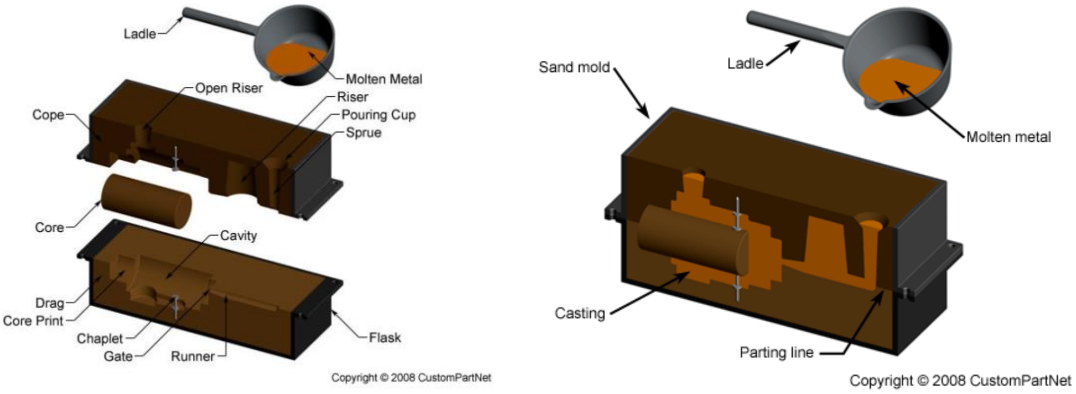

Copyright © 2008 CustomPartNet

Copyright © 2008 CustomPartNet

Figure 2-5. *Sand casting process overview* [19].

2.4.1.2 Nobake Sand Casting

Nobake sand casting even called air-set method or chemically bonded sand casting is similar to green sand casting. The main difference between the two methods is that the nobake casting method is using chemical binders and catalyst to cure and harden the moulds. The high productions rates achieved with green sand casting are not possible due to the curing time for the chemicals to harden in the mould. The well compacted mould results in nobake sand casting yields, better surface finishes and tolerances than green sand casting [20].

2.4.1.3 Croning shell moulding process

Johannes Croning [21] developed the croning shell moulding process during World War II. This sand casting process uses sand mixed with phenolic resin and hexamine catalyst plus binder, which maintains the characteristics of loose sand. The model is usually steel plates formed as the desired product. The plates are first heated to about 250°C before brought in contact with the sand and forms a shell. After cooling and model removal, the shell remains approximately 25 mm thick. Cores are applied to produce hollow castings before the two half shells are put together, ready to be filled with liquid metal, see Figure 2-6. This process is more expensive than other sand casting processes but presents better casting tolerances and surface finishes [21].

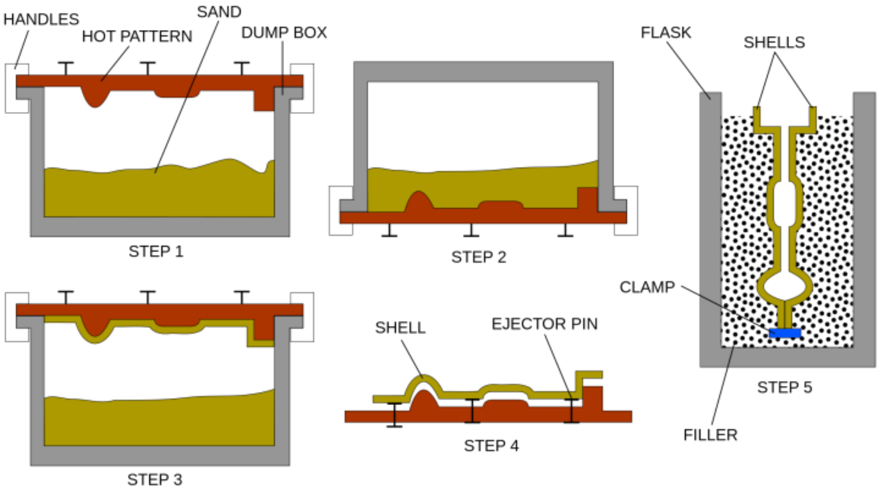

Figure 2-6. *Croning shells making process* [22].

2.4.1.4 Investment casting

Investment casting or lost wax casting process, can produce complex components with high precision and accuracy. The high tolerances reduce the need for machining [19].

Like other casting processes, investment casting follows the some steps and a pattern need to be created. With investment casting the pattern will be made in wax followed by dipping in a fine ceramic particles slurry to create the mould. This shell created is then placed into an oven to let the wax melt out. The mould is then preheated to approximately 1000°C and molten metal is poured into the gating system. The molten metal cools down, solidifying, and the cooling time depends on the mould thickness and material used. The casting is removed by breaking the mould and the parts can be removed from the pattern tree by sawing or cold breaking. Figure 2-7 shows schematically the process. As a final step, some finishing operations may be needed depending on the part requirements [19].

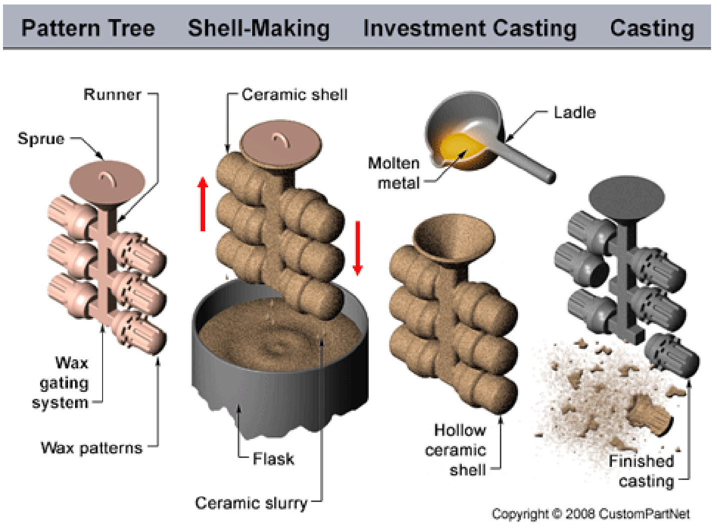

Figure 2-7. *Investment casting process overview* [19].

2.4.1.5 Lost foam

Grede, a company leader in the development and production of lightweight, ultra-high-strength ductile cast iron components for commercial vehicle chassis applications, for instance, presents lost foam casting process as a way to accomplish its goals [23].

This company is producing various suspension and exhaust brackets using the lost foam process which are up to 32% lighter than alternative designs. As an example, a spring hanger produced for one customer, is casted with as many as 27 cored places in an austempered ductile cast iron to reduce weight [23].

The lost foam process is a casting process that is ideally suited to the manufacturing of geometrical complex parts. This casting process uses “lost” patterns made of organic foam materials. These patterns are inserted into a mould material which is free of bonding agents by using vibration compression. During pouring, the pattern is vaporized by the molten steel, creating a hollow space which molten steel fills up. So, an exact metallic cast copy of the pattern is created. It is possible to create very complex shapes with this method. The castings produced by lost foam process present excellent surface quality and dimensional accuracy. Figure 2-8 shows schematically the process [24].

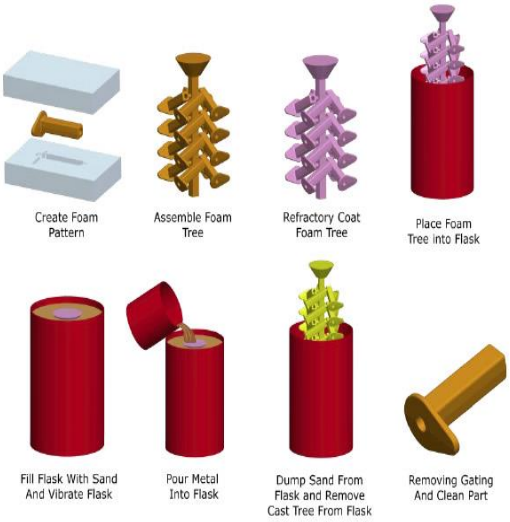

Figure 2-8. *Lost Foam process steps* [25].

Table 2-4 shows some areas of application and limitations of lost foam process.

Table 2-4. *Areas of application and limitations of lost foam process* [24].

Areas of Application/Advantages
• Suitable for geometrically complex parts • Component dimensions up to 600 x 600 x 600 mm • Component weight 1 - 100 kg • Casting of low alloyed up to high alloyed cast steel • Series cast parts from 500 to 10,000 pieces/year with foam patterns • Wall thickness able to be cast from 3 mm • Dimensional tolerances according to ISO 8062 CT07 – CT09 • Surface quality R_a 6.3 and better • Holes and slots can be cast
Application limitations
• Cast steel with less than 0.1% carbon are not able to be casted • The component must be technically suited to feeding • The interior of the component must be suitable for moulding with bonding agent free sand

2.4.2 Surface Finishes in Casting Processes

Casting processes can provide various surface finishes and for the most common process, sand casting, a root mean squared (RMS) of 250-900 can be achieved. American Foundry Society presents a table with surface finish capabilities by process, see Table 2-5.

Table 2-5. *Surface finish capabilities by process (in RMS, with extreme low values in parentheses)* [26].

Sand Processes	Ceramic Mold Processes
Shell 75-150 (40)	Plaster 40-125 (25)
Nobake 150-600 (40)	Ceramic 60-175 (25)
Lost Foam 125-175 (100)	Investment 50-125 (32)
Horizontal Green Sand 250-900 (100)	------------
Vertical Green Sand 250-900 (100)	------------

A C-9 microfinish comparator displays surface finishes from 20 to 900 RMS, see Figure 2-9.

Figure 2-9. *C-9 microfinish comparator* [26].

2.4.3 Advantage and disadvantage of the casting processes

Casting processes have different advantages and disadvantages and it is up to the part design, quantity and use to determine which method is the best in each case. An overview of some common casting processes and its advantages and disadvantages is presented in APPENDIX E.

2.5 Castability

The designer should take into account some rules regarding steel castings design to improve the castability and casting quality. These rules are based on the steel fluidity and solidification, mechanical principles involving cores and moulds production, cleaning, machining requirements, functionality, heat treatments and weight considerations [27].

2.5.1 Minimum section thickness

The minimum thickness of a section needed to withstand a given load is the requirement that governs its design. Although, in some cases, a very thin section may be enough for the application, depending on strength and rigidity calculations, and therefore, the castability becomes the main factor of a design. For these cases, the minimum section thickness per length should be followed, to ensure that steel castings sections will be entirely filled [27].

There is no common sense about the minimum thickness suggested for the design of a steel casting when conventional techniques are applied. A minimum thickness of 6 mm [27] and 6.5 mm [28] are suggested in the literature. For grey cast irons is 4.5 mm [29]. There are steels, like the new ausferritic cast steel, which has gained importance in recent years, possessing high silicon content and because of that, better castability is expected. From this steel it is possible to cast a component with 3 mm wall thickness [14]. Other more expensive processes can produce thicknesses approximately 1.5 mm in the case of investment casting and sections tapering down to 0.76 mm are possible to obtain [27].

The liquid steel cools faster just when it enters in the mould. A thin section will fill readily if it is placed near the gate, where the molten metal is hot. When the thin section is far from the gate, the metal may be too cold to fill the section [27].

It is important to note that for a given thickness, the molten steel flows easily in a narrow, rather than in a wide section. The minimum thickness of section depends on its length and should follow the values provided by the chart in Figure 2-10.

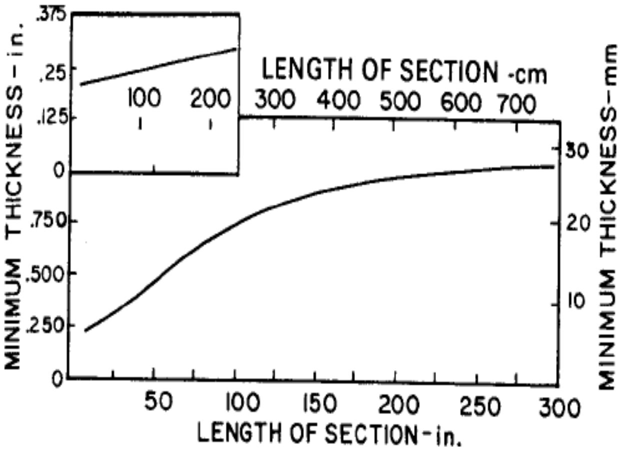

Figure 2-10. *Minimum thickness of sections as a function of their largest dimension* [27]**.**

The chart of Figure 2-10 shows the best combination, thickness versus length, when liquid steel enters into a position of a casting and have to run the lengths given in the chart. There are some special techniques/actions that can be applied by the foundries to fill longer lengths through thinner sections prescribed on the chart. The disadvantage of applying such techniques is costs increasing [27].

The recommended dimensional relationships for cores to avoid fusion are presented in Figure 2-11.

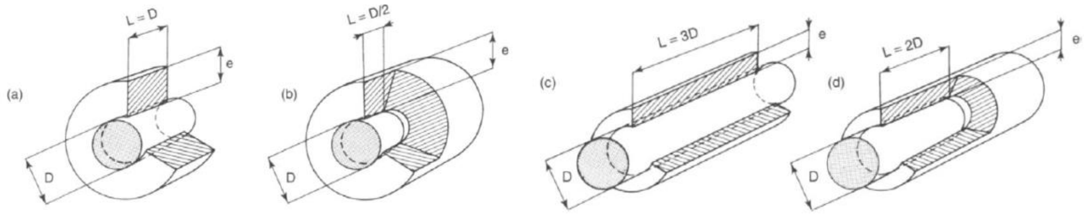

Figure 2-11. *Recommended dimensional relationships for cores to avoid fusion. (a) Cylindrical hole with D less than 2e, Maximum length =D; (b) blind hole with D less than 2e, maximum length = D/2; (c) cylindrical hole with 2e ≤ D ≤ 3e, maximum length = 3D; (d) blind hole with 2e ≤ D ≤ 3e, maximum length = 2D* [29].

2.5.2 Internal soundness

The solidification of steel casting starts at the mould wall, where a continuously thickening envelope forms, as heat is removed through the mould-metal interface. During solidification a volumetric contraction takes place within the cross section of a casting part, which must be compensated by molten metal from an adjacent thicker section, or through a riser which works like a reservoir of liquid metal and is placed next to, or on top of, the heavier section [27].

Shrinkage cavities will form, if there is not enough feed metal to replace the empty places left by the volumetric contraction, at the solidification time. They can appear in sections that have to be fed through thinner sections. Thinner sections will solidify first and the fed molten metal cannot travel from the riser to the heavier sections [27].

There are some limitations in which the risers are effective. In some design situations, it is impossible to compensate volumetric contraction in isolated sections of increased mass. For instance, the section A of Figure 2-12 will have a shrinkage cavity at the position of the heavier section, if the section were not fed by a riser placed in the thicker section as shown in section B. The section C presents a boss placed on the lower part of casting which will contain a shrinkage cavity. Chills can be used to increase the cooling rate of this part and turn this part virtually a thin section, as the riser will not feed a heavy section through a lighter section in a regular sand mould [27].

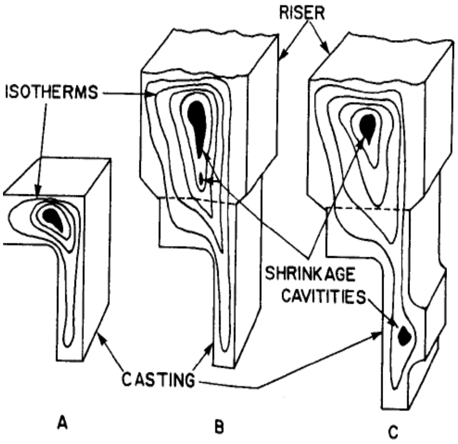

Figure 2-12. *Predictive shrinkage cavities* [27].

A work relation between design engineers and foundry engineers is needed to achieve optimum soundness of the casting. The shape of the part can be finalized for functionality as well as directional solidification. The shrinkage cavities can be avoided through directional solidification, beginning at the thinnest section, running through progressive thickest sections to the riser, ensuring feeding [27].

2.5.3 Tapers

Taper shape is a part where dimension progressively increase towards one or more available places, where risers can be placed to compensate the shrinkage. In Figure 2-13 some examples of good design practices are shown to avoid shrinkage cavities [27].

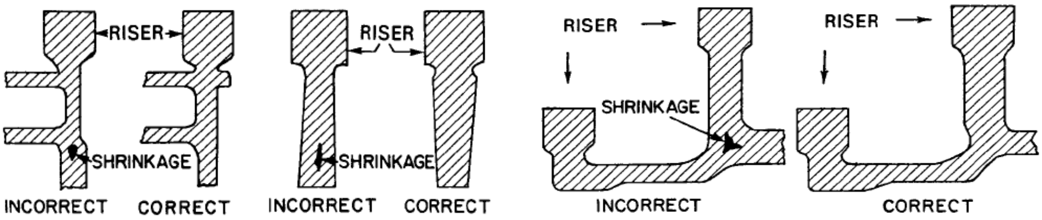

Figure 2-13. *Some examples of sections showing correct design to prevent shrinkage cavities* [27].

Suggested casting sections tapers are defined according to the following equation (1), where *W* represents the width (cm) of the section and *T* its thickness (cm):

$$Taper = -0.0164\ W + 0.0648\ T \qquad (1)$$

In the case of plates, the value of *W* should be twice of the *T* [27].

2.5.4 Padding

Padding is used in sections where a continuous taper is not admissible, because of design requirements. An example of a cast design requiring the use of metal padding is illustrated in Figure 2-14.

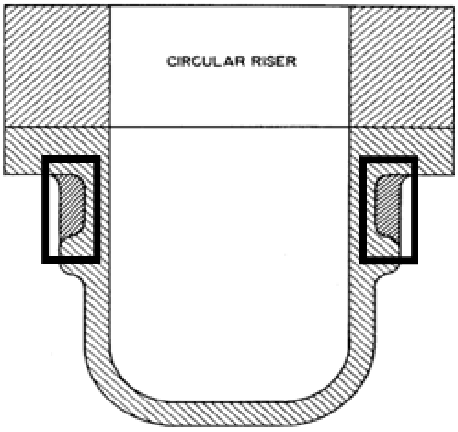

Figure 2-14. *Cut section of pressure vessel drawing showing added padding in the rectangles to feed and isolated heavy section* [27].

2.5.5 Chills

Using chills can reduce or eliminate shrinkage. Chromite or zircon sand may be used as a chill. Metal chills also are widely employed. Chills shape are according to the contour surface of the casting to be chilled. Metallic chills can incorporate into the mould or a core by pressing the sand around the chill during moulding or core making. The function of chills is to increase the cooling rate at the surface of casting compared with the surrounding mould wall. If chills are well implemented, the foundry can transmit directional solidification to a riser from an adjacent heavier section preventing shrinkage cavities. The Figure 2-15 gives two examples of implemented chills [27].

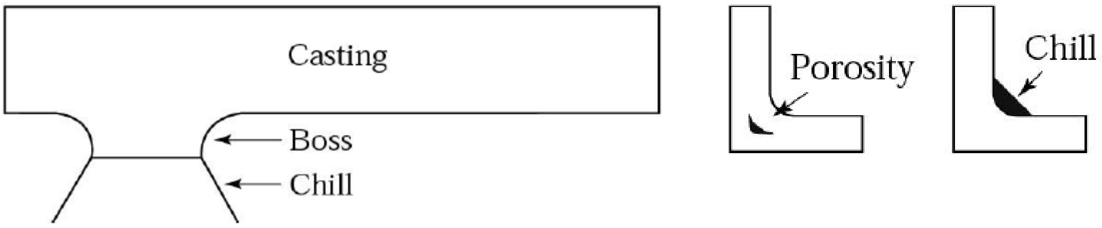

Figure 2-15. *Chill applied to a boss increase the heat extraction* [30].

2.5.6 Joined Sections and Ribs

One of the great advantages for a designer to work with steel castings is the flexibility to place metal exactly where the designer wants it. However, some cautions should be taken when sections are joined together, because an increase in mass can occur. Shrinkage cavities can occur in these areas if a riser is not used. The inscribed circle method is used to minimize heat concentration in joining sections and ribs. This method can be seen in Figure 2-16. The increase mass at the joint is proportional to the square of the diameters ratio, $(D/d)^2$, which must be as small as possible [27].

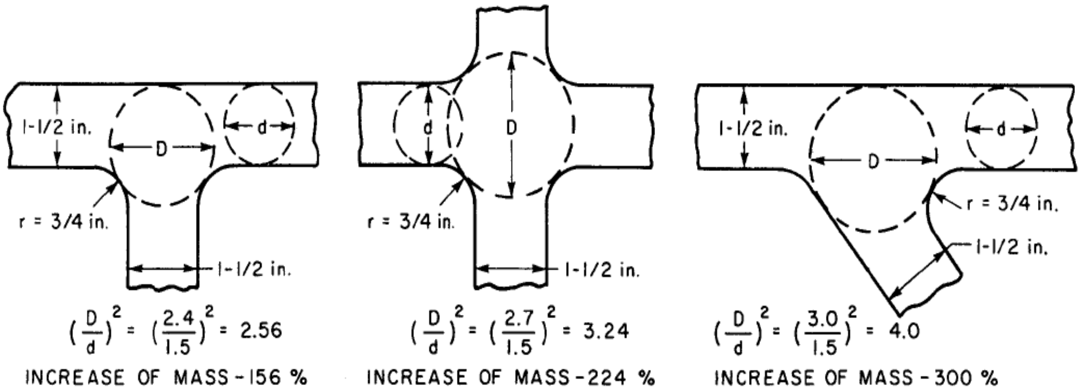

Figure 2-16. *Increasing of mass resulting from joining sections shown by inscribed circle* [27].

Ribs and webs as shown in Figure 2-17 should be as thin as possible regarding other requirements like design, strength, *et cetera*.

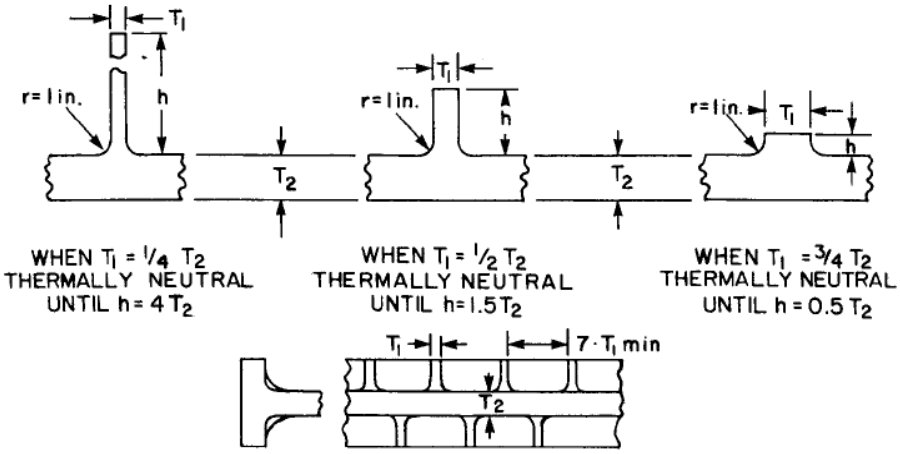

Figure 2-17. *Rib thickness with several T-junctions thermally neutral* [27].

The Figure 2-17 shows the correct proportion of ribs and parent sections. Another important thing is to place the ribs as shown in the figure to avoid X-junctions [27].

The heavy section in A shown in the Figure 2-18 would be hard to feed in some parts, so the design can be changed to a thinner section, and employ reinforced ribs as illustrated in B. The junction between the rib, flange and body will originate a hot spot. To avoid this hot spot, a cored hole can be placed as shown by Figure 2-18 to the right [27].

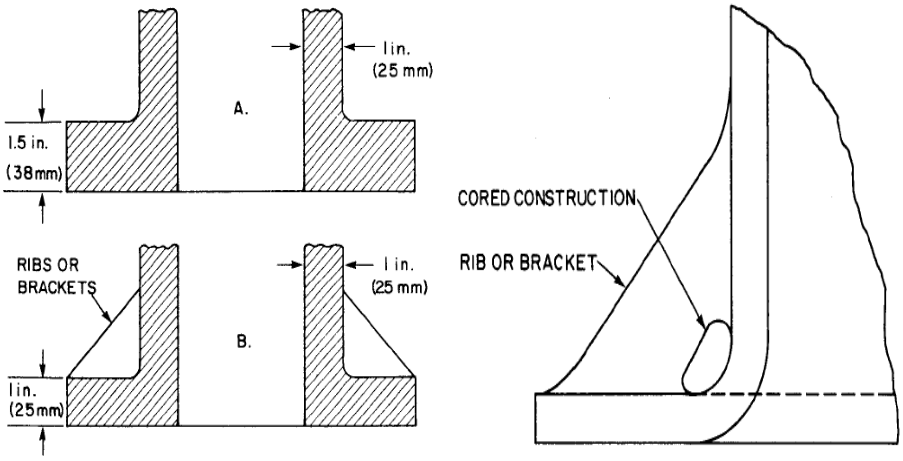

Figure 2-18. *To the left: Rib addiction to increase rigidity and reduce weight. To the right: Eliminate hot spot in rib using a core* [27]**.**

2.5.7 Surface integrity

Besides soundness of the casting, the designer should take into account the surface integrity of the casting, meaning prevent surface discontinuities [27].

Changes in section or junctions tend to produce cracks and hot tears and good design practices are necessary to avoid these defects. Formation of discontinues, such as hot tears and cracks cause costly removal, repair and production delays. These recommendations can be followed to avoid such problems [27].

2.5.8 Changes in Section Size

When it is strictly necessary implement abrupt changes in section thickness, some considerations should be taken into account. Sharp corners and small radius at a change of section should be avoid, due to stresses concentration during solidification and even in service [27].

Changes in section thickness should be progressive. Figure 2-19 shows how a section change should be done. To the left we can see how the change of section thickness should not be done and to the right how it should be done [27].

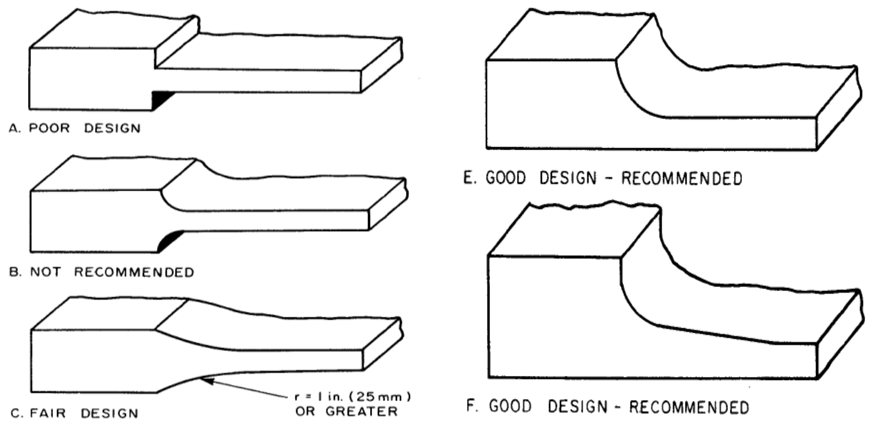

Figure 2-19. *Design for changing section thickness* [27].

The section thickness changing can be done preventing problems following some rules as:

1. Sharp angles or small fillets are not recommended (Figure 2-19, A and B).
2. A common centre line of both sections results in fair design (Figure 2-19, C).
3. The best option (Figure 2-19, F) is in which the change in section just takes place on one side of the thinner section and respecting the design as expressed in Figure 2-20 [27].

There are rules to apply on cylindrical sections of different diameters to be joined on a common axis. In the following considerations, T1 represents the thickness of the smaller section and T2 the thickness of the larger section.

1. If T_1 = 25 mm, and T_2 = 41 mm join with a 15° taper.
2. If T_1 = 25 mm and T_2 = 51 mm join with a fillet having a radius between 13 to 28 mm.
3. If T_1 = 13 mm and T_2 = 41 mm do not join [27].

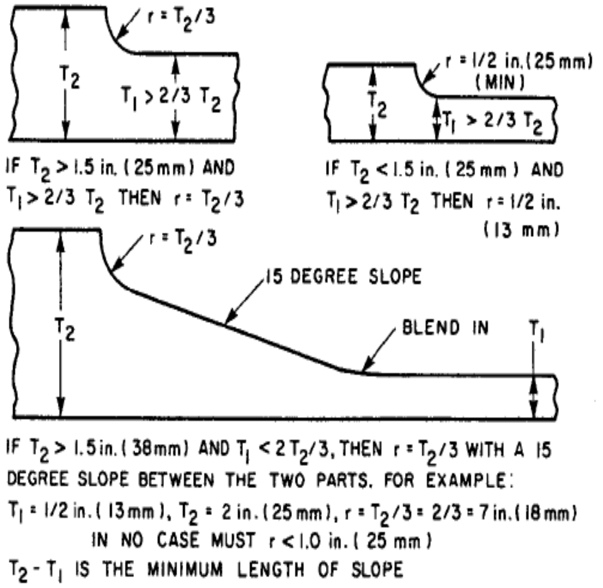

Figure 2-20. *Design rule for section thickness change (T= thickness)* [27].

2.5.9 External corners

External sharp corners must be avoided, due to high residual stresses that may take place when these corners cool quickly from high temperatures. This can be particularly problematic for quenched steels. Employing an external radius will preventing these high stress gradients [27].

In order to prevent high thermal gradients a radius between 0.1 and 0.2 T is needed [27].

2.5.10 Wave construction

This type of design aims to minimize internal stresses through the use of curved spokes. In many types of wheels for instance, the rim, hubs and the spokes cool at different rates due to different cross sectional areas, originating internal stresses. Using curved spokes will reduce internal stresses by allowing movement of the part after solidification [27].

2.6 Steel Castings tolerances

Service and manufacturability requirements influence the shape of a cast steel component. Casting shapes must follow guidelines for draft allowances to properly produce the mould. Machining allowances are needed where more precision and improved surface finishing is needed [31].

Another factor that must be taken into account is the shrink rules or pattern allowances, whose are important in order to meet customer dimensional tolerance requirements [31].

2.6.1 Draft tolerances

Table 2-6 presents general draft suggestions for steel castings. The draft allowances presented are for all surfaces perpendicular to the mould parting line. It is recommended to meet or exceed these suggested draft allowances to ensure mouldability [31].

Table 2-6. *Typical draft allowances* [31]**.**

Moulding Process	**Typical Draft (Taper) Angles**	
	Most features	**Deep Pockets**
Green Sand – Manual	1.5°	2.0°
Green Sand – Automated	1.0°	1.5°
Nobake & shell moulding	1.0°	1.5°

Some aspects about draft allowances must be discussed with foundry. A minimum amount of draft is required for machine moulding. In green sand mould interior surfaces usually require more draft, compared with exterior surfaces. Draft can be eliminated through the use of precision casting processes like investment casting or through the use of cores [31].

2.6.2 Machining allowances

The casting must have extra metal in all surfaces requiring machining. The required machining allowance (RMA) depends mainly on the casting size and shape, surface to be machined, steel hardness, surface roughness and its distortion tendency. The required machining allowance superimposes the draft and pattern allowances. The APPENDIX F presents the required machining allowances for steel castings [31].

The machining allowances presented in APPENDIX F are conservative. For high production castings series these machining allowances should be reduced when adequate machining trials have been conducted.

The faces position related to the mould influences the machining allowances. The cope surfaces of a large casting will require higher machining allowances than side walls for instance [31].

2.6.3 Dimensional tolerances

Dimensional tolerances should be discussed between producer and purchaser. Using tight tolerances on not critical areas just increase final casting cost without any added value to the purchaser [31].

The casting quantities, design and dimension type, all play an important role on the casting tolerances definition, which can be accomplished by the process.

The table presented in APPENDIX G shows dimensional tolerances from SS EN-ISO 8062-3:2007. Appropriate casting tolerance grades for each casting process, for long and short-production series, are pointed out in Table 2-7.

Table 2-7. *Steel casting tolerance grades for long-production series, SS EN-ISO 8062-3:2007* [31].

Conditions	**Tolerance Grades for long-production series**	**Tolerance Grades for short-production series**
All sand moulding process fully capable, most appropriate for large castings	CT 12-14	CT 13-15
Appropriate for most casting types and sand moulding processes	CT 10-12	CT 11-13
Within process capabilities, but not appropriate for all casting types and sand moulding processes	CT 8-10	CT 9-11
Investment Casting	CT 5-7	------

The casting geometry, moulding process and production techniques are the main factors which influence the dimensional tolerance. Some experienced foundries may develop production techniques and process control allowing produce castings with tighter tolerance than indicated in Table 2-7 [31].

2.6.4 Moulding process

The moulding process influences the dimensional capabilities. For a given size and shape, shell moulding is expected to be a more dimensionally capable process than nobake and green sand moulding, respectively. These differences in dimensional capabilities between processes are in less extension than foundry to foundry variation, for a given moulding process. So, while a given steel foundry may need to use the more expensive shell moulding process to meet close dimensional tolerances, another foundry may be capable to achieve close dimensional tolerances using green sand moulding [31].

Some special operations can be employed when the tolerances are tighter than the process capability. Table 2-8 presents some of these additional operations that may be conducted in order to produce castings with tighter tolerance limits compared with expected from standard process capabilities [31].

Table 2-8. *Additional operations to be conducted to produce castings with tighter tolerance limits* [31].

Pattern Upgrading	Molding and core making	Finishing
Changes in construction, mounting and/or material. Alteration of patterns after production of sample castings.	Changes in mould making equipment or moulding process. Upgrading of core boxes or adjustments in core processes.	Gage grinding Straighten or press to gage Coining to gage Machine locating points Rough machine to gage Target machine casting Finish machine part

2.6.5 Geometrical casting tolerances

Geometrical casting tolerances are applied to the shape features of a casting. Geometrical tolerances for features like straightness, flatness, circularity, perpendicularity, symmetry, and coaxiality are presented in APPENDIX H.

General comparison of casting requirements between the different casting methods is shown in Table 2-9. This information is general and should be used as comparison and not as design tolerances in drawings. Each foundry has its capacity and experience and some foundries may produce greater dimensional capabilities, lower costs and better lead times compared with data in Table 2-9 [31].

Table 2-9. *Comparison of steel casting methods – General* [31].

Casting requirements	Green Sand	Nobake	Shell Mould	Investment
Surface smoothness	Fair	Good	Good	Excellent
Minimum thickness [mm]	6	5	4	2
Total tolerance for a 100 mm features [mm]	3.4	2.5	1.7	0.8
Added total tolerance across a parting face [mm]	3	4	2	No parting line
Intricacy	Fair	Good	Very good	Excellent
General machine finish allowances [mm]	6	Most 5	2	Least 0.5
Pattern costs	100%	80%	250%	175%
Lead time (pattern)	18 weeks	12 weeks	20 weeks	22 weeks
Lead time (existing pattern)	6 weeks	6 weeks	6 weeks	8 weeks
Economical quantities [pieces]	Less than 100 but also high-volume depending on the automation	1-5000	High volume production but 10-500 may be economically	Most suitable for 10-1000 but also high volume with automation

2.7 Defect characterization in cast steels

The most common defects found in steel castings are porosity, inclusions (oxide, slag and non-metallic), shrinkage cavities, hot tears and primary grain boundary fracture [32].

Porosity is a common and deleterious casting defect. The gases dissolved in the molten steel, hydrogen, nitrogen or oxygen, or core gases decomposed from the sand core and absorbed by the liquid, are important parameters in porosity formation in castings [33]. This defect is formed during solidification due to the decrease gas solubility and often in combination with oxide and slag inclusions. Normally, the upper parts of castings are more sensitive to this defect, once are the last part to be filled. The gases and inclusions not retained in the gating system neither expelled by vent channels in the mould (gas case), will be retained in front of the filling. The inner surface of gas porosities is smooth. This defect can be identified in Figure 2-21, to the left [32].

In order to avoid this defect the use of dry materials and ladles, clean charge, properly degasification of the melt and improved quality of mould sands (permeability of gas, vent) should be done [32].

Figure 2-21, to the right, presents another common defect identified as inclusions. Inclusions are defects formed during casting process of the molten steel. Inclusions can be non-metallic impurities, slag or oxides, whose can be classified as endogenous, when are caused by reaction products during the process of the molten steel (especially during deoxidation), or exogenous when derived from external causes, like slag [34].

Manganese added to interact with sulphur producing manganese sulphide (MnS) inclusions instead of iron sulphide which presents a brittle effect is an endogenous inclusion [32].

The inclusions also can be classified by the size, as macro-inclusions (> 20 μm) or micro-inclusions (< 20 μm) [32].

This type of defect is frequently found at surface as described before. This happens because these particles easily float on the molten steel. The conditions which increase the appearance probability of this defect are:

- Overheating at a temperature and during a period of time;
- Gating and feeding system with dimensions and geometry which allow the absorption of air and mould erosion;
- Turbulent metallic flux which does not allow the maintenance of oxides and other particles at the molten steel surface;
- Oxygen dissolved in liquid [34].

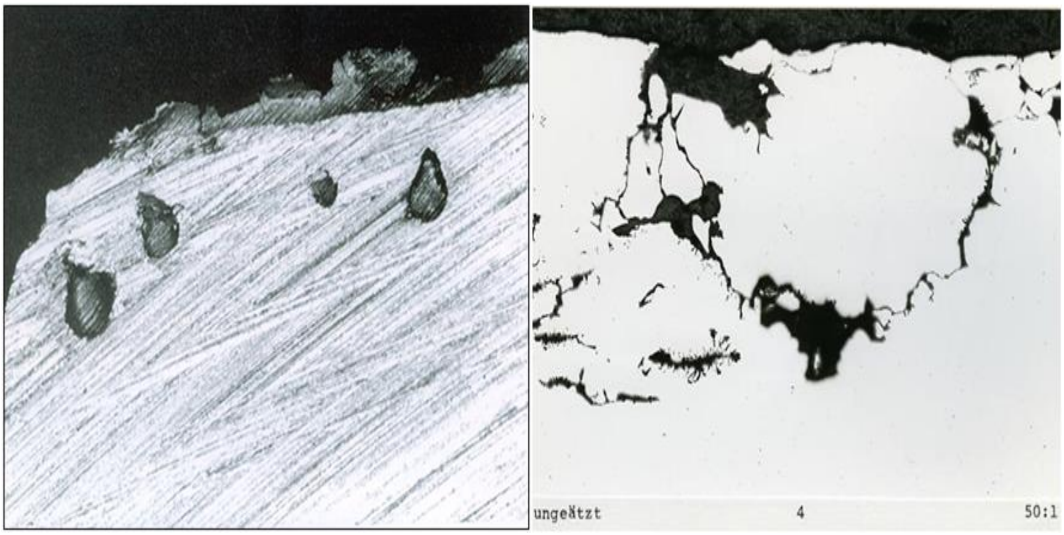

Figure 2-21. *To the left: Gas cavities. To the right: Inclusions* [32].

The molten steel specific volume is higher than the solid specific volume, resulting in a contraction during solidification and cooling, which is about 4 to 7% in cast steel. To compensate this contraction, feeding is necessary through risers placed in zones in which it is possible to create a solidification path. If the feeding is not enough, formation of shrinkage cavities takes place. The surface of shrinkage cavities is rough and looks like as shown in Figure 2-22, to the left. To avoid this type of defects it is important to ensure an optimal feeding system, which can be tested through simulation programs, warranty of directional solidification, use of exothermic riser sleeve and decrease the pouring temperature, in order to avoid some shrinkage that already happens during the cooling of molten steel [32].

Hot tear is another defect which can appear in steel castings. The reason of its appearance is stresses caused by contraction during solidification (residual stresses). The main variable for formation of hot tears is the casting geometry. Figure 2-22, to the right, shows the appearance of this defect [32].

Hot tears are intercrystalline discontinuities and cracks run along the grain boundaries. The risk of cracks increases for alloys with high freezing range. The hot tearing tendency rises with the increase of carbon content up to ~0.4%, then decreasing. Alloys with carbon below 0.2% have low tendency for this defect. Sulphur increase the appearance of hot tear but the addition of manganese compensate the effect of sulphur forming manganese sulphides. Wide difference in the wall thickness and hot spots may contribute to increase residual stresses and should be avoided through properly design to casting (as referred in *Castability*) [32].

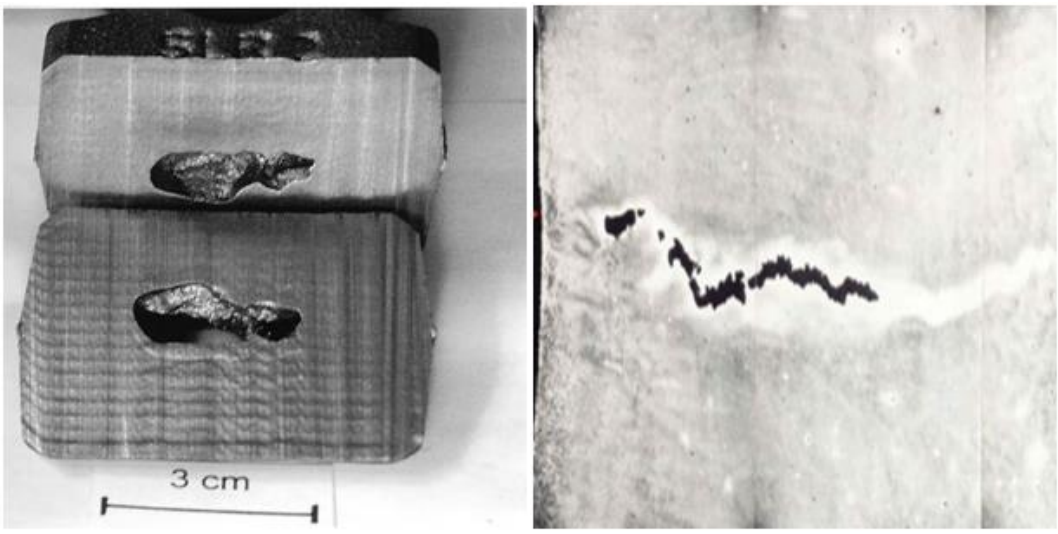

Figure 2-22. *To the left: Shrinkage. To the right: Hot tear* [32].

Primary grain boundary fracture is caused by precipitation of Al-N. High content of these elements and thick-walled castings are sensitive to the appearance of this defect [32]. Figure

2-23 shows, to the left, a primary grain boundary fracture, and to the right, Al-N precipitates are visible.

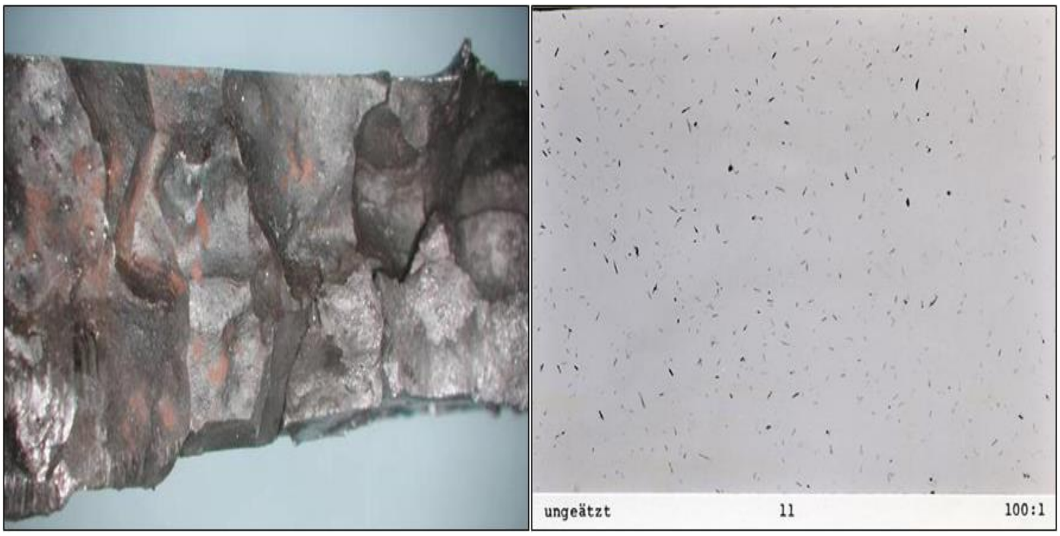

Figure 2-23. *To the left: Primary grain boundary fracture. To the right: Al-N precipitates* [32].

2.8 Bulk and surface cast steels heat treatments

There are two types of heat treatments applied to steels including cast steels, surface hardening and bulk heat treatments. The first changes the microstructure of the surface layer while the second changes the microstructure in the whole component mass.

2.8.1 Surface hardenings

In this work diffusion methods and selective hardening methods are described. The diffusion methods are carburizing, nitriding and carbonitriding. The selective hardening methods include flame, induction and laser hardening.

The diffusion methods introduce surface compressive residual stresses that are beneficial for fatigue strength. However, in the selective hardening some residual tensile stress may exist in the border region between the hardened and unhardened zones. So, methods such as flame or induction hardening should be applied away from geometric stress concentrations. The diffusion methods provide good resistance to surface fatigue. In bending fatigue resistance, the ideal hardening depth is achieved where the failure initiation point is transferred from the core to the surface [35].

2.8.1.1 Carburizing

Carburizing is a surface hardening process in which carbon is dissolved by diffusion in the surface layers of a low-carbon steel part (0.10-0.25% C) at a temperature where austenitization occurs, followed by quenching and tempering resulting in a martensitic microstructure [36].

This treatment causes a gradient in carbon content below the surface of the part leading to a hardness gradient. Materials are carburized to increase the surface hardness, wear and fatigue resistance [37][38][39].

There are some variants of carburizing but the most used is gas carburizing. This type uses a carbon rich furnace atmosphere produced either from gaseous hydrocarbons, for instance, methane, propane and butane or from vaporized hydrocarbon liquids [37].

Liquid carburizing can be also used and the carburizing is conducted at 840-890°C to have <0.75 mm of thickness carburized and 900-950°C for a thickness up to 3 mm [40].

2.8.1.2 Nitriding

Gas nitriding is a thermochemical heat treatment process used to hardening the surface. This process introduces nitrogen in the steel surface layer. High surface hardness (between 1000 and 1200 HV) promotes the wear and scuffing resistance that also increase the fatigue strength due to surface compressive stresses. This nitriding layer has some tenths of millimetre [41].

Parts are first heat treated and machined then exposed to active nitrogen under a controlled temperature range (496 to 529°C). This temperature shall be less than the tempering temperature of steels for the process does not affect substantially the base metal mechanical properties or the dimensions. Higher temperatures also can promote the formation of a eutectoid constituent between iron and nitrogen, very brittle, and decrease the nitriding layers properties. To avoid hardening in some areas, the part can be masked to easily be machined after nitriding [41][42][43].

2.8.1.3 Carbonitriding

Carbonitriding is more a modified form of gas carburizing than a nitriding form. The goal is to introduce carbon and nitrogen in the steel surface layer. The simultaneous introduction of carbon and nitrogen creates a harder superfici layer than the carburizing layer. This process is conducted introducing ammonia into the gas carburizing atmosphere to add nitrogen. Nitrogen is formed at the work surface by the dissociation of ammonia in the furnace atmosphere and diffuses into the steel with carbon [37][44].

The temperatures used in this treatment lie between 550 and 900°C forming carbonitring layers with 0.075 to 0.75 mm of thickness with hardness between 1000 and 1200 HV [44].

2.8.1.4 Flame hardening

This process consists of austenitizing the steel surface by heating with an oxyhydrogen or oxyacetylene torch followed by quenching in water or polymer solution. This process results in a martensitic hard surface layer. There is no change in composition, so the steel should have adequate carbon content for the flame hardening be effective. It is limited to steels such as medium-carbon, and medium carbon alloyed [35].

The process is generally applied for very heavy cases, in the range of approximately 1.2 to 6 mm, because for thin cases depths are difficult to control [35].

2.8.1.5 Induction hardening

Induction hardening is an electromagnetic process for hardening the surface where the components are heated above the transformation range followed by immediate quenching. The parts are placed inside a copper coil where a current is applied to induce an alternating magnetic field within the workpiece. This causes the outer surface to harden and enhance the mechanical properties in a ferrous component localized area. This process is suitable for components that are subjected to heavy loading and surfaces that experience impact loads [45]. Carbon steels containing more than 0.4% carbon are usually used for induction hardening [2].

2.8.1.6 Laser hardening

In this hardening process, a laser beam warms the outer layer to between 900 and 1400°C depending on the material. The temperature should reach to just under melting point then the laser beam starts moving. The heat causes the iron atoms to change their position and when the laser beam moves, the surrounding material cools down the heated surface, this calls self-quenching. Rapid cooling produces a martensitic structure which is very hard. The advantages with this process are the abilities to process irregular and difficult areas on the workpiece and require less refinishing work and reduce therefore the costs [46]. Laser hardening is used in carbon steels with more than 0.4% carbon and in low alloyed steels with good hardenability [35].

2.8.1.7 Comparison between hardening processes

Different surface hardening methods have different hardening depths, as can be seen on Figure 2-24.

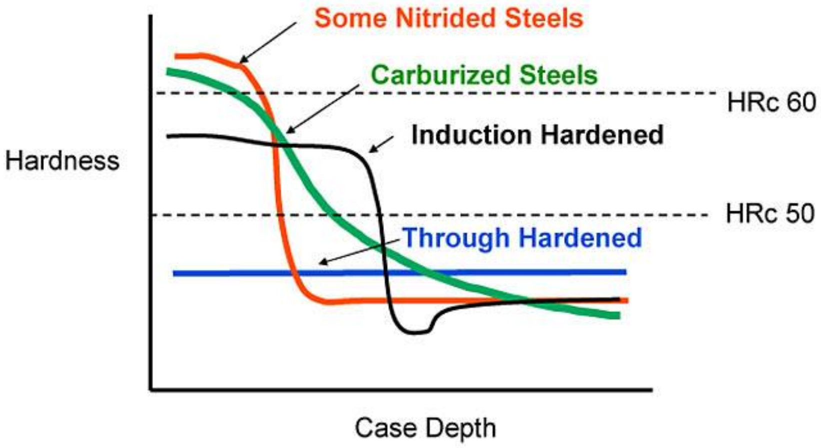

Figure 2-24. *Typical gear tooth hardness profiles, where HRc 60 is a hardness measurement on the Rockwell C scale* [47]**.**

2.8.2 Bulk heat treatments

Bulk heat treatments are applied in steels to accomplish two goals: decrease mechanical strength but increase ductility to improve the workability of steel (like machinability for instance) or increase mechanical strength with loss of ductility to achieve high performance. In some cases, it is possible to increase mechanical strength and keep good ductility like ausferritic cast steels as example. In some cases, heat treatments, like solution annealing, are applied in order to improve physical properties as corrosion.

Following will be presented the most common heat treatments applied to cast steels: solution annealing, normalizing, quenching, tempering and austempering.

2.8.2.1 Solution annealing (+AT)

Solution annealing is normally applied in austenitic cast stainless steels to prevent alloy sensitization. The treatment is composed by holding time at high temperatures in the range of 1040 to 1205°C in order to dissolve the carbides, followed by severe cooling to prevent carbides re-precipitation. Normally, the solution annealing heat treatment is followed by an aging treatment in order to promote a fine dispersed precipitation of carbides, improving creep resistance [17].

2.8.2.2 Normalizing (+N)

Normalizing is usually applied in order to improve machinability, grain-structure refinement, homogenization and decrease the residual stresses. This heat treatment also provides a better response to further heat treatments and refines the dendritic structure in castings. The temperatures of normalizing are between 880 and 980°C and the cooling should be done in still air [48].

2.8.2.3 Quenching (+Q)

Quenching is the process of austenitization at temperatures typically in the range of 815 to 870°C followed by cooling, fast enough to prevent pearlite and bainite formation [49].

The holding time at austenitization temperature should be the lowest possible, to avoid the austenite grain growth. This holding time aims to ensure the dissolution rate necessary of carbides into austenite and formed austenite homogenization [49].

The initial microstructure has influence in the holding time. It is beneficial to have an initial normalized microstructure, being thin structures allow a quick homogenization, decreasing the holding time at high temperatures and give the possibility to obtain an austenite with small grain size [49].

2.8.2.4 Tempering (+T)

As-quenched steels are too brittle to enter directly in service. Tempering is a heat treatment applied in order to improve ductility and toughness of quenched steels. The process consists of reheating the steel after quenching heat treatment to obtain the mechanical properties required, release stresses formed during quenching and to ensure dimensional stability. Tempering can also be used to relieve stresses and reduce hardness developed during welding and machining operations [50].

Usually, tempering is conducted at temperatures in the range of 175 to 705°C and for times from 30 min to 4 h [50].

2.8.2.5 Austempering

Austempering is defined as a steel alloy isothermal transformation at a temperature between pearlite and martensite formations. The steel austempering includes some potential advantages such as increased ductility, toughness and strength for a given hardness, reduced distortion, scrap and energy savings, due to the short overall time cycle to harden thoroughly [51][12]. It is a one step reaction where the austenite directly decomposes into acicular ferrite and carbide (bainite). Under lower temperatures, the distribution of carbides is finer, the ferrite needles thinner and the product is called lower bainite. Using higher transformation temperatures, the product obtained is upper bainite composed by lath or plate-shaped ferrite with packets and interlath carbide precipitates. Regarding the steel, lower bainite produces higher yield strength but lower toughness [12].

New developments are in the basis of a new third generation of advanced high strength, high toughness steel [52]. These steels were designed using austempered ductile iron (ADI) concepts [12].

For ADI the austempering transformation can be divided in two stages, first the austenite decomposes into ferrite and high carbon austenite is retained and after a long time, the second stage comprises the transformation of high carbon austenite into ferrite and carbide. This causes an iron carbide dispersion in a ferritic matrix [12].

When silicon or aluminium are added to steel in certain amounts (exceeding 2%), a special microstructure containing bainitic ferrite fine plates separated by high carbon austenite thin films is formed. The second bainitic transformation reaction is retarded due to silicon steel content and an unique ausferritic microstructure is possible to obtain without carbides [12]. The Figure 2-25 shows an austempering heat treatment (dashed line) in a TTT diagram. From Figure 2-25, it is possible to oberve that the transformation ($\gamma \rightarrow \alpha + \gamma_{HC}$) has stopped before the second stage ($\gamma \rightarrow \alpha + C$) start.

The austempering process consists of heating at austenitization temperature, normally between 790 to 915°C, depending on the alloy, quenching in a bath kept at constant temperature, usually in the range of 260 to 400°C, allowing the isothermical transformation of austenite followed by cooling to room temperature [51].

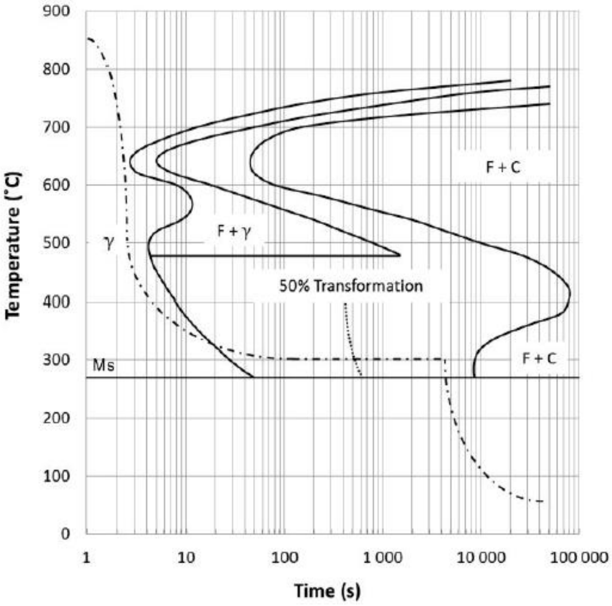

Figure 2-25. *Temperature time transformation (TTT) for 0.55C-1.62Si-0.78Mn-0.77Cr steel. The dashed line represents austempering heat treatment* [53].

2.8.3 Main defects caused by heat treatments

Quenching is the most critical heat treatment applied in steels because normally requires high cooling rates and consequently exaggerated thermal shocks that can originate defects. The main defects caused by this treatment, causes and consequences are described in Table 2-10.

Other defects can appear in different heat treatments when not conducted on the right way. Intergranular corrosion can occur in some stainless steels if the heat treatment applied (solution annealing) was incorrect and allow chromium rich carbides precipitation on the grain boundaries.

Scania has STD4100 *Defects in castings – Cast iron and cast steel* which deals with casting defects. There is an ongoing feasibility study for a new SIS standard for defects in steel castings [54].

Table 2-10. *Main defects in steel castings heat treatment* [32][49].

	Defects	**Causes**	**Consequences**	**Recover**
1	Presence of a ferritic matrix fraction	Austenitization temperature not enough	Lower hardness	Annealing and quenching again with the correct austenitization temperature
2	Coarse grain of austenite, more brittle	Exaggerated austenitization temperature	Higher deformation, crack initiation	The same as 1: if cracked, part becomes scrap
3	Burned piece, melting of the grain boundaries, growth of austenitic grain, stabilization of austenite and martensite transformation more difficult	Too exaggerated austenitization temperature	Lower hardness, crack, early fractures	Part becomes scrap
4	Descarburization; Superficial layer of austenite with lower carbon	Heat treatment without protective atmosphere	Lower surface hardness but as predicted in the core	The same as 3
5	Heterogeneous austenite, no time for carbon alloyed elements diffusion	Heating rate too fast	Hardness too irregular	Annealing and quenching again with an appropriate heating rate
6	Carbon diffusion during cooling is not avoided, may originate pearlite or bainite	Cooling rate too low	Lower hardness	Annealing and quenching again with an appropriate cooling rate
7	Thermal shock too high	Cooling rate too fast	Higher deformation and cracking	The same as 6; if cracked, part becomes scrap

2.9 Machinability

Machinability is a term which tells how ease a material can be machined (machining, drilling, milling, *et cetera*) to achieve adequate shape and desirable surface finish. A material with good machinability will be easy to process and will require little power to cut and does not wear excessively the tools. These materials are called free machining materials [55].

Many factors will influence the machinability and factors that improve the material performance often reduce the machinability. It can be difficult to predict the machinability due to the work material condition that includes eight factors: microstructure, grain size, heat treatment, chemical composition, fabrication, hardness, yield strength, and tensile strength [56].

2.9.1 Machinability Index

Machinability of different materials can be compared by machinability index which is defined as [57]:

$$\textit{Machinability index} = \frac{\begin{array}{l}\textit{Cutting speed of metals for}\\ \textit{20 minutes tools life}\end{array}}{\begin{array}{l}\textit{Cutting speed of a standard}\\ \textit{steel for 20 minutes tool life}\end{array}} \tag{2}$$

When comparing machinability, different materials are cut under the same conditions to compare power required, tools life surface and finish *et cetera*. Heat treatments affect the machinability. Normalizing processes increase the machinability because it reduces the hardness or stabilize the microstructure, whilst quenching and hardening processes decrease the machinability since the processes harden the material [57].

The machinability can be improved by adding sulphur for example. Methods like heat treatment, use of proper coolant, making use of quality tools, improving microstructure of the material or hot working alloy will also improve the machinability [57].

2.9.2 Relative machinability

Alloying elements, heat treatments and manufacturing processes (forging, casting, *et cetera*) will affect the stainless steels machinability. Higher alloying elements content decrease in general the machinability.

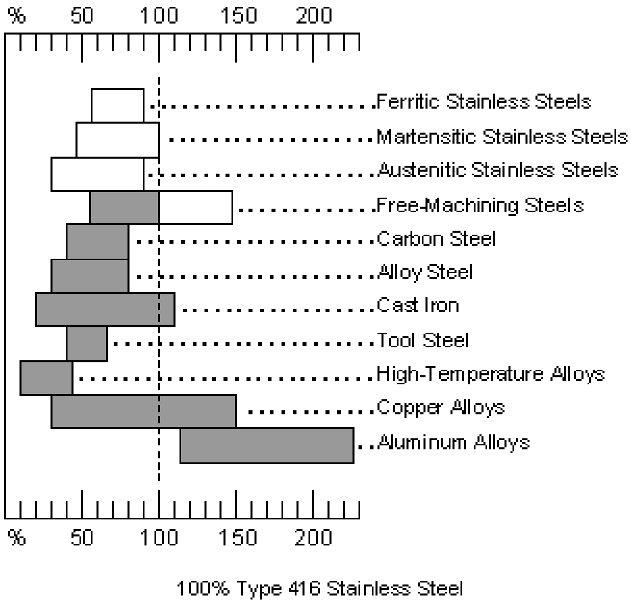

Figure 2-26. *Comparative machinability of common metals* [58].

The hardness of the material will determine the cutting speed, the cutting feed and the depth of cut. The recommended cutting speed must be multiplied by a factor obtained from Figure 2-27 if the hardness differs from the Coromant Material Classification (CMC) code [59].

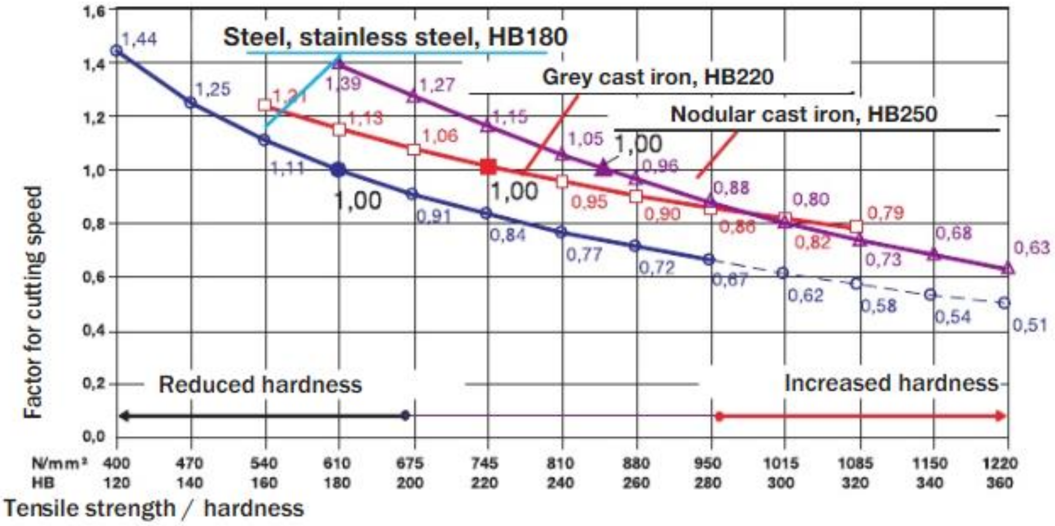

Figure 2-27. *Diagram comparing the hardness and factor for cutting speed* [59]**.**

For example HK30, presents a hardness in as-cast state of HB 180. After solution annealing followed by aging, the hardness increased up to HB ~230. The recommended cutting speed will be reduced by 20% to compensate the increased hardness. The cutting speed should be adjusted with a factor 0.80 as shown in Figure 2-27 [59].

2.10 Welding

Welding is a joining process to fuse metal components together with pressure or heat applications.

In Guideline - Simulation driven design of optimized sheet metal bracket at Scania states that *"Welding is good for statically loaded structures, such as load-bearing structures in buildings that only burdened by the gravitational field where the weld has the same strength as the base material. For Scania articles that are affected by dynamic loads welds are not good when their fatigue strength is significantly reduced relative to the static resistance. The weld fatigue strength is considerably lower for high cycle fatigue, i.e., more than 100 000 cycles, than for static strength. The weld static strength is basically the same as the base material"*, see Figure 2-28 [60].

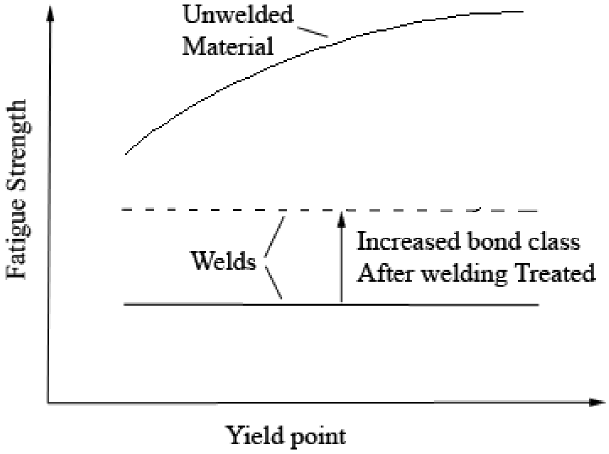

Figure 2-28. *Fatigue strength versus yield point in the weld* [60].

2.10.1 Welding process

A heat source will create a liquid weld pool in the fusion zone. The area around the fusion zone will be affected by the heat from the procedure and this zone is called heat affected zone (HAZ), see Figure 2-29 [61].

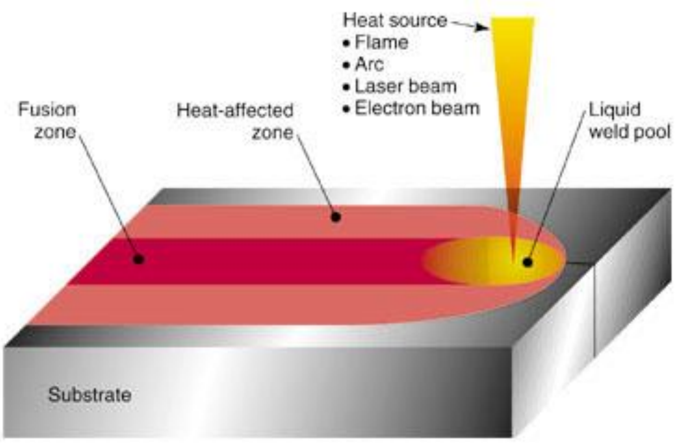

Figure 2-29. *A schematic diagram showing the welding process* [61].

A thermoplastic process in the base metal occurs in the formation of a welded joint. For welded steel structures, this causes brittleness in the HAZ that can exhibit a limited resistance to failures. Figure 2-30 shows the different formations in the heat-affected zone.

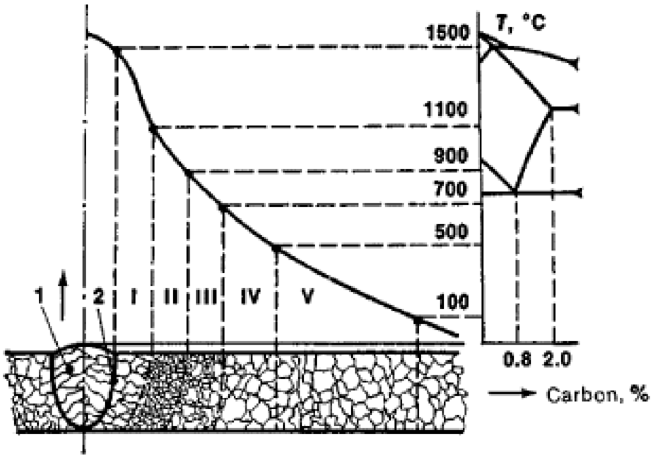

Figure 2-30. *The diagram shows the different formations in the heat-affected zone; (I) overheated section, (II) grain-refined (normalized) section, (III) partially grain-refined section, (IV) recrystallized section, (V) aging section; (1) weld metal, (2) fusion zone* [62]**.**

The components being joined by welding methods will be reduced in dimension, both in longitudinal and transverse direction. The shrinkage and the effect from the welded zone must also be considered when choosing welding method [62].

High-temperature rupture and creep strength characteristics can be affected by welding operations [63].

2.10.1.1 Choice of methods

The microstructure in the weld zone will be different depending on steel classification. The properties from the diluted metal will be determined by the chemical composition.

The Schaeffler diagram allows predict the expected structure that can be obtained and shows an indication of the ferrite-austenite balance for different compositions, see Figure 2-31. Through the equations in Figure 2-31 the Schaeffler diagram can be read.

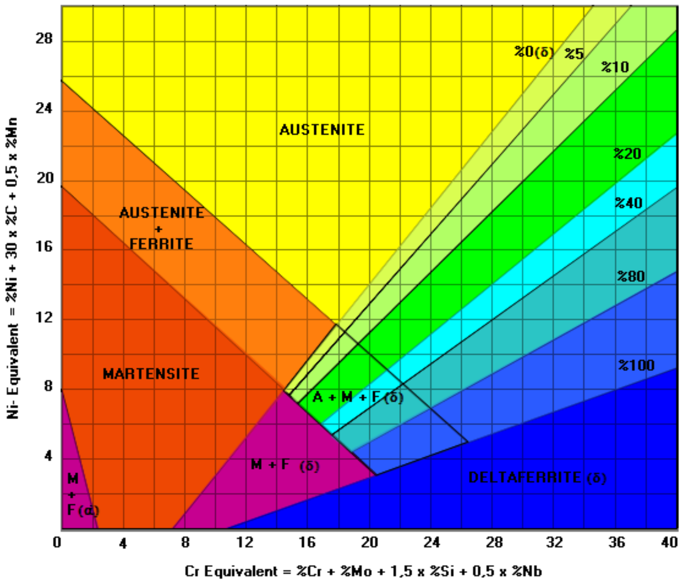

Figure 2-31. *A Schaeffler diagram shows the limits of the austenitic, ferritic and the martensitic phases in relation to the chromium and nickel equivalent* [64].

Regarding the Schaeffler diagram, ferrite levels can be predicted from the composition by comparing the effects of austenite and ferrite stabilising elements. This is important since ferrite is less prone to hot cracking. Knowing the composition, we will make the choice of welding methods easier.

2.10.1.2 Welding methods

A variety of welding methods are used for structural connections. The most common welding method is MAG welding and one of the reasons for this is that it is very easy to automate.

In order to fulfil the requirements of welded joint tensile strength it is important to pick the right method and filler material, so the HAZ will be effected as little as possible.

Table 2-11. *Common welding methods* [65]**.**

Welding method	Possible problems*	Solution (before pickling)
MMA (SMAW)	Slag inclusions, tarnish (heat tint)	Brushing (grinding)
MIG, MAG (GMAW)	Heavy bead oxidation, slag inclusions, spatter	Grinding (brushing)
TIG (GTAW)	Small slag islands ("black spots"), Tungsten inclusion	Grinding (if possible)
SAW	Sometimes slag inclusions	Brushing (grinding)

*Depending on filler metal, welding position, overheating, gas mixture, etc.

Table 2-12 shows the same design considerations for the different welding methods used on cast steels.

Table 2-12. *Design considerations for different welding methods on steels* [66].

Welding method	Thickness min. [mm]	Thickness max. [mm]	MWR [mm]	Tolerances [mm]	Unequal thickness
MMA (SMAW)	1.5	200	≥ 10	± 1.0	Difficult
MIG, MAG (GMAW)	0.5	80	≥ 5	± 0.5	Possible
TIG (GTAW)	0.2	6	≥ 5	± 0.5	Difficult
SAW	5.0	300	≥ 40	± 2.0	Very difficult

2.10.1.3 Carbon equivalent

Equivalent carbon content formula was developed to give a numerical value for a steel composition where its carbon content contributes to the hardenability of that steel.

Generally, the cracking trend during welding is controlled by the carbon equivalent. Higher carbon content means higher strength, but lower weldability and machinability [67].

Mathematical formula for carbon equivalent is as follows [67]:

$$C_{eq} = \%C + \frac{\%Mn}{6} + \frac{\%Cr + \%Mo + \%V}{5} + \frac{\%Ni + \%Cu}{15} \tag{3}$$

The carbon equivalent will give the weldability of steel, see Table 2-13.

Table 2-13. *Carbon equivalent levels to compare the weldability* [68].

Carbon equivalent (CE)	Weldability
Up to 0.35	Excellent
0.36-0.40	Very Good
0.41-0.45	Good
0.46-0.50	Fair
Over 0.50	Poor

Certain element content will affect the weldability, preferred and maximum weight percent can be seen in Table 2-14.

Table 2-14. *Preferred and maximum weight percent content of some elements* [69].

Element	Composition	
	Range for satisfactory weldability [%]	Minimum Level requiring special care [%]
Carbon	0.06 to 0.25	0.35
Manganese	0.35 to 0.80	1.40
Silicon	0.10 or less	0.30
Sulphur	0.035 or less	0.05
Phosphorus	0.030 or less	0.04

It is possible to weld steel with high carbon equivalent through alternative ways such as preheating, altered joint geometry or with special electrodes. SS-EN 10293:2005, Annex A, gives guidance data for steel castings welding for general engineering uses with pre-heat temperatures and suggestions for post weld heat treatments.

2.10.1.4 Weldability

When selecting steels, engineers usually select the specific steel based on mechanical properties. The steel chemistry sets the terms of weldability, which describes how easily the steel can be welded. Almost all steels can be welded but not with the same degree of ease. Cost and weight savings can be made with weldable steels.

When welding, the base metal temperatures will rises up in which a microstructural transformation occurs. The changes and their effect on the finished weldment depends upon alloy content, thickness, filler material, joint design, weld method and welder skills. The aim when welding stainless steels is a joint with qualities equal to the base material or even better.

Weldability of Stainless steels

Stainless steels weldability varies strongly with the chemical composition and structure. A first rough distinction of weldability can be seen in Table 2-15.

Table 2-15. *Stainless steels weldability* [68].

Type of Steel	Weldability
Austenitic	Good – very good
Ferritic	Relatively good
Martensitic	Poor
Martensitic-austenitic	Relatively good
Ferritic-austenitic	Relatively good – good

There are many welding processes to choose between, if one method does not work maybe another will, but common to all methods is that the joint surfaces and any filler materials must be clean to avoid weld imperfections.

Weldability of Austenitic stainless steels

Austenitic stainless steels have austenite as its primary phase and contain chromium and nickel.

Austenitic steels are not hardenable by heat treatment. These cast steels are the most weldable within the high-alloy steels group. They can be welded by all fusion and resistance welding processes. About 80% of the stainless steel welded is austenitic type [70].

In fully austenitic structures weld metal solidifications cracking also known as hot cracking might appear. The presence of 5-10% ferrite is extremely beneficial as a ferrite is less prone to this type of cracking. The filler material composition is crucial in restrain the risk of cracking [71].

CF-8 is a cast stainless steel and may be welded by the shielded metal arc welding (SMAW), gas tungsten arc welding (GTAW also called TIG) and gas metal arc welding (GMAW so-called MIG or MAG) processes [72].

HK, HN alloys have good weldability. They can successfully be welded by the SMAW, GTAW and GMAW processes using filler metal of matching composition [72].

Weldability of Ferritic stainless steels

Ferritic stainless steels can be considered to be predominantly single phase and non-hardenable. They can be welded with fusion welding to join materials of similar compositions and melting points. Hot cracking is a major risk if the ferritic steel contains significant sulphur content. Fillers with sufficiently high niobium content can prevent this [71]. Niobium and/or titanium also can be used to stabilize the steel, preventing chromium carbides precipitation which could promote intergranular corrosion after welding. These elements combine with carbon and nitrogen leaving the chromium dissolved in the matrix. Besides this, these elements act as a grain growth controllers which also improve the weldability of these alloys, reducing cracking risks. These elements should be used in the minimum amounts necessary to stabilize the material, because higher amounts could be detrimental in terms of toughness [73].

The main problem when welding ferritic grades is poor HAZ toughness because it is coarse grained which can lead to cracking in thick section material or highly restrained joints. Thinner section materials less than 6 mm will not need any special precautions. In thicker sections it is necessary to minimize the width of the grain-coarsened zone. This can be done with low heat input and an austenitic filler will produce a tougher weld metal. Material preheating will decrease the HAZ cooling rate and also reduce residual stresses, by keeping the weld metal above the ductile-brittle transition temperature [71].

CC-50 alloy, equivalent to cast grade 446 (wrought), or HC grades for high temperature applications, may be welded by the SMAW and GTAW processes, but is considered difficult to weld [74].

Weldability of carbon steels

The weldability of carbon steels are very good, if the carbon is less than 0.25% and the sulphur and phosphorus contents are less than 0.04% [75]. Carbon steels welding does not encounter any big problem and produces quality welds. The basic carbon steels properties will not be changed by heating to melt or to weld. Carbon steels are easily welded by any arc (Covered electrode, TIG, plasma arc, MIG, Submerged arc), gas or resistance welding processes.

2.10.2 Defects in welds

Weld imperfections are flaws that compromise with the welds serviceability. It can be irregularity or discontinuity in a weld which may affect in a negative way.

The most commonly imperfections in welds are [76]:

- Porosity
- Solidification cracking (hot cracking)
- Hydrogen cracking
- Reheat cracking
- Slag inclusion
- Tungsten inclusion
- Fulfilling defect
- Lack of fusion
- Incomplete penetration

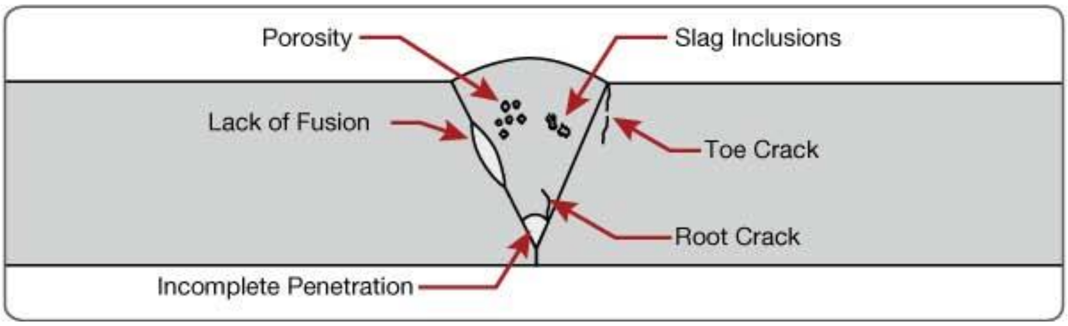

Figure 2-32. *Some of the most commonly flaw types that can be found during welding processes* [76]**.**

2.11 Castings after treatment

2.11.1 Surface treatment

There are some typical surface defects occurring in castings for different reasons. Heat tint and oxide scales are caused by processes such as heat treatments or welding and will affect the castings oxidation resistance. Other weld defects like pores, slag inclusions and incomplete penetration, may also require surface treatment to restore the oxidation layer protecting the surface.

A rough surface increases both the risk for corrosion and product contamination by collection deposits and reduces the fatigue strength. Different casting methods varies in surface roughness (R_a value), but also cleaning treatments like grinding or sand blasting will affect the surface roughness and rough surfaces should generally be avoided. Organic contamination occurs whenever the castings are machined or in other way handled. The contamination can be in the form of grease, oil, dirt and remains of paint, glue and fingerprints. All this can cause crevice corrosion in aggressive environments [77].

Therefore it is important restoring the surface with a cleaning process. Depending on quality and environment, pitting corrosion and galvanic corrosion are both quite common. The incubation period for these types of corrosion can vary from a few hours to many months. This local corrosion can have devastating effect on a construction and some surface treatments are needed to prolong the component life [77].

2.11.1.1 Sand blasting and shot blasting / Shot peening

Sand blasting can be used to remove high temperature oxides, iron contaminations and burnt sand from steel and stainless steel castings. Sand particles are thrown into a compressed air stream, being shot at high speed against the workpiece, having as main task to clean the surfaces [78], preparing the surface for painting or coating and can also have a positive influence on the mechanical properties, increasing the fatigue strength and stress corrosion resistance [79].

When workpieces are shot penned, the surface is bombarded with high quality media of steel, stainless steel, glass or ceramic [80]. Shot peening may remove oxides, but is primary used to convert surface stresses to compressive stress improving the fatigue strength and prevents stress-corrosion cracking (SCC) [73].

Figure 2-33. C*omponent before (to the left) and after (to the right) shot peening* [81]**.**

2.11.1.2 Steel degreasing

Organic contaminations like dirt, grease and oil must be removed before any chemical cleaning treatment or as a prelude to surface finishing. This is necessary to achieve overall access to the workpiece and avoid irregular pickling. The contaminations will be removed with a non-chlorinated solvent [77].

2.11.1.3 Pickling

Pickling is a surface treatment for metals to remove impurities in the surface in heat treated and welded stainless steel (Figure 2-34). The main ingredients for the stainless steel pickling are hydrofluoric acid (HF), nitric acid (HNO_3) and water. Pickling removes oxides, residues from grinding wheels, abrasive belts, any iron impurities and abrasives from the stainless steel surface [82].

At room temperature, the pickling time can be from 30 minutes to several hours, depending on the heat tinting darkness to be removed and the metal contaminants concentration on the bath. The easiest way is with a pickling bath but the pickle can also be applied as a paste. For larger areas spray pickling and circulation pickling can be used. A steel etch can occurs as a side pickling effect, affecting a few micron thickness, which can promote some accuracy concerns and/or increase the steel surface roughness [83].

Ferritic and martensitic steels are easier to pickle and need less time than austenitic and austenitic-ferritic (duplex) steels to avoid the overpickling risk. They can also need a less aggressive acid content in their pickling bath [65].

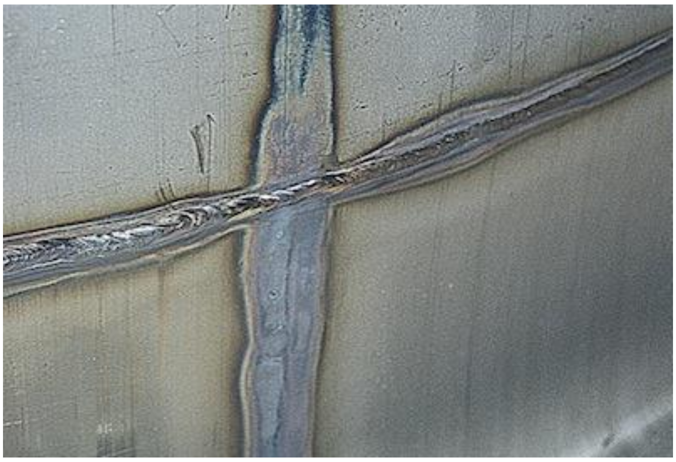

Figure 2-35. *A heat tinting that shall be removed and the easiest way to do this is by pickling process* [65].

2.11.1.4 Grinding and polishing

Grinding and polishing are processes by which surface layer is removed from an object to produce a fine surface finish (Figure 2-36). Coarse grinding is generally performed with 80-120 grit papers, followed by fine grinding with 240-600 grit papers. Thereafter a polishing with rotating disks can be performed covered with napless cloth, impregnated with diamond dust pastes or other slurries with different particle sizes [84].

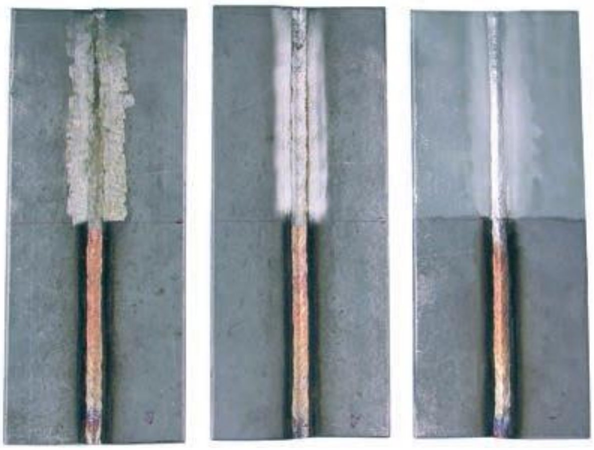

Figure 2-37. *Appearance of different cleaning methods. Grinding to the left, polishing in the middle and pickling to the right* [77].

2.11.1.5 Passivation

The passivation process improves and purifies the component surface and is often used after machining, for example. This process restores the passive film, back to its original specifications by removing dirt and grease.

Passivation usually occurs naturally on the stainless steels surfaces. So this process may not be needed to improve the corrosion resistance, if the component has been properly pickled [77].

The passivation process also contains a bath but here it is only nitric acid (HNO_3) for about one hour. This process will not affect the surface roughness [83].

2.11.1.6 Paint coatings

The most common way to protect steel is by painting the surface, and like painting wood, the preparation steps are the most important. If the surface is too smooth there might be needed to roughening it up before coating. This can be achieved by shot peening, light hand abrasion or chemical etching. The surface must be clean and free from rust, grease and other foreign materials using organic solvents, for example acetone [85].

2.11.1.7 Thermal barrier coating

Thermal barrier coatings (TBC) are advanced material systems applied to metallic surfaces that operate at elevated temperatures. These coatings insulate components from heat loads and allow higher operating temperatures. The thermal exposure will be limited, reducing oxidation and thermal fatigue that will extend the part life. This exhaust heat management reduces heat loss from the engine exhaust system components [86].

Thermal barrier ceramic coatings are becoming more common in the automotive applications due to the protection from oxidation, corrosion and thermal fatigue. The TBC is built in different layers, all with its own function. First there is the super alloy substrate with physical properties needed to be matched to form a robust TBC. Then there is the metallic bond coat (BC) that will improve the contact between substrate and the top coat. It will also protect the substrate from oxidative and corrosive attacks [87]. The top coat is a ceramic layer in different thicknesses depending on the working conditions. A common top coat is yttrium-stabilized zirconia (YSZ) applied via plasma spraying [86]. During service a thermal growth oxide (TGO) layer occurs between the top coat and the bond coat, see Figure 2-38 [88].

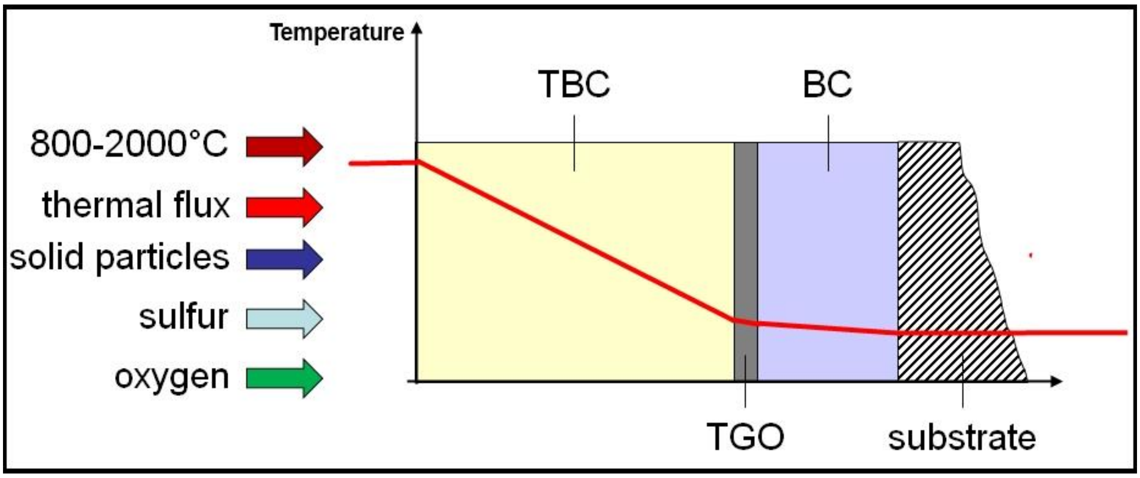

Figure 2-38. *Thermal barrier schematic structure coating and corresponding temperature profile* [89].

It is difficult to prepare the internal surface of exhausting systems and problems have been found with some TBC [86].

In master thesis STR7026701, tests on five different TBC for SiMo51, D5S and HK30 has been conducted [90]. These kinds of TBC can improve the fatigue life as well as fuel savings among other, see Table 2-16.

Table 2-16. *Improvements that can be achieved through TBC use* [91].

Benefit	**Change percentage [%]**
Fuel savings	11
Engine life extension	20
Power output increase	10
Reduction of emission	20-50
Reduction of particulate	52
Lubricating oil savings	15
Maintenance cost reduction	20
Exhaust valve life extension	< 300
Reduction of component temperature	< 38°C

3 Practical work

3.1 Compile a cast steel guideline

This master thesis aims to compile a guideline, STR7030111 *Cast Steel Guideline* and this work will take place after the completion of this report. Some reference material has been use in addition to the literature studies in form of STR7019798 – *Guideline för design av gjutna & smidda komponenter:* version 1.

3.2 Introduction to Materials Selection

One of the goals of this work besides produce a cast steel guideline, was studying the possibility to use cast steel effectively to produce two truck components: a turbo manifold and a bracket.

3.2.1 Challenges of the components

All components are exposed to different mechanical loads and environments. This puts some challenging requirements to the Design Engineer in material selection, especially facing the coming Euro 7 legislation.

For example turbo manifolds are exposed to new challenges. The exhaust system endures high gas temperatures, and cyclic thermal strains put high demands on the thermal fatigue life of the system. It is also a highly corrosive environment caused by condensation of exhaust gases during the engine cooling. This set extremely high requirements on the selected material.

Brackets are under cyclic loads, therefore the material must have high fatigue resistance to avoid fatigue failure. To achieve weight reduction without risking safety requirements, higher strength and fatigue resistant material is needed. However, mechanical properties are not the only constraint that needs to be fulfilled regarding cast materials. Other properties like castability, minimum section thickness, tolerances and maximum size of the casting needs to be analysed. Even a strong material must be designed to minimize fatigue failures in high risk areas, such as welded parts, holes, sharp radiuses and in materials accumulations. To protect against corrosion and improve fatigue resistance, coatings and surface treatments must be considered.

3.2.1.1 Heat resistant cast manifolds

The turbo manifold collects the exhaust gas produced by engine. The exhaust system is exposed to high temperatures with repeated thermal strains due to the continuous start-up and shut-down operating conditions. During the start-up, a thermal expansion introduces compressive strain and tensile strain is applied during shut-down. This produces a cyclic stress similar to low cycle fatigue (LCF). Life predictions and overall assessment of the component performance can be predicted by LCF test where mechanical strain, tension and compression are exerted under isothermal testing conditions [92].

Thermal fatigue stress is the most common reason why cracks appear in turbo manifolds [93].

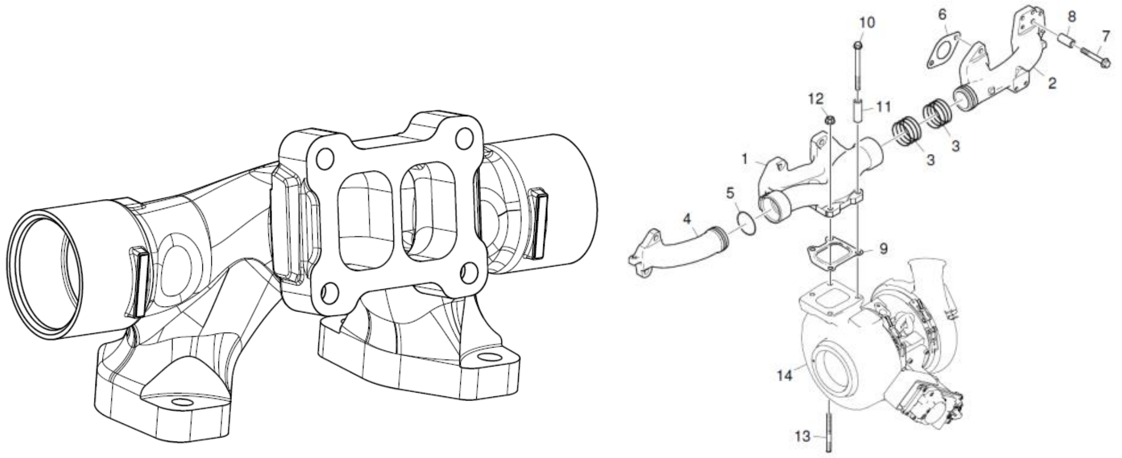

Figure 3-1. *Turbo Manifold and the assembly view of the exhaust system.*

The turbo manifolds at Scania are mostly made by ferritic spheroidal graphite iron (SiMo51). Ni-resist D5S is used for Otto-engines.

SiMo51 is working close to its limiting exhaust temperature. So, the study of other materials for turbo manifolds that can be used in more severe conditions keeping high durability and reliability of the component is necessary [4].

The turbo manifolds, Figure 3-2, is a double channel compound, subjected to high loads in part due to the mass flow of exhaust gases and also to the additional load from the weight of the turbo charger [4].

The design of this component should take into account properties like creep, corrosion and thermal fatigue and oxidation resistance [4].

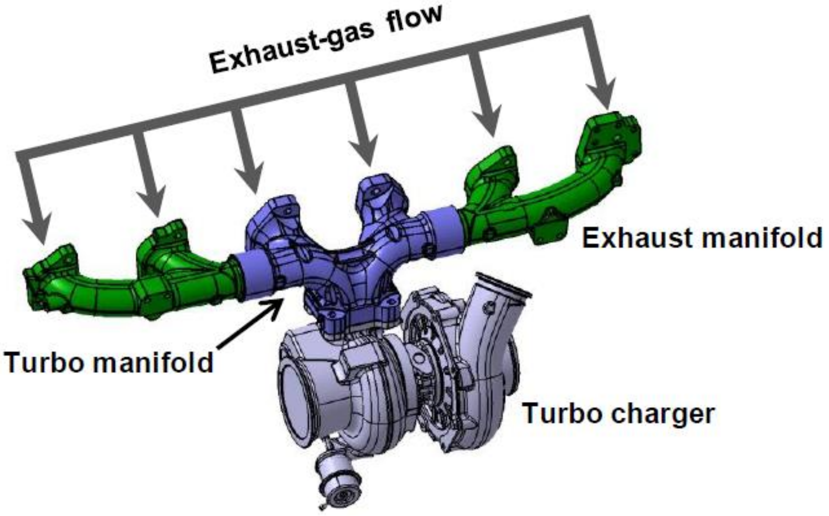

Figure 3-2. *Schematic description showing a turbo manifold attached to a turbo charger and connected to exhaust manifolds* [4].

Creep resistance

Creep is a time-dependent strain that occurs under load at elevated temperatures. When temperatures overcome 480°C, creep starts to be relevant. With time, creep may cause excessive deformation or even fracture at stresses below those determined in room-temperature and elevated-temperature short term tests [17].

When the deformation rate is the constraint factor, the design stress is based on the minimum creep rate and required life time of the component. The stress that causes a specified minimum creep rate of a material or a specified amount of creep deformation in a given time, 1% total creep in 100,000 h for instance, is named as the limiting creep strength or limiting stress [17].

When the rupture is the limiting factor, stress to rupture values are used in components design [17].

The highest creep resistance is provided by the austenitic grades of the different kinds of stainless steels available [17].

One thing that has a detrimental effect on the materials performance in service at high temperatures is the creep-fatigue interaction. For temperatures high enough to cause creep strains and when cyclic strains are present, both may interact. Creep strains may seriously reduce fatigue life [17].

Corrosion fatigue resistance

Corrosion fatigue is the result of the cyclic loading and a corrosive environment combined synergistic actions. It is a discontinuous process in which crack initiation and growth take place during transient periods [94].

The exhaust gas temperature can be as high as 950°C. One problem with rising temperatures, among many, is the high temperature corrosion. Nitrogen oxides (NO_x) are compounds of nitrogen (N_2) and oxygen (O_2). This oxide is produced by high pressure, high temperature and an oxygen overflow in the engine during the combustion cycle. With more effective engines, higher temperatures are produced, the nitrogen oxide concentrations in exhaust emissions rises as well [95].

Ferritic grades have low ultimate tensile strength at temperature above 800°C compared to austenitic grades. They show good cyclic oxidation properties and low thermal expansion coefficient, therefore lower levels of stress induced by a thermal cycle are presented in ferritic grades than in austenitic grades. The difference in thermal expansion coefficient between the grades of ferrite and austenite is not enough to explain the thermomechanical fatigue (TMF). The connection between creep and oxidation seems to be the fundamental factor for the damage process especially where stress tensile state occurs at higher temperature [95].

Condensation of exhaust gases may occur during cold start or engine cooling, resulting in acid liquids covering the inner surfaces of the manifolds, affecting oxide scale and metal underneath. Penetration into the oxide scale through pores and cracks by condensed liquid may occur, contacting the metal surface and starting corrosion reactions, both at low and high temperature. The depletion of the alloy can cause corrosion reactions consuming the metal [4].

Fatigue resistance – thermal cycling

The manifolds are exposed to thermal cycling during service, as referred before, causing fatigue damage. This thermal cycling may induce stresses producing elastic or plastic deformation of the oxide scale formed on the material surface. During a long time exposure, this may cause fracture and oxide spallation resulting in both more material oxidation and oxide flakes transference at high velocity into the turbo charger. Thermal induced stress effect depends on the ratio between bulk material thermal coefficient and oxide scale, which depends on the temperature range [4].

Austenitic stainless steels (e.g. HK), seems to have higher spallation ability due to larger thermal expansion difference (ratio of 2.56) than in the ferritic alloys (e.g. SiMo51) (ratio of 0.92). However, not just the expansion coefficient should be considered, but also the oxide scales thickness. Thick scales have higher tendency for spalling, so chromium scales (formed in high chromium cast stainless steels) may be more favourable to prevent spallation than iron scales [4].

Oxidation resistance

There are two chemical reactions to consider in the corrosion process: reduction and oxidation. Reduction occurs when oxygen is withdrawn from the exhaust gas components and oxidation when oxygen is added to the exhaust gas [95].

The most frequent causes of high temperature corrosion in stainless steels are oxidation reactions [17].

High temperature stainless steels are designed in order to have the ability of producing a protective oxide scales. Stainless steels resist oxidation mainly because of their content in chromium, which has the ability to produce a protective chromium oxide layer (Cr_2O_3). Increasing nickel content decreases scale spalling, when temperature cycling is present, like in heavy-duty engines [17].

3.2.1.2 High strength brackets

The brackets, in Figure 3-3, are components of the rear air suspension system. Nowadays, Scania uses a ductile cast iron to produce this component.

The purpose of air suspension is to provide a smooth, constant ride quality. Suspension system is subjected to diverse loads types including bending, torsion, and lateral loading, due to vehicle mass and carrying-load, irregular roads, cornering, acceleration and braking. These loads occur in combination with both dynamic and transient effects in a range of temperatures and environmental conditions.

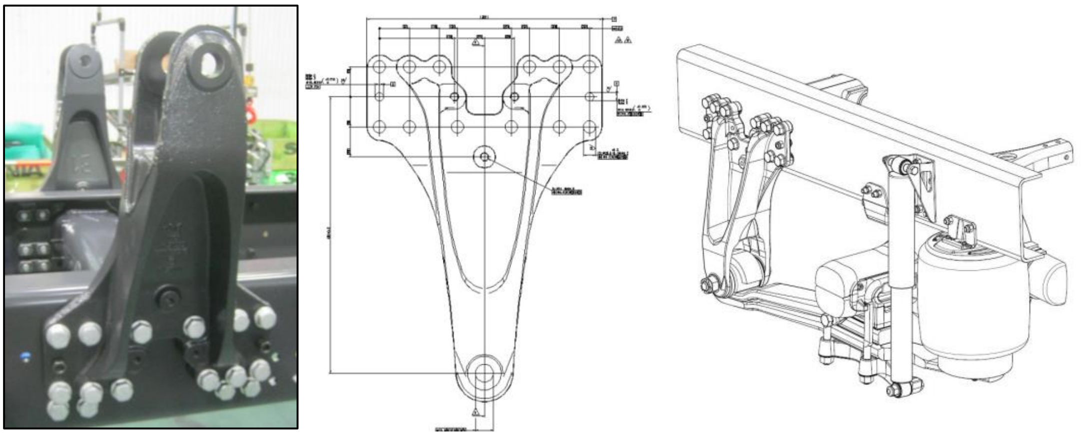

Figure 3-3. B*racket at the assembly line, bracket drawings and bracket's assembly view.*

As structural component, brackets have to be designed so that under the worst predictive cyclic load condition, there will still be a safety factor adequate for preventing fatigue failure.

This is a safety-critical component with high requirements, mainly regarding fatigue resistance.

To be a large, compact and safety-critical component with high requirements, mainly fatigue resistance, this part was chosen for this work as an opportunity to save weight. Unlike the turbo manifold, the ductile cast iron used in this component is not on the limit of its ability, so the cost here is a more important factor. Besides excellent mechanical properties and best performance per cost ratio, the material should exhibits good castability (allowing casting of thin wall sections and complex shapes) and machinability.

Fatigue resistance

Fatigue is the progressive, localized and permanent structural change caused by cycling or fluctuating strains at stresses that have maximum values lower than material tensile strength. Fatigue may cause cracks and further fracture after a sufficient number of cycles. This failure process can be divided in three steps: crack initiation, crack propagation to a critical size (at which the remaining uncracked cross section of the part becomes too weak to carry the imposed loads) and finally, abrupt rupture of the remaining cross section [96].

The simultaneous action of cyclic stress, tensile stress and plastic strain are the fatigue damage causes. To initiate and propagate a fatigue crack, these three variables have to be present. Cyclic stress induces plastic strain which initiates the cracks and tensile stress promotes propagation of cracks [96].

Fatigue limit or endurance limit should not be confused with fatigue strength. Fatigue limit is the stress value below which a material will endure an infinite number of stress cycles. Fatigue strength refers to the stress to which the material can be subjected for a specified number of cycles [96].

The steels fatigue strength is normally proportional to hardness and tensile strength, however not always this assumption is true. Toughness and critical flaw size can be the main factors for ultimate load carrying capacity in high strength steels [96].

Parameters that influence the carbon and low alloy steels fatigue behaviour are strength level, ductility, cleanliness, residual stresses and surface conditions [96].

For steels with hardness below 400 HB (except precipitation hardening steels), the fatigue limit is around half the ultimate tensile strength. However, for medium-carbon steels, higher strength may not mean higher fatigue resistance in a low cycle fatigue regime ($<10^3$ cycles) because ductility may have a bigger effect [96].

The steel cleanliness is evaluated by its relative absence of non-metallic inclusions. These defects usually decrease the steels fatigue resistance behaviour, mainly for high-cycle fatigue. Type, number, size and distribution may have a greater effect on the steels fatigue life, compared with differences in composition, microstructure or stress gradients. Large spherical inclusions, about 0.13 mm in diameter were detected in specimens fracture surfaces, which showed less fatigue resistance than specimens where no spherical inclusions larger than 0.02 mm were detected [96].

Surface imperfections and roughness can reduce component fatigue limit. This effect is more important for high strength steels. Surface depletion of carbon should be avoided (decarburization) during heat treatment processes because it significantly decreases the fatigue limit of the steel [96].

Fatigue limit can be improved by surface hardening. Surface hardening can be achieved by chemical processes like carburizing, carbonitriding and nitriding. These processes harden the surface layer and can produce beneficial surface residual compressive stresses. Surface residual stresses produced by bulk heat treatments are often tensile [96].

Surface treatment like shot peening applied to the steel component surface increases the fatigue resistance. This method induces compressive residual stresses at the surface causing improved fatigue resistance [96].

Fracture Toughness

Fracture toughness is a material property which characterizes the resistance to unstable crack propagation [97].

The plane-strain fracture toughness parameter, K_{IC}, measured by fracture mechanics test, allows the determination of how a crack or imperfection (e.g. inclusion) can exist in a critical section, without producing premature brittle fracture below the maximum design load. Designer can determine the critical combination of imperfection size and stress required to cause failure in one load application, if the K_{IC} is known. Additionally, it is possible to calculate the remaining life of a component containing a flaw, or estimate the largest acceptable flaw, using the crack growth rate and other fracture mechanics parameters [8].

Various studies have been conducted about fracture toughness of cast irons and steels. K.E. McKinney *et al.* [98], show in their experiments that a ferritic ductile cast iron is more resistant to crack extension than a cast steel, with similar strength between -40 to 27°C. Cast steel in these experiments showed much higher ductile to brittle transition temperature compared with the ferritic ductile iron, although this good toughness reported can only be expected in ferritic ductile cast irons. The presence of pearlite in the matrix, increases the transition temperature and decrease the fracture toughness of ductile cast irons, for the same tensile strength level [99] [97]. The fracture toughness tests in these referenced works, were conducted on ferritic ductile irons and cast steels with strength up to 500 MPa. Hence, some considerations should be made about these results.

When the goal is to reduce weight, more high strength materials are necessary to accomplish this goal. For ductile cast irons, increasing the pearlite content will improve the strength but the fracture toughness will drop. The Figure 3-4 shows the pearlite content effect on fracture toughness for ductile cast iron. Analysing the fracture toughness for a temperature between 0 and 50°C, we realise that increasing pearlite content present in the microstructure, a significantly decrease of fracture toughness takes place.

High strength nickel-chromium-molybdenum cast steel presents at room temperature a plane fracture toughness of 110 MPa√m at a yield strength level of 1034 MPa [8]. When requiring higher tensile strengths than 500 MPa and good fracture toughness, cast steel may be a good option. However, other characteristics like costs and castability, for instance, should also be taken into consideration.

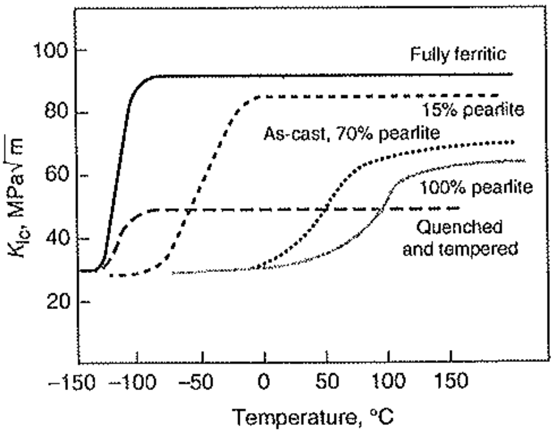

Figure 3-4. *Microstructure effect on ductile iron fracture toughness* [3].

3.2.2 Benchmarks

The benchmarking is important to validate Scania vehicles' performance towards competitors. The benchmark results show Scania's position on the market and gives the possibility to detail investigate components and systems.

Since Scania belongs to Volkswagen group, Scania has access to Volkswagen information. Thus, some material and material examinations have been received from Volkswagen.

3.2.2.1 Volkswagen

Volkswagen group research has a pre-evaluate group for material selection. Twice a year, Volkswagen invites steel suppliers to give a presentation on their newest materials and supply samples for experiments along with material data. Volkswagen then performs analysis on the materials and conduct simulations with the material data on different components.

Volkswagen has already a turbo manifold produced in austenitic cast stainless steel from Hitachi applied in a 1.4-liter twin charger. Another component is under developing, a turbine house produced in cast stainless steel GX40CrNiSi25-20.

3.2.2.2 Hitachi

Hitachi is an exhaust components supplier of automotive companies. They have a range of their own materials used in these components. These materials can be ductile cast iron, Ni-resist cast iron and cast stainless steels [100].

The company offers an interesting solution which is the turbo manifold casted together with the turbo charger, see Figure 3-5. This leads to fewer parts needed and less problem related to the joining between turbo manifold and the turbo charger [100].

Hitachi also offers a set of cast steel alloys like A5N which can withstand temperatures in service around 1050°C [100].

Figure 3-5. *Exhaust turbo manifold casted together with turbo housing* [100]**.**

3.2.2.3 Hyundai

Also Hyundai integrates the turbo manifold and the turbo housing, see Figure 3-6.

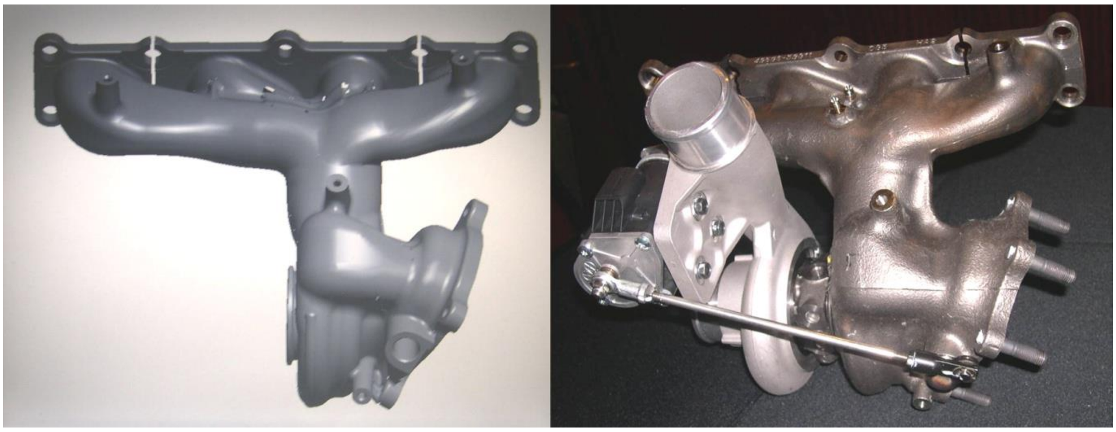

Figure 3-6. *To the left: A single austenite stainless steel casting that integrates the turbo manifold and turbine housing. To the right: A complete manifold assembly* [101].

3.2.2.4 MAN

A truck from MAN was analysed in order to obtain ideas about competitors' solutions around the components in this study. After analysing the bracket used by MAN, the first impression was that it is thinner and consequentially lighter compared to a Scania bracket for the same axle load. After research, SiboDur® 700-10 was found to be the material used [102].

SiboDur®, an ultra-high strength ductile iron alloy, is patented (expires in 2022) by Switzerland's Georg Fischer Automotive Group (GF) and just a few companies have licence to produce components in this material. Figure 3-7 shows the bracket used in MAN trucks. The companies allowed to produce it are Georg Fischer Automotive Co. Ltd. in Kunshan China, Georg Fischer GmbH in Mettmann Germany, Georg Fischer Automobilguss GmbH in Singen Germany and Grede Holdings LLC in Southfield United States.

Figure 3-7. *A SiboDur® spring hanger bracket* [103].

3.2.3 Materials from benchmarking

3.2.3.1 Sibodur®

The SiboDur® is not so expensive compared with cast iron 0727. The elements added in SiboDur® are Silicon (greater than 2.4%) and Boron (at least 60 ppm), inexpensive elements. The castability may be slightly lower than for cast iron 0727 due to the higher silicon content [104]. The Table 3-1 shows the SiboDur® 700–10 chemical composition analysed by Scania.

Table 3-1. *SiboDur® 700–10 chemical analysis according to Scania Internal Document*

Material	C%	Si%	Mn%	Mg%	Cu%
SiboDur® 700–10	3.62	3.04	0.35	0.046	0.77

One advantage, besides being a stronger material, SiboDur® does not need to be heat treated to achieve high strength. Figure 3-8 shows a comparison with process and material type versus yield strength cost per unit and SiboDur® presents better yield strength ratio cost per unit compared with ductile iron.

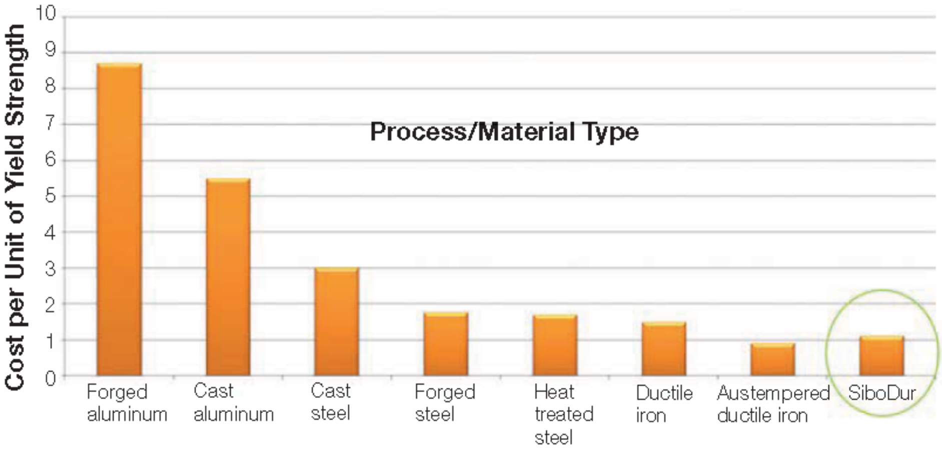

Figure 3-8. *The current market cost/unit strength position for a forged or cast aluminium process carries an exponential cost burden vs. alternative higher-strength alloys when considering yield strength behaviour* [105].

Scania internal reports have been referring bending fatigue tests and material investigation on SiboDur® grades 450-17 and 700-10, see Table 3-2 for a summary.

Table 3-2. *Material properties of two SiboDur® grades compared to cast iron 0727*

Material	**Ultimate Strength (R_m) [MPa]**	**Yield Strength ($Rp_{0.2}$) [MPa]**	**A %**	**Fatigue limit [MPa]**	**Fatigue for 10^5 cycles [MPa]**
Cast iron 0727	500-720	320-440	7	224	285
SiboDur® 450-17	441	375	24.7	216	292
SiboDur® 700-10	769	627	8.8	264	360

A short analysis from a Design Engineer at RTCB - Basic chassis development at Scania, shows that a reduction in weight by about 20% can be achieved if the article is well drawn when increasing the fatigue life for 10^5 cycles from 285 MPa for traditional material to 360 MPa for SiboDur® 700-10.

3.2.3.2 Austempering ductile iron (ADI)

Figure 3-9 shows X-link member of a MAN truck with the function of ensure axle location functional integration in longitudinal direction and vertical axle load support. The first generation was produced by forged quenched and tempered steel 42CrMo4. Now, an ADI cast X-Link solution has been used with a final weight benefit of 33%. Savings in tool costs due to casting (forging tools are expensive) admit the production of a range of different sizes. Small batches can be cost-effectively produced and individual solutions for customers can be realized [106].

Figure 3-9. *X-link used on heavy duty MAN TGA truck. It ensures the directional and vehicle stability and damping control.*

The designers recognized potential benefits of casting: lower weight and energy content compared to steel forging, more supplier capacity, ability to cast complex shapes and thin sections, less work on casting, rapid prototyping and less machining. Additionally, casting simulation can be used to optimize the process and achieve high quality demands of safety critical components [106].

The original forged X-Link manufactured from quench and tempered 42CrMo4 (.

Table **3-3**) had a solid profile, including four “eyes” which must be machined to accommodate the rubber joints. This X-Link weighed 65 kg (assembled weight 60.4 kg) [106].

The use of cores and satisfactory mechanical properties of ADI (.

Table **3-3**), permit the part to be casted with hollowed central zone and reduced section thickness. The four “eyes” are also cored and comparing to the forging minimal machining is required before assembly. The final casting weighs 40.8 kg [106].

Table 3-3. *Mechanical properties of the ADI alloy used to produce the X-Link and forged steel 42CrMo4 for thickness higher than 20 mm, EN 10083-3:2006* [106].

ADI Alloy	**R_m [MPa]**	**$R_{p0.2}$ [MPa]**	**A [%]**
MAN M3201 GGG 100B	1000 min	750 min	6 min
42CrMo4	900 min	650 min	12 min

3.2.4 Materials selection for turbo manifold and bracket

The steps followed for the materials selection are presented in Table 3-4.

Table 3-4. *Selection of materials for turbo manifold and bracket*

Selection process	Turbo Manifold	Bracket
What conditions must be met?	Goal: Support higher exhaust temperatures	Goal: Weight reduction through thickness decrease
What are the component requirements?	Component requirements: Oxidation resistance Thermal fatigue resistance Creep resistance Corrosion fatigue resistance Temperature service > 900°C	Component requirements: High Fatigue Resistance Stiffness Cost effective
What are the material requirements to meet the component requirements?	Material requirements: Low oxidation rate Low thermal coefficient High thermal conductivity High creep strength High corrosion resistance	Material requirements: Fatigue resistance >285 MPa Fracture toughness highest possible Young Modules ≥ 175 MPa
Materials which accomplish the material requirements.	List of materials: All presented on APPENDIX D	List of materials: G24Mn6 Ausferritic cast steel* From Benchmark: SiboDur® 700-10 MAN M3201 GGG 100B (ADI)
Process requirements to produce the component	Process requirements: Complex shape 6 mm wall thickness possible ~15 kg component Grade CT9 tolerances	Process requirements: Complex shape Thin wall thickness Up to 27 kg > 400 mm length
Material and production process which can accomplish the requirements	Material: GX40CrNiSi25-20 GX40CrNiSi22-10 Process: Shell moulding	Material: SiboDur® 700-10 Process: Sand casting

**material with potential application*

3.2.4.1 Turbo manifold

All the alloys presented on APPENDIX D fulfil the material requirements presented in Table 3-4. Although the material selection process for turbo manifold results in two grades, both are austenitic cast stainless steels. The ferritic grade, despite its lower thermal expansion and lower price, was rejected due to its poor castability and it will be difficult to cast sound parts. Thus, two grades of austenitic cast stainless steels were selected, one due to its performance in terms of creep resistance and lower price compared with GX40CrNiSiNb24-24. The other one, GX40CrNiSi22-10 was selected because its lower price compared with HK30. The creep resistance of this alloy, although lower than for HK30, may be enough for applications up to 950°C. Hence, for temperatures up to 950°C this alloy should present the best performance/cost ratio. Above these temperatures HK30 should have better performance which compensates the higher cost.

The component size eliminates the investment casting as a possible cast process. Sand cast process cannot be applied due to the casting tolerances. Shell molding process seems to be the best choice because it is less expensive than lost foam.

3.2.4.2 Bracket

As for the manifold, a similar analysis has been conducted for brackets. The first analysis of material requirements resulted in a four potential cast steels list. The selection focus was in the fatigue resistance and materials used by other truck companies in the same component or components with similar service conditions. The first one was selected from the alloys presented in APPENDIX C. This cast steel, G24Mn6 was chosen because presents a fatigue limit much higher than ductile cast iron 0727 used nowadays (345 MPa for fatigue limit against 285 MPa for 10^5 cycles, respectively).

The ausferritic cast steel is added in the table because of its potential as a future structural material. It presents high strength, high fracture toughness, high fatigue resistance, adequate ductility, good castability (3 mm wall thickness are possible), stiffness and all of this is achieve just using inexpensive elements like silicon.

From benchmark two alloys compete with cast steel, SiboDur® 700-10 (used in MAN truck brackets) and austempered ductile cast iron used on X-Link component with similar requirements to those for bracket.

The product size restricts the processes to sand casting. The G24Mn6 was rejected as an option for this component. The reason for this derives from the benchmark study. The SiboDur® bracket of MAN truck was analyzed and the component average wall thickness was around 6 mm. It is known that the castability of ductile cast irons is better compared with cast steels. The minimum wall thickness for cast steel using sand casting is 6 mm. For a component of this size, using cast steel will not give any weight reduction advantage, even using a material with much higher fatigue resistance. The reasons of that is the limitation in section thickness. Another relevant feature with SiboDur® is that it is less expensive than cast steel, Table 3-5 (21 against 30 SEK/kg) and for the same volume it is 10% lighter than cast steel due to graphite. However, comparing with ductile iron, SiboDur® 700-10 is about 62% more expensive (Table 3-5). Considering weight reduction by about 20% achieved changing the material from ductile iron 0727 to SiboDur® 700-10 to produce brackets (as referred in "*Materials from Benchmarking*") we will get about 5 kg of weight effective reduction (~27 to 22 kg). Additional cost for weight savings in chassis should be up to 15 SEK/kg [107] so 5 kg of weight reduction means an additional cost of ~22 SEK/kg, 7 SEK/kg higher than the recommended, see Table 3-6. However, SiboDur® is a patented material and its utilization by the foundries is limited, being expected a price decrease when the patent ends and in that time may fulfil the cost requirements.

Table 3-5. Price comparison on average material price for some materials.

Material	Average price (SKR/kg)	Accessed	From
Ductile Iron	13	2014	Scania
Gray Iron	6	2014	Scania
Cast Steel	30	2014	Scania
SiboDur® 700-10	21	2013	Grede Holdings LLC

Scania always use two suppliers for each component and that requirement becomes more difficult due to the SiboDur® patent.

ADI can be a good option also but it is heat treated and may become less cost effective comparing with SiboDur®.

The ausferritic cast steel will be probably a good alternative in the future. As referred, it is possible to cast 3 mm wall thickness components and this steel would consequently have an advantage over SiboDur® or other cast iron. It presents higher stiffness which allows the production of very thin wall components with less tendency to bend, comparing with any cast iron, excellent mechanical properties and comparable cost per performance than ADI and ductile irons [14][108].

Table 3-6. Comparison of weight and price between materials needed to produce bracket.

Material	**Weight of bracket (Kg)**	**Price of material needed (SEK)**	**Difference of cost (SEK/kg)**
Ductile Iron	27	351	22
SiboDur® 700-10	22	462	

3.3 Materials examination – materials and methods

Besides writing a Scania *Cast Steel Guideline*, two turbo manifolds, one made in SiMo51 and one in HK30 were examined in this thesis work. The HK30 manifold is a prototype and the SiMo51 manifold is used in Scanias' diesel engines. The examinations purpose is to compare the HK30 manifold properties with the SiMo51 manifold, concerning the microstructure and hardness.

3.3.1 Samples characterization in the as-cast state

Two turbo manifolds, one made using SiMo51 for Scanias' diesel engines and one prototype made using HK30 were delivered, see Figure 3-1. Cross-section samples were selected for microstructural characterization. The chemical composition of each alloy is given in Table 3-7.

Table 3-7. *Chemical compositions of HK30 and SiMo51*

	C%	**Si%**	**Mn%**	**Cr%**	**Ni%**	**Mo%**	**Cu%**
HK30	0.34	1.40	1.11	24.37	19.13	0.38	0.37
SiMo51	3.09	4.01	0.32	0.03	0.02	0.80	0.06

The white rectangles shown in Figure 3-10 represent the as-cast samples removed from the manifolds. Two samples of each material with different wall-thicknesses were removed, in order to analyze the possible effect of different cooling rates. The analyzed surfaces were perpendicular to the surface showed in Figure 3-10.

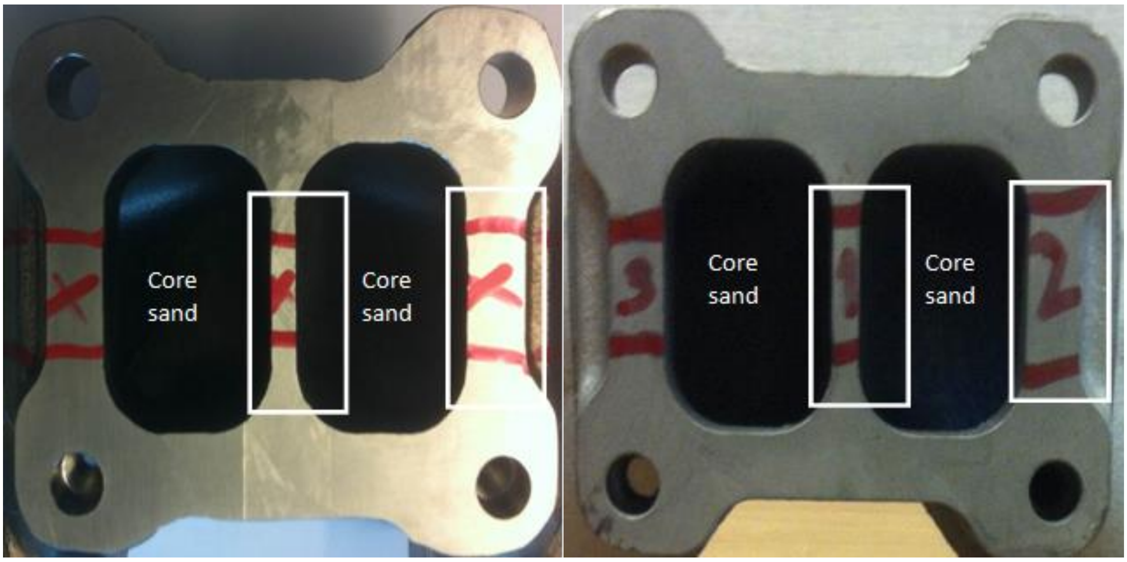

Figure 3-10. *To the left: Samples removed from the prototype produced in HK30. To the right: Samples removed from the manifold SiMo51.*

The materials' characterization was conducted through microstructure analyses and hardness measurements. All the samples were cut, mounted, polished and etched. The etch reagent used for HK30 samples was Kallings Etsmedel etchant (5 g copper chloride, 100 ml hydrochloric acid, 100 ml ethanol, 100 ml water) and for SiMo51 samples was used Nital 2%.

A Carl Zeiss AX10 optical microscope with an incorporated AXIOCAM MRC digital camera was used for microstructure observation. Micro and macro hardness measurements were performed with a Matsuzawa MxT30 and a KB 3000 BVZ (ball diameter of 2.5 mm with a nominal test load of 187.5 kg) testing machines respectively, for both materials. The results presented were obtained by 5 measurements average.

For HK30, some microstructural analyses in scanning electron microscope (SEM) and x-ray microanalyses (EDS) were conducted with a FEG-SEM/EDS Zeiss Sigma VP provided with Gemini field emission column and element microanalysis was carried out with an Energy Dispersive Spectrometer, EDS INCA Oxford Instruments.

3.3.2 Heat treatments

The heat treatments were performed in a Naber N60/HR oven. The samples were covered in full by steel filings in order to protect against oxidation and descarburization. The samples presented a rectangular shape with 20 mm of length and around 6 mm of thickness.

After the heat treatment, the samples were characterized concerning the microstructure and hardness.

3.4 Results and discussions

3.4.1 Ductile cast iron SiMo51

The expected as-cast microstructure for SiMo51 presents nodular graphite distributed in a ferritic matrix, stable M_6C carbides and intercellular zones with spheroidized pearlite precipitated [109].

The microstructures obtained by thin and thick sections in the SiMo51 are very similar, composed of graphite nodules surrounded by ferritic matrix, intercellular M_6C carbides and spheroidized pearlite, as expected.

APPENDIX K shows the as-cast microstructure obtained for material SiMo51 for thin and thick samples. No visible relevant differences in microstructure were observed for these samples.

This alloy presented 236±6 HBW 2.5/187.5 macro-hardness, while 238±12 HV1 was obtained for matrix micro-hardness.

3.4.2 Austenitic cast stainless steel - HK30

The HK30 is a 25Cr/20Ni alloy, so it is an iron-chromium-nickel alloy, being expected a microstructure composed of an austenitic matrix containing relatively large carbides in the form of either unconnected islands or as networks [110].

Figure 3-11 shows vertical sections of ternary equilibrium system for 55% weight in iron. The HK30 composition is represented by the line (25% Cr and 20% Ni). From Figure 3-11 we can verify that the alloy composition fall into austenitic field, so, a fully austenitic microstructure is expected. The transformation of austenite to σ-phase may occur in this alloy, when the compositions are unbalanced and after long exposition at temperatures in the range of 760 to 870°C [17]. From Figure 3-11 we can see that σ-phase formation may happen at lower temperatures, between 400 and 800°C.

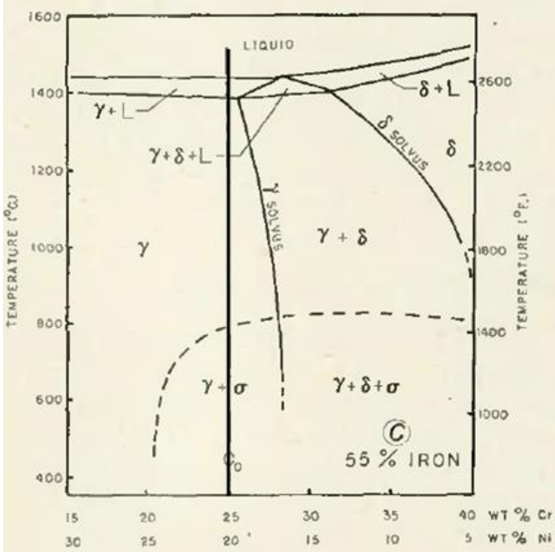

Figure 3-11. *Vertical sections of ternary equilibrium system for 55% weight in Fe* [111].

By observation of the microstructures presented in Figure 3-12, for thin and thick samples respectively, a microstructure composed of a fully austenitic matrix and carbides can be confirmed, as individual islands and networks.

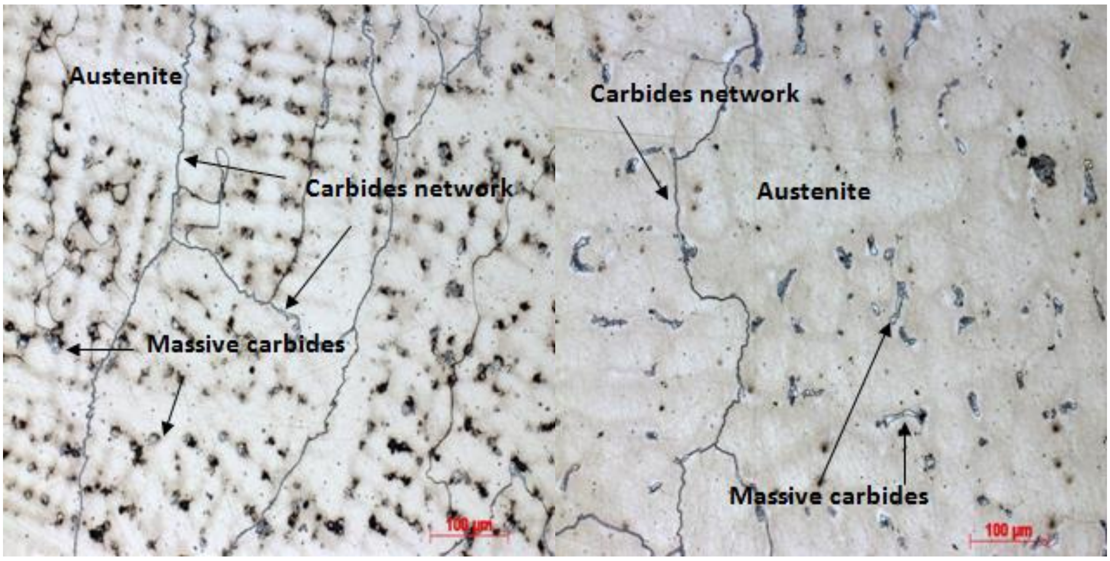

Figure 3-12. *To the left: Microstructure obtained in as-cast state for thin part composed of a fully austenitic matrix, grain boundaries chromium rich carbides and massive carbides into the matrix; Objective: 20X; Kallings Etsmedel etch. To the right: Microstructure obtained in the as-cast state for thick part composed of a fully austenitic matrix, grain boundaries chromium rich carbides and massive carbides into the matrix; Objective: 50X; Kallings Etsmedel etch.*

The literature refers the susceptibility of stainless steels intergranular corrosion when chromium carbides precipitate at the grain boundaries, during high temperature exposure [17][112]. These chromium carbides, type M_7C_3 and $M_{23}C_6$ (M=Fe, Cr) [113], will deplete the surrounding matrix of chromium and make the alloy more sensitive to intergranular corrosion. This is easy to understand since these chromium carbides present chromium content between 24 to 60% [114]. These carbide networks usually appear when the alloy is cooled very slowly through high temperature ranges, in which the carbon rich austenite reject the carbon as grain boundary networks instead of dispersed particles [17] [112].

Both microstructures obtained in Figure 3-12 show a network and unconnected islands of carbides (massive carbides) into austenite matrix. From Figure 3-12, both thin and thick samples present grain boundary carbides, but they are more visible in the thin sample. Looking just for the samples thickness, would be expected a faster cooling rate for the thin sample during solidification and consequently, may avoiding the presence of carbides in the grain boundaries. However, we should take into account the samples source and in what conditions they were subjected. Looking for the place where the thin sample was removed (Figure 3-10), it was in the middle of two thick metal walls. During solidification, these thick walls release heat through mould sand to outside and to the thin wall through core sand. For this reason, the thin sample during cooling remains more time at high temperatures than the thick sample.

The carbides network formed at the grain boundaries can promote material intergranular corrosion, as said above. Furthermore, the ductility is reduced and the material becomes brittle [17].

When the thin sample microstructure is observed (Figure 3-12), we can conclude that grain size is smaller compared with the thick part. Actually, taking a look of a microstructure at low magnification (Figure 3-13, to the right in the picture), it is clear a grain growth from the surface on right to the left (visible surface on Figure 3-13, to the left). This may be caused by an initial high cooling rate verified during casting. The molten steel when arrived at this narrow cold end surface of the mould sand solidifies very fast and cooling rate decrease along the arrow represented (Figure 3-13). Consequently, the grain size becomes bigger with the distance. Despite of this initial sample fast cooling, it is not enough to avoid the grain boundaries carbides precipitation as shown in Figure 3-12, to the left. The reason for this may be that in the beginning the cooling rate starts very high, reaching at an equilibrium when the sand temperature increases and consequently the heat release through the sand becomes slower.

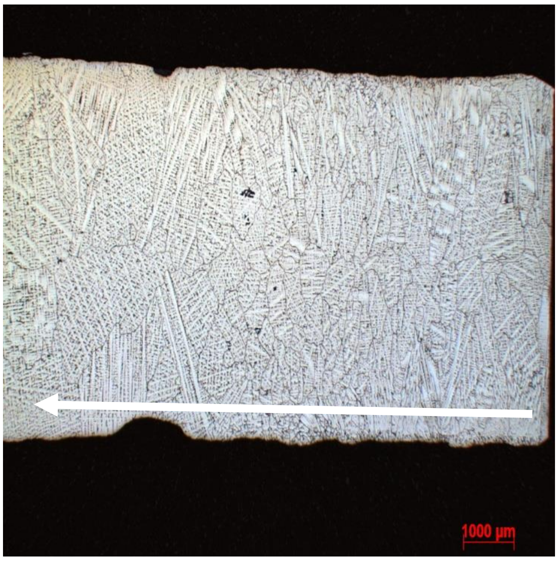

Figure 3-13. *Microstructure showing the grain growth from the right to the left (from surface showed in* Figure 3-12 *to middle); Objective: 1.25X; Kallings Etsmedel etch.*

If chromium carbides form and grow in the solid state, chromium depletion of the matrix happens and the alloy sensitization is present [115].

For those reasons, heat treatments tests were designed in order to eliminate these carbide networks and improve the ductility, creep and corrosion resistance. Adding elements to form carbides like niobium or titanium, may avoid further precipitation of chromium carbides at grain boundaries presented in the samples [112].

3.4.3 Heat treatments

3.4.3.1 Samples source

Totally, 11 samples were taken from the HK30 manifold prototype and two of them, were analyzed in the as-cast state. The goal of this as-cast analysis was to verify if the samples of both sides present similar microstructure, in order to ensure that each sample starts the heat treatment at the same level.

The two as-cast samples analysed in this section presented similar microstructure and like the previous as-cast samples in Figure 3-12, showing a fully austenitic matrix and carbides, as individual islands and networks. Figure 3-14 to the left, shows an as-cast sample SEM micrograph where the grain boundary carbides and the unconnected carbide island are visible. The unconnected islands present a lamellar structure as we can see in Figure 3-14, to the right. These lamellar carbide islands were not visible in the previous as-cast samples.

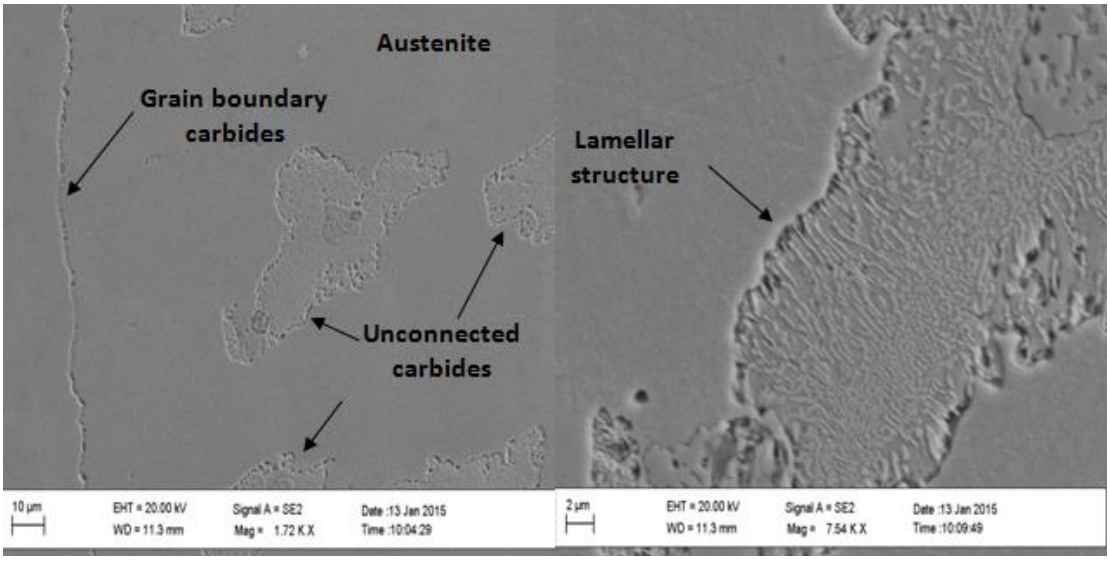

Figure 3-14. *To the left: SEM image of grain boundary carbides and unconnected carbide islands in as-cast sample. To the right: SEM image of an unconnected carbide island showing a lamellar structure in as-cast sample.*

As the as-cast samples of each side presented similar microstructure and hardness (HBW ~180), the heat treatments could be performed.

3.4.3.2 Heat treatments design

A solution annealing heat treatment can be applied in order to dissolve the grain boundary carbides back to the matrix, followed by water quenching, just enough to prevent the re-precipitation of carbides during cooling [112]. This heat treatment is conducted in the range of temperatures between 1040 and 1205°C [28]. The temperature depends on the alloying elements present, principally the molybdenum content that may increase the solution annealing temperature needed (close to the maximum) to dissolve the more stable carbides [112]. A solution annealing heat treatment followed by aging is usually employed to reach maximum creep strength [17].

A series of heat treatments were conducted, changing three variables: solution annealing heat treatment holding time, quenching medium (after the solution treatment holding time) and the aging holding time. The heat treatment effectiveness was evaluated through microstructural analysis by optical and scanning electron microscopes and hardness measurements.

The experimental method used was the 2^k factor analysis [116]. Table 3-8 shows the chosen variables with the values range.

Table 3-8. *Variables and experimental parameters*

Variables	**-**	**+**
ST – Solution temperature holding time	1.5 h	3 h
QM – Quenching Mean	Oven	Water
AT – Aging Holding Time	0	24 h

Table 3-9 shows the experimental matrix obtained after variables decomposing.

Table 3-9. *Matrix of experiments*

Sample number (Designation)	**ST**	**QM**	**AT**
1 - (ST/1.5 + O.C.)	-	-	-
2 - (ST/3 + O.C.)	+	-	-
3 - (ST/1.5 + W.Q.)	-	+	-
4 - (ST/3 + W.Q.)	+	+	-
5 - (ST/1.5 + O.C. + AT)	-	-	+
6 - (ST/3 + O.C. + AT)	+	-	+
7 - (ST/1.5 + W.Q. + AT)	-	+	+
8 - (ST/3 + W.Q. + AT)	+	+	+

Fixed temperatures were selected for solution and aging heat treatments, 1200 and 760°C, respectively. The solution heat treatment temperature (1200°C) was defined because it is almost the maximum temperature referred by literature [28] to ensure the effective grain boundary carbides dissolution in the matrix. At 760°C [17], precipitation of a fine, uniformly dispersed carbides is promoted resulting in a high strength level and can be kept up to temperatures around 980°C, where the carbides start to agglomerate and spheroidize, decreasing the creep strength [17]. The cooling applied after the aging holding time was still air. Figure 3-15 shows schematically the different thermal cycles employed.

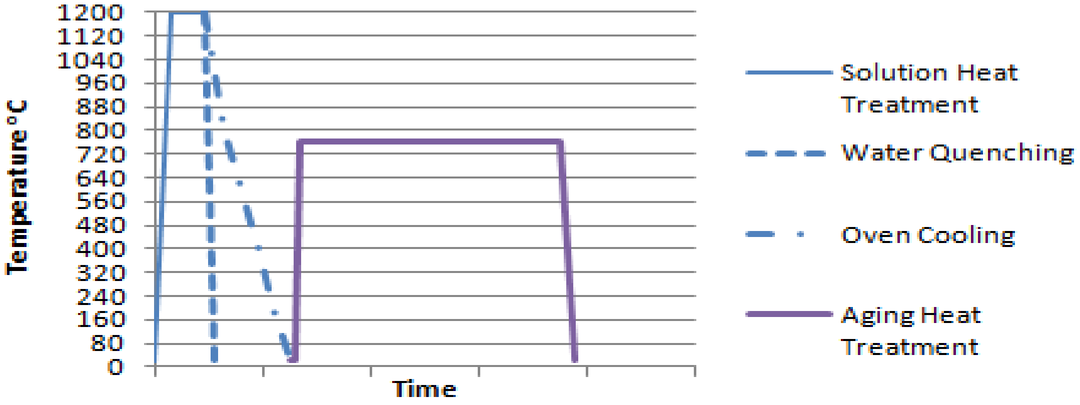

Figure 3-15. *Thermal cycles applied in heat treatments.*

3.4.4 Microstructures

3.4.4.1 Solution annealing followed by water quenching

As referred before, the solution annealing heat treatment can be applied to dissolve the grain boundary carbides back to the matrix. This is possible due to the increase of carbon solubility in austenite with the temperature increasing. Figure 3-16 shows a chart where two lines are visible, a dashed line and a solid line, both representing the solubility of carbon in austenite. The solid line represents 18Cr-12Ni alloy and the dashed line 20Cr-25Ni stainless steel [115]. Despite of differences in chromium and nickel contents of HK30 alloy comparing with the alloys represented in Figure 3-16, the main conclusion is the same, with the temperature increase, the carbon solubility in austenite increase and consequently, more carbides will be dissolved. Another important consideration is that some carbon carbides always will be present in microstructure for alloys with carbon contents greater than 0.20%, like HK30 alloy, regardless of solution annealing treatment [73]. For instance, in the Figure 3-16, the 20Cr-25Ni alloy presents a solubility limit in austenite for carbon around 0.15%. This means, compositions with carbon content above ~0.15%, will present carbides in the microstructure, regardless the solution annealing treatment.

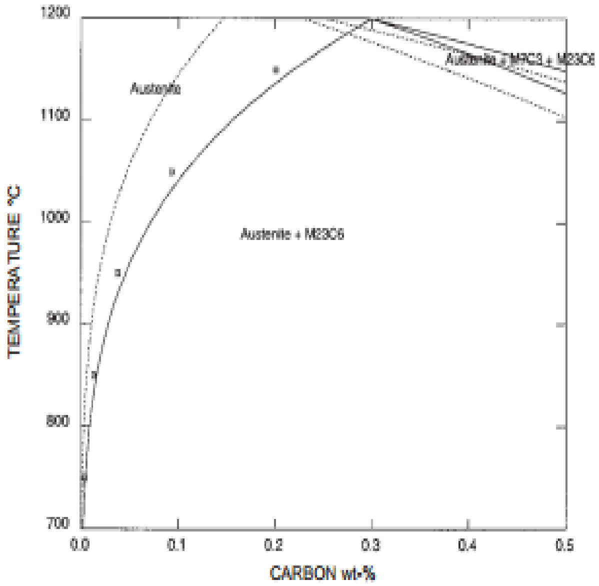

Figure 3-16. C*arbon solubility in austenite for 18Cr-12Ni and 20Cr-25Ni austenitic stainless steels represented by solid line and dashed line, respectively* [115]**.**

Figure 3-17 shows microstructures obtained on samples after solution annealing treatment. The quenching mean for both samples was water. The Figure 3-17, to the left, represents the microstructure of the sample solution annealed at 1200°C for 1.5 h. It is possible distinguish some differences compared with the as-cast state sample. Lamellar carbides are not visible and a decreasing of grain boundary carbides is clear. The carbides were somewhat dissolved back to the matrix, becoming thinner and are disconnected as we can see in the Figure 3-18, to the left, in more detail. For the sample solution annealed at 1200°C for 3 h (Figure 3-18, to the right), the grain boundary carbides are less compared with the sample solution annealed for 1.5 h, which was expected, since the carbides solution is also a time dependent process. A sufficient amount of time is necessary to accomplish the maximum carbon solution in austenite [73]. From X-ray microanalysis the chromium content near carbides was higher (26.33%) than in the middle of matrix (24.52%) for the sample ST/1.5 h, see APPENDIX L. This can be explained by the dissolution of grain boundary carbides during solution annealing, increasing the chromium contents close to carbides.

For both samples in Figure 3-17, very small carbides are present near massive and grain boundary carbides. These small carbides or decomposed carbides may be the result of the lamellar massive and grain boundary carbides dissolution during the solution annealing, since they are not visible in the as-cast state. In Figure 3-18 with higher magnification, these carbides and dissolution of grain boundary carbides are visible and clear compared with the as-cast sample (Figure 3-12).

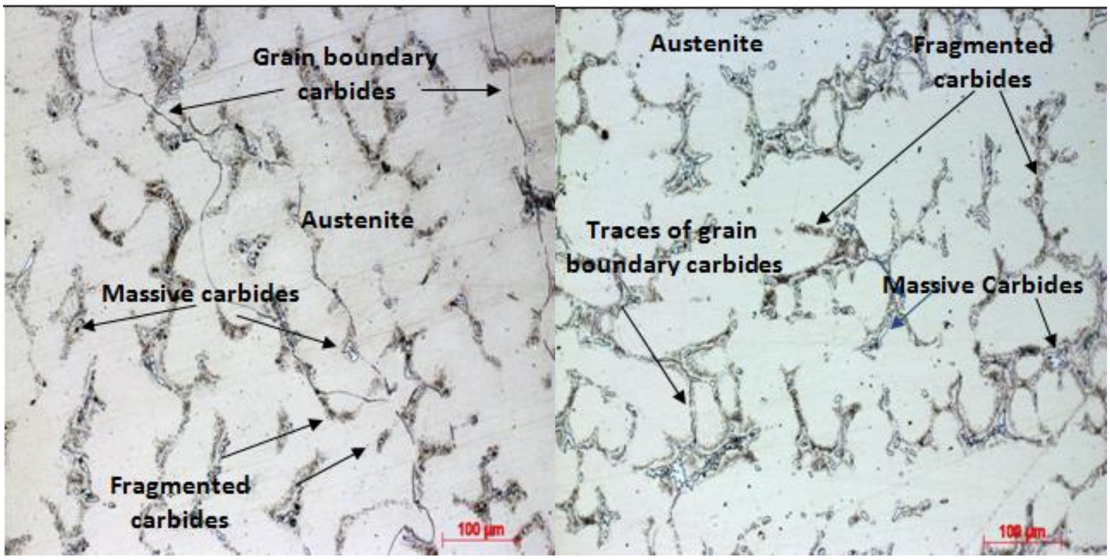

Figure 3-17. *To the left: Microstructure obtained after solution annealing at 1200°C for 1.5 h followed by water quenching composed of a fully austenitic matrix, very thin grain boundaries chromium rich carbides, massive carbides in the matrix and decomposed carbides; Objective: 20X; Kallings Etsmedel etch. To the right: Microstructure obtained after solution annealing at 1200°C for 3 h followed by water quenching composed of a fully austenitic matrix, massive carbides, decomposed carbides and small traces of grain boundary carbides; Objective: 20X; Kallings Etsmedel etch.*

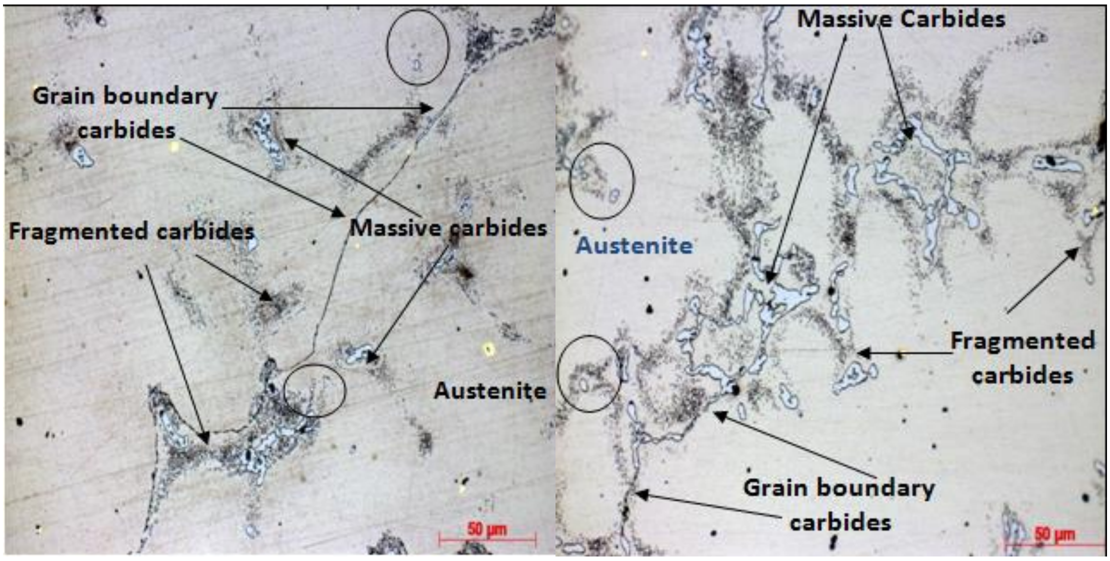

Figure 3-18. *To the left: Microstructure obtained after solution annealing at 1200°C for 1.5 h followed by water quenching composed of a fully austenitic matrix, thin grain boundaries chromium rich carbides and massive carbides, decomposed carbides and spheroidized carbides highlighted by circles; Objective: 50X; Kallings Etsmedel etch. To the right: Microstructure obtained after solution annealing at 1200°C for 3 h followed by water quenching composed of a fully austenitic matrix, grain boundaries chromium rich carbides and massive carbides, decomposed carbides, and spheroidized carbides highlighted by circles; Objective: 50X; Kallings Etsmedel etch.*

The literature refers that at high temperatures, like used in this experiment, carbides can be dissolved or spheroidized [73]. These spheroidized carbides can be seen highlighted with circles in Figure 3-18. From these figures we can conclude that increasing the solution annealing holding time, the massive carbides become bigger, possibly due to the decomposed carbides agglomeration to the previous massive carbides. In Figure 3-18, to the right (solution annealed for 3 h) bigger massive carbides are visible compared with the massive carbides present in Figure 3-18, to the left, for a solution annealing time of 1.5 h. Even from Figure 3-17 (at lower magnifications), it is visible a difference between massive carbides size, being bigger for the sample solution annealed for 3 h than 1.5 h.

From these experiments, we can conclude that during solution annealing heat treatment, the carbides dissolution takes place until the maximum carbon solubility in austenite is reached. When this happens, carbides dissolution stops and carbides agglomeration starts, due to the high temperature [17].

3.4.4.2 Solution annealing followed by oven cooling

Microstructures obtained for samples solution annealed at 1200°C, followed by oven cooling, are presented in Figure 3-19, for 1.5 and 3 h holding time. Comparing samples solution annealed for 1.5 h (Figure 3-17), larger massive carbides and thicker grain boundary carbides are visible in the sample oven cooled than the sample water quenching. The sample solution annealed for 3 h followed by oven cooling presents grain boundary carbides in more quantity compared with the sample water quenched. The slow cooling in oven (around 120°C/h) may be sufficient to keep the samples at high temperatures long enough for the carbides agglomeration process takes place. Also a higher carbides concentration in the microstructure (increase of ratio carbide/matrix) is visible. This can be explained also by the slow cooling, which enables further carbide precipitation, due to the decreasing carbon solubility in austenite with temperature (Figure 3-16).

The carbide precipitation (due to the carbon excess in the austenite) at high temperature ranges, takes place at grain boundary networks, instead as dispersed particles in matrix [73]. In Figure 3-20 (sample solution annealed at 1200°C for 1.5 and 3 h followed by oven cooling), this carbide precipitation in grain boundaries tendency can be seen by the more continuous carbides networks presented comparing with both samples water quenched (Figure 3-18). The conclusion at the final of these trials is that slow cooling after solution annealing heat treatment promotes the carbides agglomeration and precipitation at grain boundaries and previous massive carbides. So, the dissolution effect of carbides in austenite after solution annealing lose its effect, if further cooling is slow enough to admit carbides precipitation and agglomeration at high temperatures.

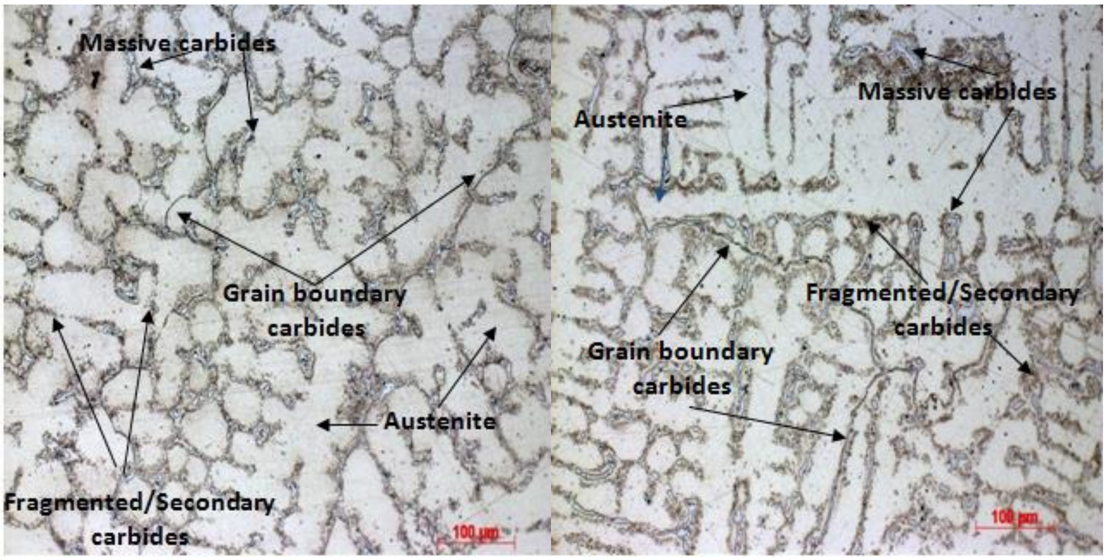

Figure 3-19. *To the left: Microstructure obtained after solution annealing at 1200°C for 1.5 h followed by oven cooling composed of a fully austenitic matrix, thin grain boundaries chromium rich carbides, massive carbides into the matrix and decomposed/precipitated carbides; Objective: 20X; Kallings Etsmedel etch. To the right: Microstructure obtained after solution annealing at 1200°C for 3 h followed by oven cooling composed of a fully austenitic matrix, thin grain boundaries chromium rich carbides, massive carbides into the matrix and decomposed/precipitated carbides; Objective: 20X; Kallings Etsmedel etch.*

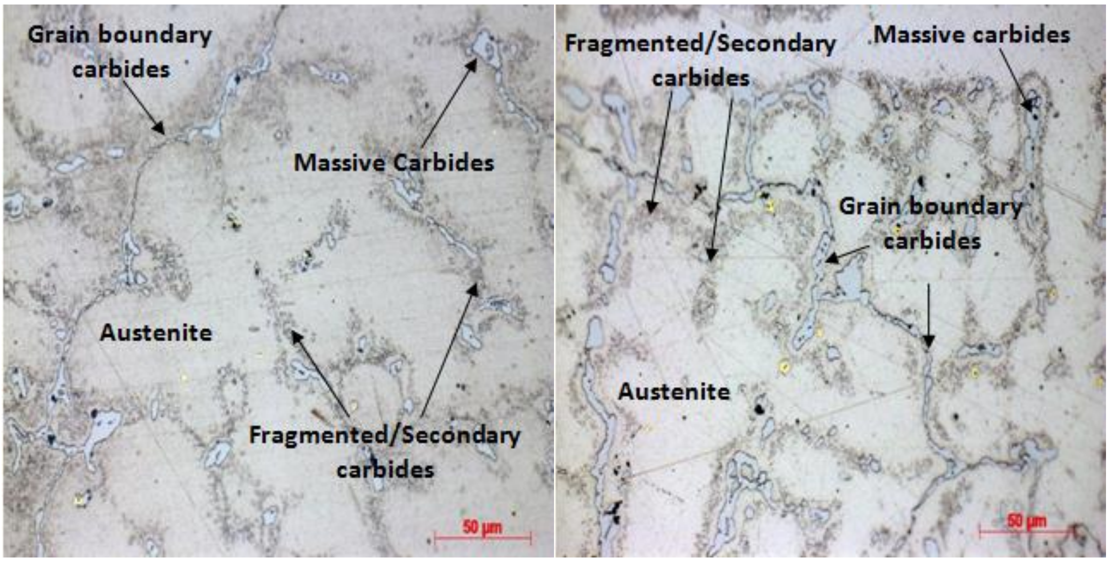

Figure 3-20. *To the left: Microstructure obtained after solution annealing at 1200°C for 1.5 h followed by oven cooling composed of a fully austenitic matrix, thin grain boundaries chromium rich carbides, massive carbides into the matrix and decomposed/precipitated carbides; Objective: 50X; Kallings Etsmedel etch. To the right: Microstructure obtained after solution annealing at 1200°C for 3 h followed by oven cooling composed of a fully austenitic matrix, thin grain boundaries chromium rich carbides, massive carbides into the matrix and decomposed/precipitated carbides; Objective: 50X; Kallings Etsmedel etch.*

3.4.4.3 Aging heat treatment

Samples solution annealed followed by water quenching

The aging treatments were applied after solution annealing heat treatments. One aging heat treatment was conducted with the sample in the as-cast state, to compare the effect of the solution annealing in the aging treatment.

Figure 3-21 presents the samples microstructures after aging. To the left represents the sample previous solution annealed for 1.5 h and to the right for 3 h, both were quenched in water.

The microstructures presented in Figure 3-21, show a big difference comparing with the samples that have been just solution annealed for both quenching media. Fine dispersed carbides in the matrix are visible as we can see with higher magnification in Figure 3-22. Carbon far from grain boundaries remains in supersaturated austenite and much longer times and greater supersaturation are needed for nucleation and growth of these precipitates [117]. Thus, the previous samples (without aging) did not remain enough time at high temperatures to admit precipitation of these fine dispersed carbides. The samples aged, both present fine dispersed carbides in austenite matrix. However, as referred previously, for the samples solution annealed and quenched in water, the sample solution annealed for 1.5 h presents thin grain boundary carbides whereas the sample solution annealed for 3 h, grain boundary carbides are not visible in Figure 3-21. As for solution annealed samples after water quenching, the higher the holding time the larger the massive carbides are.

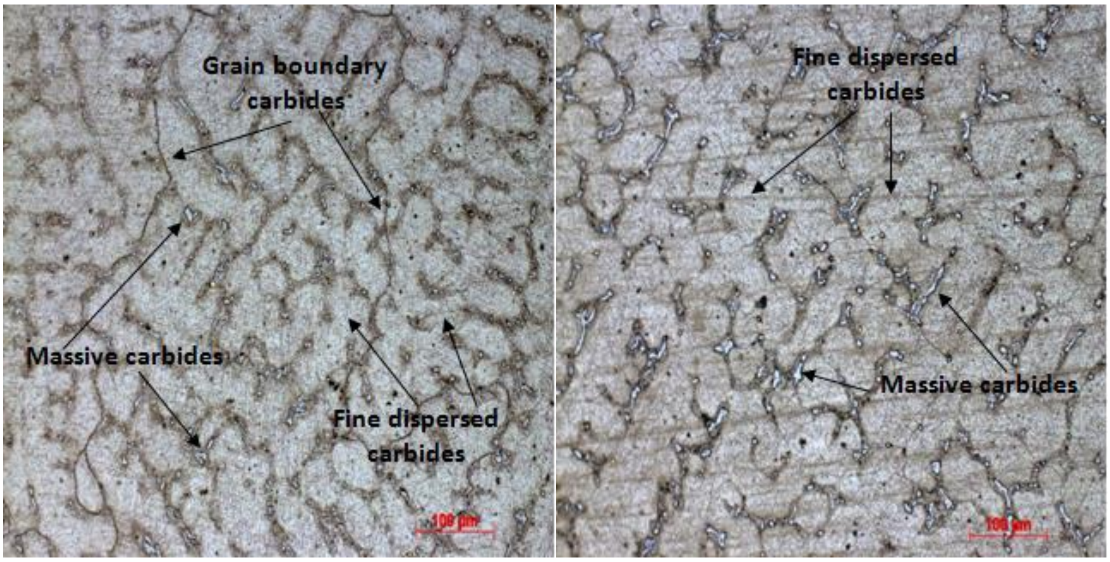

Figure 3-21. *To the left: Microstructure obtained after solution annealing at 1200°C for 1.5 h followed by water quenching and aged at 760°C for 24 h, which contains a fully austenitic matrix, thin grain boundaries chromium rich carbides, massive carbides and fine dispersed carbides into a austenitic matrix; Objective: 20X; Kallings Etsmedel etch. To the right: Microstructure obtained after solution annealing at 1200°C for 3 h followed by water quenching and aged at 760°C for 24 h, which contains massive carbides and fine dispersed carbides into a austenitic matrix; Objective: 20X; Kallings Etsmedel etch.*

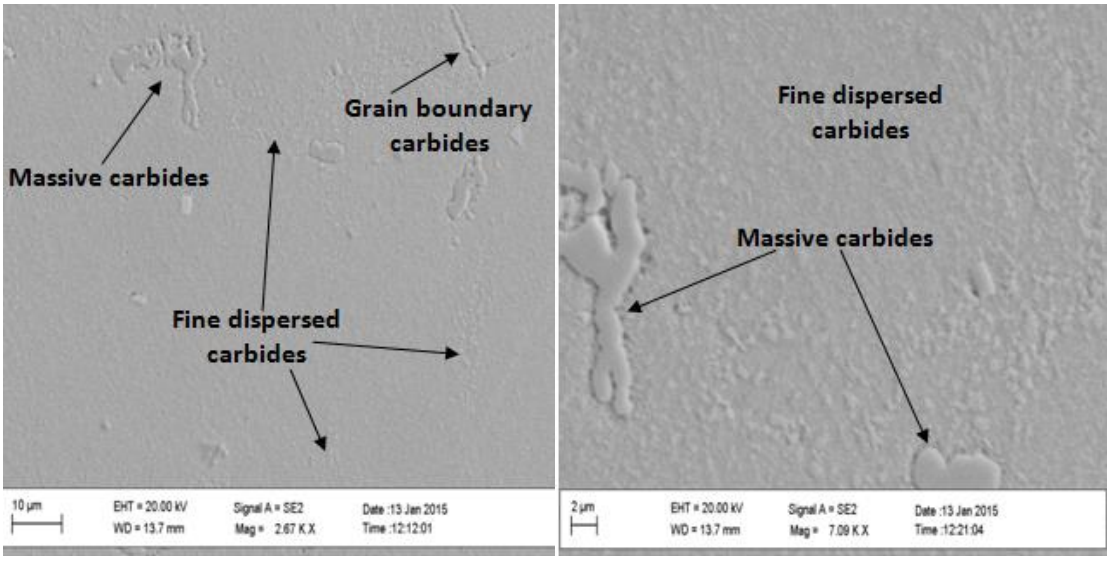

Figure 3-22. *To the left: SEM micrograph showing fine dispersed carbides into the matrix for the sample solution annealed for 1.5 h water quenching and aged for 24 h; Kallings Etsmedel etch. To the right: SEM micrograph showing fine dispersed carbides into the matrix for the sample solution annealed for 1.5 h water quenching and aged for 24 h; Kallings Etsmedel etch; Higher magnification.*

Samples solution annealed followed by oven cooling

The effect on aging treatment of samples oven cooled after the solution annealing was also evaluated.

From Figure 3-23, one thing is clear: the precipitation of fine dispersed carbides was much less intense compared with the samples water quenched. Actually, the sample solution annealed for 1.5 h and aged does not present fine dispersed carbides into the matrix. The reason for the sample solution annealed for 3 h present less fine dispersed carbide precipitation is, as mentioned before, the precipitation of carbon far from grain boundaries needs besides much longer time, greater supersaturation. During the slow cooling in the oven, the carbides precipitation takes place, depleting the matrix in carbon. When the aging treatment is applied, the austenitic is less supersaturated in carbon, decreasing the possibility of fine dispersed carbides precipitation far from the grain boundaries.

The lower holding time at solution annealed temperature, less carbide are dissolved and consequently there will be less supersaturated austenite. Therefore, for the sample solution annealed for 1.5 h (Figure 3-23, to the left) none fine dispersed carbide in matrix is visible and for the sample with higher holding time (3 h), some are visible in Figure 3-23 to the right.

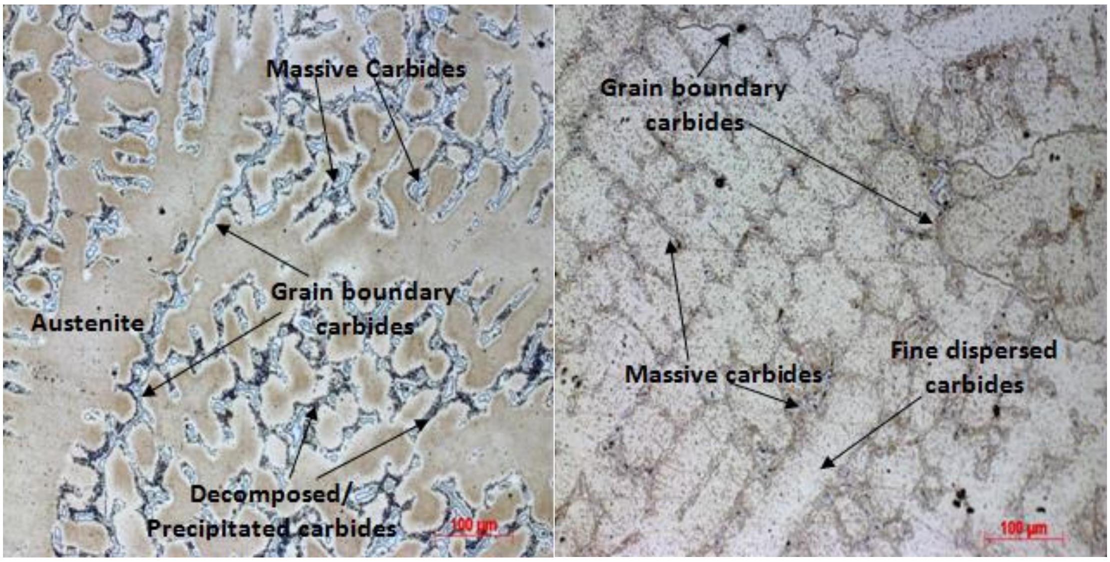

Figure 3-23. *To the left: Microstructure obtained after solution annealing at 1200°C for 1.5 h followed by oven cooling and aging composed of a fully austenitic matrix, grain boundaries chromium rich carbides, massive carbides and decomposed/precipitated carbides; Objective: 20X; Kallings Etsmedel etch. To the right: Microstructure obtained after solution annealing at 1200°C for 3 h followed by oven cooling composed of a fully austenitic matrix, thin grain boundaries chromium rich carbides, massive carbides and fine dispersed carbides; Objective 20X; Kallings Etsmedel etch.*

3.4.5 Hardness measurements

The Figure 24 presents the macro-hardness obtained for each heat treatment.

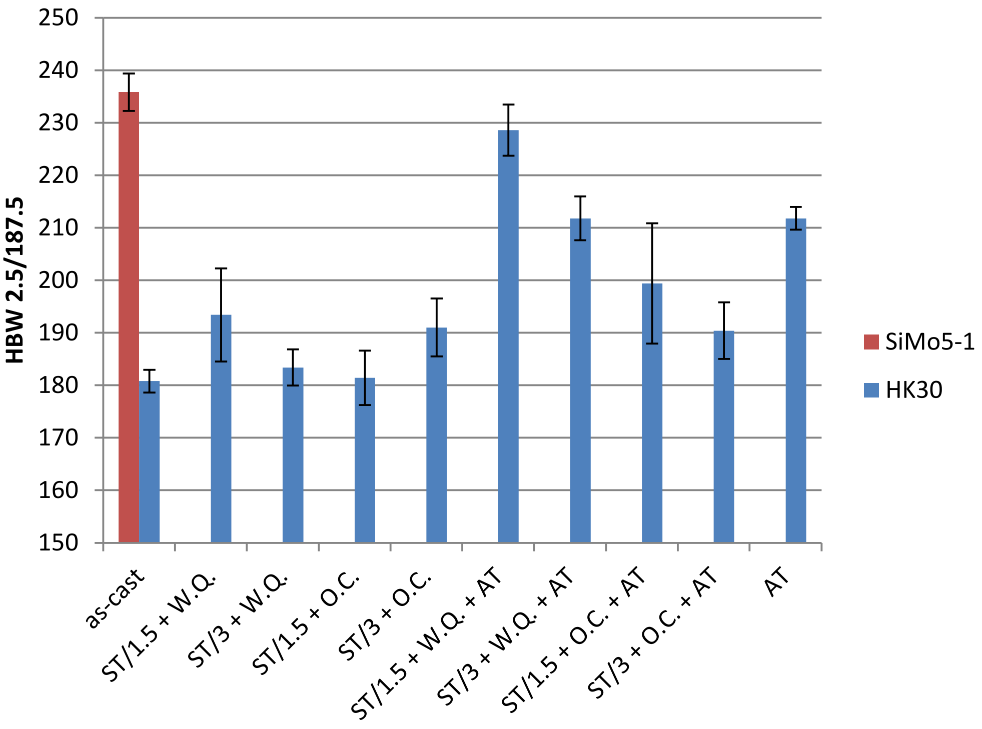

Figure 3-24. *Macrohardness obtained for different heat treatments.*

Figure 25 shows micro-hardness measured on the matrix of each heat treated sample. Note that the micro-hardness measurements for the cast stainless steel were conducted at three different places on samples, namely inside, in the middle and outside. These three places on the samples were analysed in order to test the different cooling rates that may be subjected, even though the relative low thickness of the samples (~6 mm). The inside surface represents the surface in contact with the core sand, outside the surface in contact with the mould sand and in the middle is the core of the sample.

Returning to Figure 3-24, there are two main conclusions coming up from the results. First, SiMo51 presents higher hardness compared with HK30, when both are in the as-cast state. Second, the sample ST/1.5 + WQ + AT, clearly presents the highest HK30 samples hardness, approaching the SiMo51 sample in the as-cast state.

For the first one, the reason for what SiMo51 presents higher hardness in the as-cast state compared with HK30 in the same state, can be explained looking for matrix micro-hardness results in Figure 3-25. The micro-hardness measured on matrix is higher for SiMo51 compared with the inside and middle surfaces of HK30. The outside surface (HK30) presents higher hardness compared to SiMo51 (in all places), although its impact is not expressive on macrohardness (large area of indentation), because it represents a small area compared with the middle and inside surfaces together.

Before analysing the second conclusion, let us focus on micro-hardness differences verified for HK30 in the as-cast state. As referred before, the outside surface presents the higher hardness compared with the inside and middle surfaces. This may result from different cooling rates in each edge. The inside surface in contact with the sand core, and middle surface suffered lower cooling rates leading to lower hardness and the higher cooling rate of the outside surface resulting in higher hardness. The differences explanation on cooling rate between the inside and outside surface, is the same as given to explain the different cooling rates for the initial as-cast samples (thin and thick samples).

For the as-cast HK30 sample in Figure 3-25, a higher error range in micro-hardness is visible at the outside surface indicating some matrix heterogeneity. Actually, the highest error ranges were verified on the outside surfaces for the different heat treatments.

From X-ray microanalysis the matrix presented less chromium content in the middle (23.06%) than in the outside surface (24.05%). This also shows that carbon content in the middle may be less than in the inside surface. From APPENDIX L can be seen that the outside surface shows higher carbides fraction compared with the middle. This may be the reason for the higher hardness in the outside surface.

The difference on hardness between the different zones is lower for the samples that have been solution annealed, which decrease the effect of the different cooling rate, experimented during the casting process.

The microstructures analysed showed the presence of higher carbides concentration in the outside surface.

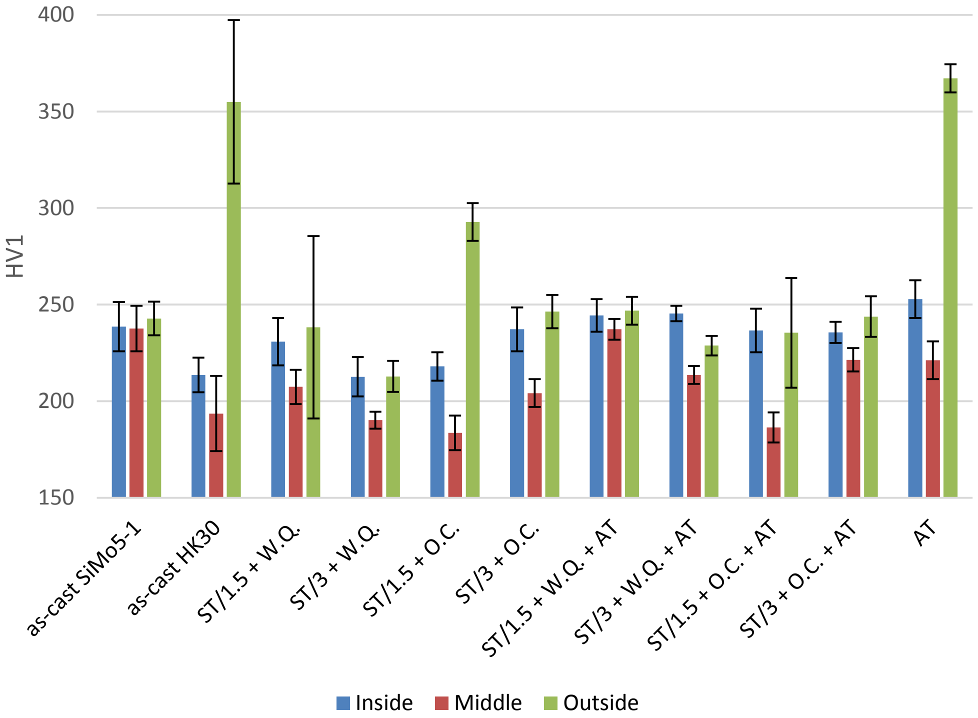

Figure 3-25. *Microhardness measured on matrix obtained for each heat treatment.*

The second main conclusion was already expected before the trial, since applying a solution annealing followed by aging heat treatment result in the highest creep resistance [17], due to the fine dispersed carbides precipitation and consequently, increasing the hardness. Analysing the microstructure and SEM micrographs, is visible a fine carbides dispersion on the matrix, as expected. This precipitation may be the reason for the higher hardness in the sample solution annealed for 1.5 h followed by water quenching and aged for 24 h.

Comparing the micro-hardness obtained for the middle section, this sample presents the highest hardness compared with HK30 samples for the same zone. In the real application the aging treatment is not needed to be applied to promote the precipitation of fine dispersed carbides. Once in service the component will achieve the temperatures needed to promote this precipitation.

The sample ST/3 + W.Q. + AT (Figure 3-25) presents lower average micro-hardness than the sample ST/1.5 + WQ + AT. The only difference between the samples is the solution annealing time. Comparing the microstructures of both (Figure 3-21) the only visible difference is the presence of grain boundary carbides on the ST/1.5 + WQ + AT sample, which may not is the reason of this difference. Both samples present fine dispersed carbides in the matrix, although, longer time at solution annealed temperature, may have resulted in austenite grain boundaries growth and consequently hardness decrease for the sample ST/3 + W.Q. + AT.

The samples ST/1.5 + OC + AT and ST/3 + OC + AT presented lower hardness compared with the sample ST/1.5 + WQ + AT. This can be explained by the slow cooling rate verified in oven, causing carbides precipitation and agglomeration at high temperatures during the slow cooling, reducing the carbon available into the matrix. Consequently, the carbon available for fine dispersed carbides formation (and to increase the hardness) during aging treatment is lower and less carbides will precipitate. From the microstructures (Figure 3-23), lower precipitation is visible compared with the samples quenched in water (Figure 3-21), correlating with referred before. Actually, the sample ST/1.5 + OC + AT does not present any fine dispersed carbide (Figure 3-23, to the left) as referred before. Despite the microstructure of the sample ST/1.5 + OC + AT does not show visible fine carbides dispersion, this sample shows higher hardness than the sample ST/1.5 + OC (Figure 3-24). The cause of this difference may be a fine precipitation occurred during aging near the massive carbides, resulting on a darkest zone of precipitates showed in the Figure 3-23 compared with the Figure 3-19. This further precipitation may result in that hardness increase.

Comparing both samples oven cooling and aged, we can conclude that the hardness is similar (Figure 3-24) due to the higher error range of the sample (ST/1.5 + OC).

The table 3-10 show a factorial analysis of the effect of each parameter or combination of parameters on hardness. From this results, the parameter AT presents the highest influence. Coming back to the Figure 3-24, we can see that sample just aged, shows hardness increase compared with the as-cast state, much higher than the samples which were not aged. Actually, the samples which were not aged show small differences in hardness, regardless the differences on solution annealing time and quenching medium.

The second parameter with higher effect on hardness is the quenching medium. Again from Figure 3-24, looking for the samples aged, the hardness difference is higher comparing the samples with different cooling media but the same solution annealed times than the opposite.

In the third place is the combination of parameters quenching medium and aging time, as have a positive effect on hardness.

Table 3-10. *Calculation of the parameters effect on hardness. Factorial analysis.*

Effect		Hardness
ST	(-Y1+Y2-Y3+Y4-Y5+Y6-Y7+Y8)/4	-6.5
QM	(-Y1-Y2+Y3+Y4-Y5-Y6+Y7+Y8)/4	14
AT	(-Y1-Y2-Y3-Y4+Y5+Y6+Y7+Y8)/4	20.5
STxQM	(+Y1-Y2-Y3+Y4+Y5-Y6-Y7+Y8)/4	-7
STxAT	(+Y1-Y2+Y3-Y4-Y5+Y6-Y7+Y8)/4	-6.5
QMxAT	(+Y1+Y2-Y3-Y4-Y5-Y6+Y7+Y8)/4	12
STxQMxAT	(-Y1+Y3+Y3-Y4+Y5-Y6-Y7+Y8)/4	3

3.5 Cast steels/casting process selection

The Figure 3-26 shows the selection process steps used to select cast steels and casting processes for truck components. The reasons which lead to the selection of each (cast steel and casting process) to produce the truck components were already described in this work.

For both decision centres in the Figure 3-26, when the materials or casting processes do not meet the requirements, the selection process returns to component design. This happens because there is a great need for an interaction between the designer, material specialist and the foundry. The components should be design not just for function but also for manufacturing in order to reduce the occurrence of scrap and to be produce in a higher efficiency manner. Hence, when cast steels and/or casting processes do not meet the function requirements, changes needs to be conducted on the design (shape of the component or thickness alterations, adding ribs to strength, for instance) for producing components which meet the functions and manufacturing needs.

It is not enough meet the design requirements for a material to be selected to produce a component. The manufacturing process requirements have to be included in the material selection due to the manufacturability limitations, castability in this case.

All the parts referred should work together in order to produce components which meet or even exceed the truck industry increasing demands for reducing weight, fuel efficiency, emissions, safety and others.

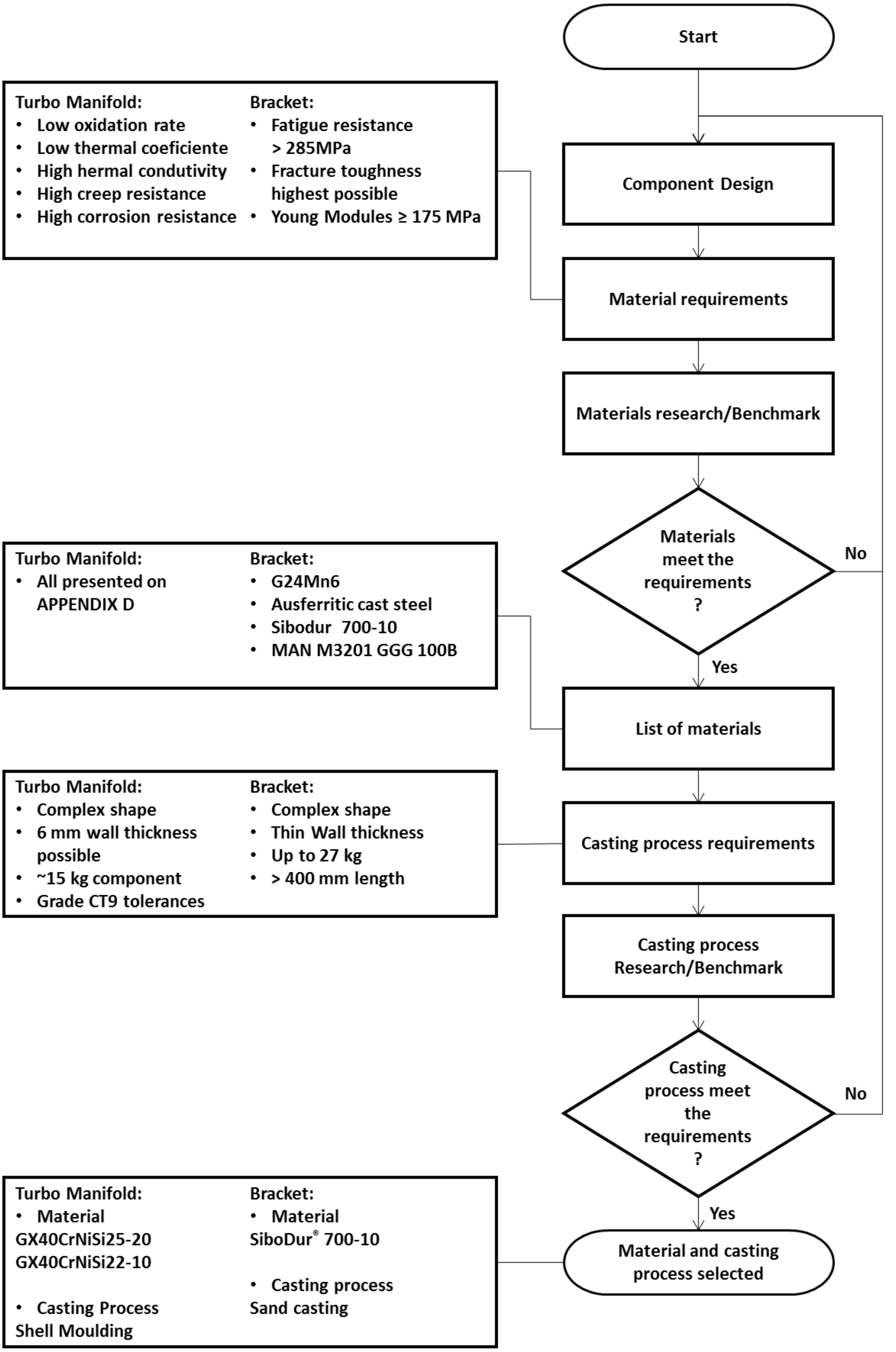

Figure 3-26. *Cast steels and casting processes selection scheme*

4 Conclusions and suggestions

The following conclusions and suggestions are the results of what we believe to be the Scania's benefits in the future.

- Steels can be advantageous when weldability, abrasion resistance, high strength, toughness, high temperature and corrosion resistance are important factors to take into account on the materials selection process.
- Cast steels present lower castability and are more expensive than cast irons.
- For brackets, cast steels do not present any advantages as a weight reduction option.
- Analysis shows that a weight reduction about 20% can be obtained in the new bracket using the patented ductile iron SiboDur® 700-10. This patent will expire within a few years, consequently the price will reduce and the amount of suppliers will increase.
- For turbo manifolds, there are a wide range of cast stainless steels that can be applied successfully.
- It is possible to increase hardness and, consequently, the creep resistance of HK30 alloy through a solution annealing followed by water quenching and aging. The aging treatment will happen naturally in service.
- Adding elements to form carbides, like niobium or titanium, may avoid further chromium precipitation.
- Carbides networks were presented at grain boundaries in the samples analyzed from the prototype HK30 manifold. This could increase the risk for intergranular corrosion and crack initiation.
- Ausferritic cast steel presents a great potential to be used as a lightweight structural material. Fatigue, fracture toughness and wear tests can be applied to this material to study the possibility of applying this material in some chassis truck components.
- It is possible to improve high temperature resistance through some changes in design; proven in simulations conducted at Scania.

Bibliography

[1] Scania, Scania in Brief, Scania, 2013.

[2] V. B. Bhandari, in Introduction to Machine Design, Tata McGraw-Hill Education, 2001, p. 77.

[3] J. R. Davis, Cast Irons, ASM International, 1996, pp. 3, 4, 6, 404.

[4] M. Ekström, “Development of a ferritic Ductile Cast Iron for Increased Life in Exhaust Applications,” KTH Industrial Engineering and Management, Stockholm, 2013.

[5] Atlas Foundry Company, “Understanding Cast Irons,” [Online]. Available: http://www.atlasfdry.com/cast-irons.htm. [Accessed 17 12 2014].

[6] H. Santos (n° 16), “Aula n° 16 - As principais famílias de ferros fundidos - composição química, microestrutura e propriedades; normas ISO,” Faculdade de Engenharia da Universidade do Porto - Internal Document, Porto, 2007.

[7] M. König, “Cast Iron 0727 - Spheroidal graphite iron,” Scania STD510727, Internal Document, Södertälje, 2012.

[8] M. Blair, “Steel Castings,” in Volume 1 - Properties and Selection: Irons, Steels, and High-Performance Alloys, ASM International, 1990, p. 368.

[9] H. Santos (n°7), “Aula n°7 - Aços não ligados de baixo e medio carbono,” Faculdade de Engenharia da Universidade do Porto - Internal Document, Porto, 2007.

[10] H. Santos (n°8), “AULA Nº 8: Aços ligados de baixo e médio carbono,” in Materiais Metálicos, Porto, Faculdade de Engenharia da Universidade do Porto - Internal Document, 2007, pp. 1,2.

[11] S. K. Putatunda, “Influence of austempering temperature on microstructure and fracture toughness of a high-carbon, high silicon and high manganese cast steel,” Materials and Design 24, p. 436, 1 April 2003.

[12] S. K. Putatunda, A. V. Singar, R. Tackett and G. Lawes, “Development of a high strength high toughness ausferritic steel,” Materials Science and Engineering A 513-514, p. 330, 10 February 2009.

[13] D. Melgarejo, “Surface Hardening and Wear Performance of Ausferritic Silicon Steels,” Luleå University of Technology, Luleå, 2007.

[14] P. Guillen and N. Moroz, “Light Weighting With Advanced High Strength Steel Castings,” 2014. [Online]. Available: http://www.autoharvest.org/images/members/detroit_materials/light_weighting_w_cast_AHSS.pdf. [Accessed 29 01 2015].

[15] Detroit Materials, “DM Thin Wall Castable Steels,” [Online]. Available: http://static1.squarespace.com/static/549345b1e4b0ced4156a3af9/t/54944515e4b02bd3dcd46d13/1419003157129/DataSheet+DM+1300-16v1.pdf. [Accessed 18 02 2015].

[16] H. Santos (n°12), “Aula n°12 - Aços inoxidáveis,” Faculdade de Engenharia da Universidade do Porto - Internal Document, Porto, 2007.

[17] J. R. Davis, “Heat-Resistant Materials,” ASM International, 1997, pp. 125, 128, 129, 159, 202, 203, 214.

[18] Engineer's Handbook, “Green Sand Molding,” 2006. [Online]. Available: http://www.engineershandbook.com/MfgMethods/greensandmolding.htm. [Accessed 02 02 2015].

[19] Custompart, 2009. [Online]. Available: http://www.custompartnet.com. [Accessed 19 01 2015].

[20] AFS, Nobake, “Choosing Between Green Sand, Nobake,” 2014. [Online]. Available: http://www.afsinc.org/multimedia/contentMCDP.cfm?ItemNumber=17366. [Accessed 19 01 2015].

[21] Prins, “Croning Casting,” 2014. [Online]. Available: http://www.primepro.eu/en/gietwerk/croning-gietwerk/. [Accessed 18 12 2014].

[22] J. T. Black and R. A. Kohser, DeGarmo's Materials and Processes in Manufacturing, John Wiley Sons, 2011, p. 304.

[23] Grede Casting Integrity, “Lightweighting: Lost Foam,” 2015. [Online]. Available: http://www.grede.com/capabilities/lightweighting-lost-foam.aspx. [Accessed 02 02 2015].

[24] GSL, “Lost Foam - What is it?,” 2015. [Online]. Available: http://www.gsl-lienen.de/2011/cms/upload/download/pdf_eng/GSL_4238_Produktbroschuere_LostFoam_GB.pdf. [Accessed 02 02 2015].

[25] ESP, “Lost Foam Casting,” 2015. [Online]. Available: http://www.espint.com/engineering/best-fit-manufacturing-practices/lost-foam-casting.aspx. [Accessed 02 02 2015].

[26] AFS, Surface Finishes, “Surface finishes for casting processes,” [Online]. Available: http://www.afsinc.org/about/content.cfm?ItemNumber=6915. [Accessed 20 01 2015].

[27] T. L. S. Malcolm Blair, “Supplement 1 - Design rules and Data,” in Steel Castings Handbook, Steel Founders Society of America, 1995.

[28] S. Lampman, Casting Design and Performance, ASM International - The Materials Information Society, 2009, pp. 45, 175.

[29] P. Beeley, Foundry technology (Second Edition), Elsevier, 2001, pp. 425, 427.

[30] J. S. Colton, “Casting Defects and Design Issues,” 2011. [Online]. Available: http://www-old.me.gatech.edu/jonathan.colton/me4210/castdefect.pdf. [Accessed 05 02 2015].

[31] T. L. S. Malcolm Blair, “Supplement 3 - Dimensional Tolerances (Revised),” in Steel Castings Handbook, Steel Founder's Society of America and ASTM International, 2003, pp. 1-33.

[32] C. Dommaschk, “South Africa Institute of foundrymen,” [Online]. Available: www.foundries.org.za/files/defects_cast_steel.ppt. [Accessed 23 01 2015].

[33] L. Xue, M.C. Carter, A.V. Catalina, Z. Lin, C. Lin, C. Li, C. Qiu, “Numerical Simulation of Core Gas Defects in Steel Castings,” American Foundry Society, 2014.

[34] A. I. G. C. Marques, “Diagnóstico de um defeito de fundição - Aplicabilidade da simulação numérica em FLOWCast para previsão e resolução de defeitos,” Faculdade de Engenharia da Universidade do Porto, Porto, 2008.

[35] M. J. Schneider and M. S. Chatterjee, “Introduction to Surface Hardening of Steels,” in ASM Handbook, Volume 4A, Steel Heat Treating Fundamentals and Processes, ASM International, 2013, p. 10.

[36] J. R. Davis, Volume 4 - Heat treating, ASM International, 1991.

[37] J. R. Davis, Volume 4 - Heat treating, ASM International, 1991, pp. 312, 376.

[38] Sandvik, Carburization, “Carburization,” 2015. [Online]. Available: http://www.smt.sandvik.com/en/materials-center/corrosion/high-temperature-corrosion/. [Accessed 09 01 2015].

[39] Corrosion Source, “Carburization,” 2013. [Online]. Available: http://www.corrosionsource.com/(S(hqlagt2nieaigunvm1xmr355))/FreeContent/1/Carburization#Figure. [Accessed 09 01 2015].

[40] H. Santos (n°19), “Aula n°19 - A cementação em meio sólido, líquido e gasoso,” Faculdade de Engenharia da Universidade do Porto - Internal Document, Porto, 2006.

[41] H. Santos (n°20), “Aula n°20 - Nitruração,” Faculdade de Engenharia da Universidade do Porto - Internal Document, Porto, 2006.

[42] Bodycote, Nitriding, “Gas nitriding,” [Online]. Available: http://www.bodycote.com/en/services/heat-treatment/case-hardening-without-subsequent-hardening-operation/gas-nitriding.aspx. [Accessed 09 01 2015].

[43] Metlab, “Nitriding,” 2012. [Online]. Available: http://www.metlabheattreat.com/nitriding.html. [Accessed 09 01 2015].

[44] H. Santos (n°21), “Aula n°21 - Carbonitruração e cianuração,” Faculdade de Engenharia da Universidade do Porto - Internal Document, Porto, 2006.

[45] Bodycote, Induction hardening, “Induction hardening,” [Online]. Available: http://www.bodycote.com/en/services/heat-treatment/harden-and-temper/induction-hardening.aspx. [Accessed 09 01 2015].

[46] Rofin, Laser hardening, “Laser hardening,” 2015. [Online]. Available: http://www.rofin.com/en/applications/surface_treatment/laser_hardening/. [Accessed 09 01 2015].

[47] P. Sherwin, “What is the cost difference between carburizing and nitriding?,” 2010. [Online]. Available: http://blog.eurotherm.com/blog/2010/07/08/what-is-the-cost-difference-between-carburizing-and-nitriding-2/. [Accessed 09 01 2015].

[48] H. Santos (n°8), “Aula n°8 - Recozimento dos aços,” Faculdade de Engenharia da Universidade do Porto - Internal Document, Porto, 2006.

[49] H. Santos (n°10), “Aula n°10 - Têmpera e temperabilidade,” Faculdade de Engenharia da Universidade do Porto - Internal document, Porto, 2006.

[50] H. Santos (n°15), “Aula n°15 - Revenido,” Faculdade de Engenharia da Universidade do Porto - Internal Document, Porto, 2006.

[51] Nunes and e. al., “Austempering of steel,” in Volume 4 - Heat treating, ASM International, 1991.

[52] C. J. Martis, S. K. Putatunda and J. Boileau, “Processing of a new high strength high toughness steel with duplex microstructure (Ferrite + Austenite),” Materials and Design 46, p. 168, 25 October 2012.

[53] A. Leiro, “Microstructure Analysis of Wear and Fatigue in Austempered High-Si Steels,” Luleå University of technology, Luleå, 2014.

[54] Gjuteriföreningen, “Forskningsgrupp Stål,” 2014. [Online]. Available: http://www.gjuteriforeningen.se/svenska/forskn/fou-dag-2014/BA9A869ABC324694AC033370FBD6ED49. [Accessed 18 12 2014].

[55] PM, “Anatomy Of Free Machining Steel,” 2002. [Online]. Available: http://www.productionmachining.com/articles/anatomy-of-free-machining-steel. [Accessed 05 02 2015].

[56] G. Schneider, Cutting Tool Applications - Chapter 3, Southfield: Lawrence Technological University, 2002.

[57] S. L. Kakani, Material Science, New Delhi: New Age International, 2006, pp. 266, 267.

[58] SSINA, “Designer Handbook: Stainless steel for machining,” 2010. [Online]. Available: http://www.ssina.com/download_a_file/machining.pdf. [Accessed 05 02 2015].

[59] Scribd, “CoroKey_2010,” 2014. [Online]. Available: http://www.scribd.com/doc/46193798/CoroKey-2010. [Accessed 19 12 2014].

[60] F. Petersson and P. Landqvist, “Guideline - Simulation driven design of optimized sheet metal bracket,” 2013. [Online]. Available: Scania Guideline - Internal document. [Accessed 08 01 2015].

[61] LLNL, “Welding Science: A New Look at a Fundamental Technology,” 2001. [Online]. Available: https://str.llnl.gov/str/November01/Elmer.html. [Accessed 14 12 2014].

[62] The free Dictionary, “Welded Joint,” 17 12 2014. [Online]. Available: http://encyclopedia2.thefreedictionary.com/Welded+Joint.

[63] NiDI, “A designers' handbook series No9014,” in Design Guidelines for the selection and use of Stainless Steel, American Iron and Steel Institute and Speciality Steel Institute of North America, 2014, p. 16.

[64] Magmaweld, “Schaeffler diagramm,” 2010. [Online]. Available: http://www.magmaweld.com/magmaweld_de/schweissen_von_edelstahlen.html. [Accessed 30 01 2015].

[65] APPS, “Avesta Pickling handbook 2009,” 2014. [Online]. Available: http://www.picklingandpassivation.com.au/SiteFiles/picklingandpassivationcomau/Avesta_Pickling_Handbook_2009_Edition.pdf. [Accessed 17 12 2014].

[66] B. J. D. Swift K. G., Process Selection - From Design to Manufacture, Edward Arnold, 2003, pp. 190-201.

[67] Leonghuat, “Carbon Equivalent,” 2014. [Online]. Available: http://www.leonghuat.com/articles/carbon%20equivalent.htm. [Accessed 17 12 2014].

[68] SIS, Svetsning av stål, MNC handbok 15, Standardiseringskommissionen i Sverige (SIS), 1986.

[69] C. W.F and E. Lui, “Steel Structures,” in Handbook of Structural Engineering, Second Edition, CRC Press, 2005, pp. 4-7.

[70] NiDI, “A Designers' handbook series no 9002,” in Welding of Stainless Steels and other joining methods, American Iron and Steel Institute and Speciality Steel Institute of North America, 2012.

[71] Stainless Steel World, “Weldability,” 2014. [Online]. Available: http://www.stainless-steel-world.net/basicfacts/ShowPage.aspx?pageID=477. [Accessed 18 12 2014].

[72] E. A. Schoefer, “Supplement 7 - Welding of high alloy steel castings,” in Steel Castings Handbook, Steel Founders' Society of America, 2004, pp. 34-45; 90-95.

[73] J. R. Davis, Stainless Steels (ASM Specialty Handbook), ASM International, 1995, pp. 70, 78, 171, 202, 368, 459.

[74] Kubota, “Alloys Data sheets,” [Online]. Available: http://www.kubotametal.com. [Accessed 12 02 2015].

[75] E. L. Elia, 2014. [Online]. Available: http://www.welding-advisers.com/Welding-steel.html. [Accessed 18 12 2014].

[76] Olympus, “Welding overview,” 2014. [Online]. Available: http://www.olympus-ims.com/en/ndt-tutorials/flaw-detection/weld-overview/. [Accessed 17 12 2014].

[77] Outokumpu, Handbook of Stainless steel, Espoo, Finland: Outokumpu Oyj, 2013, pp. 35, 73, 74.

[78] A. K. Elshennawy and G. F. Schrader, Manufacturing Processes and Materials, 4th Edition, SME, 2000, p. 624.

[79] Wirelab, “General Introduction to Shot Blasting,” 2014. [Online]. Available: http://www.wirelab.com/Cym%20Shot%20Blasting%20Info.pdf. [Accessed 18 12 2014].

[80] MIC, “Our Service,” 2014. [Online]. Available: http://www.metalimprovement.co.uk/controlled-shot-peening.html. [Accessed 18 12 2014].

[81] AAMRO, 2014. [Online]. Available: http://www.aamroco.com/shot-peening-metal-components.html. [Accessed 18 12 2014].

[82] Euro Inox, “Pickling and Passivation Stainless Steel, Material and Applications Series Volume 4,” 2007. [Online]. Available: http://www.euro-inox.org/pdf/map/Passivating_Pickling_EN.pdf. [Accessed 26 01 2015].

[83] J. R. Davis, Stainless Steels (ASM Specialty Handbook), ASM International , 1995.

[84] Damstahl, 2012. [Online]. Available: http://www.damstahl.com/Files/Billeder/2011/PDF/UK/chemical_surface_treatment.pdf. [Accessed 18 12 2014].

[85] BSSA, “Paint coating stainless steels,” [Online]. Available: http://www.bssa.org.uk/topics.php?article=119. [Accessed 18 12 2014].

[86] T. D. Bennet and F. Yu, “A nondestructive technique for determining thermal properties of thermal barrier coatings,” Journal of applied physics, 2005.

[87] R. Reidel and I.-W. Chen, “Thermal Barrier Coatings,” in Ceramics Science and Technology, Weinheim, Wiley-VCH Verlag GmbH & Co. KGaA, 2014.

[88] D. D. Vargas Carmona, “Thermal Barrier coatings for Efficient Combustion,” KTH, Stockholm, 2014.

[89] F. B. Ettouil and A. Dolatabadi, “Numerical Study of Suspension Injection in Plasma Spraying Process,” 2014. [Online]. Available: http://users.encs.concordia.ca/~dolat/Research-TS-Areas-TBC.html. [Accessed 18 12 2014].

[90] B. Christoffer, “Thermal Barrier Coatings for diesel engine exhaust application,” Karlstad University, Department of Engineering and Physics, Karlstad, 2014.

[91] D. W. Parker, “Thermal barrier coatings for gas turbines, automotive engines and diesel equipment,” Materials & design, Volume 13, Issue 6, pp. 345-351, 1992.

[92] S. J. Ko and Y.-J. Kim, “High temperature fatigur behaviors of cast ferritic stainless steel,” Material Science and Engineering A 534(2012), pp. p. 7-12, 2011.

[93] T. Gocmez and U. Deuster, “Designing Exhaust Manifolds Using Integral Engineering Solutions,” 2009. [Online]. Available: http://www.fev.com/fileadmin/user_upload/Media/TechnicalPublications/Design/ExhaustManifoldDesign.pdf. [Accessed 29 01 2015].

[94] R. B. Dooley and A. Bursik, “Corrosion fatigue,” in Boiler and HRSG tube failures, PowerPlant Chemistry , 2009, p. 586.

[95] Volkspage, “Motor Vehicle Exhaust Emissions,” 2014. [Online]. Available: http://www.volkspage.net/technik/ssp/ssp/SSP_230.pdf. [Accessed 18 12 2014].

[96] B. Boardman, “Fatigue resistance,” in Volume 1 - Properties and Selection: Irons, Steels, and High-Performance Alloys, ASM International, 1990, pp. 673-680.

[97] R. Larker, “Fracture toughness, impact energy and ductility of spheirodal graphite cast irons,” Annex F for EN 1563:2012, pp. 1, 2, 2012.

[98] W. B. a. P. G. J. K.E. Mckinney, “An Evaluation of the Toughness of Ductile Iron vs Cast Steel Using Modified Charpy Test Specimens,” AFS Transitions, pp. 248, 250.

[99] W. L. Bradley, “Toughness Properties of Nodular Iron,” Journal of Metals, pp. 75, 76, January 1985.

[100] Hitachi, “Engine/exhaust components, Hercunite® series,” [Online]. Available: http://www.hitachi-metals.co.jp/e/products/auto/. [Accessed 13 01 2015].

[101] P. Weissler, “Hyundai develops one-piece exhaust manifold-turbo housing,” 2010. [Online]. Available: http://articles.sae.org/9095/. [Accessed 13 01 2015].

[102] GF Automotive, “Commercial vehicles,” [Online]. Available: http://www.gfau.com/content/gfau/com/en/products-and-solutions/commercial-vehicle.html. [Accessed 11 02 2015].

[103] SAE INTERNATIONAL , “Lightweighting with iron,” Automotive Engineering International, pp. 25-27, 2013.

[104] Foundry Management & Technology, “Foundry Management & Technology,” An Extra Dose of Chemistry for Iron That's Hard and Ductile, 11 September 2008. [Online]. Available: http://foundrymag.com/feature/extra-dose-chemistry-iron-thats-hard-and-ductile. [Accessed 11 02 2015].

[105] J. W. Nichols, “Grede offers iron as lightweighting option,” 2013. [Online]. Available: http://articles.sae.org/12526/. [Accessed 13 01 2015].

[106] A. Rimmer, E. Muratore, X. Yong and E. Veneri, “ADI solutions in Europe,” 2009. [Online]. Available: http://www.foundrytradejournal.com/pdf/archive/July-Aug%2009%20-%20ADI%20p184-189.pdf. [Accessed 02 02 2015].

[107] H. Sieurin och E. Tolf, ”Guideline för design av gjutna & smidda komponenter: version 1,” Scania Technical Report 7019798, Internal document, Södertälje, 2013.

[108] S. K. Putatunda, “Influence of austempering temperature on microstructure and fracture toughness of a high-carbon, high-silicon and high-manganese cast steel,” Materials and Design 24, p. 435, 1 April 2003.

[109] M. Ekström, “Development of a ferritic Ductile Cast Iron for Increased Life in Exhaust Applications,” KTH Industrial Engineering and Management, Stockholm, 2013.

[110] J. R. Davis, Heat-Resistant Materials, ASM International, 1997, pp. 202, 214.

[111] J. C. L. a. W. F. Savage, “Solidification of Austenitic Stainless Steels Weldments - Part I - A Proposed Mechanism,” in AWS 60th Annual, Detroit, 1979.

[112] H. Santos (n° 14), “AULA nº 14 - Aços inoxidáveis austeníticos,” Faculdade de Engenharia da Universidade do Porto - Internal Document, Porto, 2007.

[113] M. Ekström, “High-temperature mechanical and fatigu eproperties of cast alloys intended for use in exhaust manifolds,” Materials Science & Engineering, p. 81, 2014.

[114] R. G. K. R. G. Laird, “Abrasion-Resistant Cast Iron Handbook,” American Foundry Society, 2000.

[115] T. Sourmail, “Precipitation in creep resistant austenitic stainless steels,” Materials Science and Technology Vol. 17, pp. 7, 76, 77, January 2001.

[116] M. M. F. Barbosa, “Cold Spray Deposition of Titanium onto Aluminium Substrates,” Porto, 2009.

[117] M. F. McGuire, Stainless Steels for Design Engineers, ASM International, 2008, p. 77.

[118] S. G. Ledell, “Utmattning av gjutstål,” Swerea, Jönköping, 2002.

[119] P. Guth, “Utmattningsdata för gjutstål,” Swerea, Jönköping, 2008.

[120] T. L. S. Malcolm Blair, “Supplement 5 - General properties of steel castings,” in Steel Casting Handbook, Steel Founders' Society of America, 1985, p. 26.

[121] “SS - EN ISO 8062-3:2007,” Geometrical Product Specifications (GPS) – Dimensional and geometrical tolerances for moulded parts - Part 3: General dimensional and geometrical tolerances and machining allowances for castings, pp. 1-17, 03 09 2007.

APPENDIX A 1

Chemical composition

General engineering and high-strength cast steels SS-EN 10293:2005

Material designation	**C %**	**Si %**	**Mn %**	**P % max**	**S % max**	**Cu % max**	**Ni %**	**Mo %**	**Cr %**
G20Mn5+N	0.17 - 0.23	max 0.60	1.00 - 1.60	0.020	0.020 [a)]	0.30	max 0.80	-	-
G24Mn6	0.20 - 0.25	max 0.60	1.50 - 1.80	0.020	0.015	-	-	-	-
G26CrMo4	0.22 - 0.29	max 0.60	0.50 - 0.80	0.025	0.020	-	-	0.15 - 0.30	0.80 -1.20
G28Mn6 +N	0.25 - 0.32	0.60	1.20 - 1.80	0.035	0.030	-	-	-	-
G34CrMo4	0.30 - 0.37	0.60	0.50 - 0.80	0.025	-	-	-	0.15 - 0.30	0.80 - 1.20
GS22MnCrMo5	0.22	0.30	1.00	-	-	-	-	0.25	1.20
G42CrMo4	0.38-0.45	max 0,6	0.6-1.00	0.025	0.020	-	-	0.15-0.30	0.8-1.20
G30NiCrMo14	0.27-0.33	0.6	0.6-1.00	0.030	0.020	-	3.00-4.00	0.3-0.6	0.8-1.20

a) For casting of thickness < 28 mm, a sulphur content max 0.030 % is allowed.

APPENDIX A 2

Chemical composition

Heat resistant steel castings SS-EN10295:2002, SS-EN10095

Material designation	**C %**	**Si %**	**Mn %**	**P % max**	**S % max**	**Ni %**	**Mo %**	**Cr %**	**Nb %**	**Other**
GX40CrNiSi22-10	0.30 - 0.50	1.00 - 2.50	max 2.00	max 0.040	max 0.030	9.00 - 11.0	max 0.50	21.0 - 23.0	-	
GX40CrNiSi25-20	0.30 - 0.50	1.00 - 2.50	max 2.00	0.040	0.030	19.0 - 22.0	max 0.50	24.0 - 27.0	2.50 - 3.00	**W %** 3.00 - 3.50
GX40CrNiSiNb24-24	0.30 - 0.50	1.00 - 2.50	max 0.20	0.040	0.030	23.0 - 25.0	max 0.50	23.0 - 25.0	0.80 - 1.80	
X6CrNiNb18-10	0.080	1.00	2.00	0.045	0.030	9.00 - 12.0	-	17.0 - 19.0	10xC	
X10CrAlSi25	0.12	0.70 - 1.40	-	-	-	-	-	23.0 - 26.0	-	**Al %** 1.20 - 1.70
X9CrNiSiNCe21-11-2	0.05 - 0.12	0.70 - 1.40	-	-	-	10.0 - 12.0	-	20.0 - 22.0	-	**N %** 0.12 - 0.20
X15CrNiSi25-21	0.20	1.50 - 2.50	-	-	-	19.0 - 22.0	-	24.0 - 26.0	-	

APPENDIX B

Steel castings for general engineering SS-EN 10293:2005

Material designation			Tensile strength SS-EN 10002-1					Hardness HB SS-EN ISO 6506	Impact strength SS-EN 10045-1	
Name	Number	Heat treatment a)	Thickness t [mm]	Tensile strength R_m [MPa] min	Yield strength $R_{p0,2}$ [MPa] min	Fatigue limit [Mpa]	Elongation A [%] min		T [°C]	KV [J] Min
G20Mn5	1.6220	+N	≤ 30	480 - 620	300	244 ±7 b)	20	140 - 183	-30 RT f)	27 50
G24Mn6	1.1118	+QT3	≤ 150	600 - 800	400	∞ 345 c)	18	176 – 238 e)	-30	27
G26CrMo4	1.7221	+QT1	≤ 100	600 - 750	450	-	16	176 – 219 e)	RT	40
			100 < t ≤ 250	550 - 700	300	-	14	152 – 204 e)	RT	27
G28Mn6	1.1165	+N	≤ 250	520 - 670	260	241 d)	18	152 – 195 e)	RT	27
		+QT1	≤ 100	600 - 750	450	-	14	176 – 219 e)	RT	35
Reference	Cast Iron 0727	-	-	500 - 720	320 - 440	285	7	170 - 230	RT	7-17

a) + N means: Normalizing, + QT or + QT1 or + QT2 means: Quenching (air or liquid) + Tempering
b) Swerea report 020531 Utmattning av gjutstål, Stefan Gustavsson Ledell [118]
c) Swerea report 081220 Utmattningsdata för gjutstål, Pär Guth with data for ∞ [119]
d) Data from Steel Castings Handbook, Supplement 5, Table 2 based on tensile strength [120]
e) Conversion table for unalloyed, low alloy steels and cast steel, Annex A, SS-EN ISO 18265:2013
f) Room temperatur

APPENDIX C

High-strength cast steels SS-EN 10293:2005

Material designation			Tensile strength SS-EN 10002-1					Hardness HB SS-EN ISO 6506	Impact strength SS-EN 10045-1	
Name	Number	Heat treatment a)	Thickness t [mm]	Tensile strength R_m [MPa] min	Yield strength $R_{p0,2}$ [MPa] min	Fatigue limit [Mpa] (50 % Failure at 100000 cycles amp) c)	Elongation A [%] min		T [°C]	KV [J] Min
G24Mn6	1.1118	+QT1	≤ 50	700 - 800	550	∞ 345 b)	12	204 – 238 d)	-30	27
		+QT2	≤ 100	650 - 800	500	-	15	190 – 238 d)	-30	27
G26CrMo4	1.7221	+QT2	≤ 100	700 - 850	550	310 c)	10	204 – 252 d)	RT e)	18
G28Mn6	1.1165	+QT2	≤ 50	700 - 850	550	310 c)	10	204 – 252 d)	RT	31
G34CrMo4	1.7230	+QT1	≤ 100	700 - 850	540	310 c)	12	204 – 252 d)	RT	35
			100 < t ≤ 150	620 - 770	480	-	10	181 – 228 d)	RT	27
		+QT2	≤ 100	830 - 980	650	-	10	242 – 285 d)	RT	27
G42CrMo4	1.7231	+QT2	≤ 100	850-1000	700	427	10	252-295 d)	RT	27
G30NiCrMo14	1.6771	+QT2	≤ 50	1100-1250	1000	510	7	323-390 d)	RT	20
Reference	Cast Iron 0727	-	-	500 - 720	320 - 440	(285)	7	170 - 230	RT	

a) + N means: Normalizing, + QT or + QT1 or + QT2 means: Quenching (air or liquid) + Tempering

b) Swerea report 081220 Utmattningsdata för gjutstål, Pär Guth with data for ∞[119]

c) Data from Steel Castings Handbook, Supplement 5, Table 2 based on tensile strength [120]

d) Conversion table for unalloyed, low alloy steels and cast steel, Annex A, SS-EN ISO 18265:2013

e) Room temperature

APPENDIX D

Heat resistant steel castings SS-EN10295:2002, SS-EN10095

Material designation			Tensile strength SS-EN 10002-1			Hardness HB SS-EN ISO 6506	Creep resistans [MPa] at 700/900°C at 100000h			CTE, linear [µm/m-°C]			Thermal conductivity [W/(m·K)]		T_a max [°C]
Name (γ-Fe) - Austenitic (α-Fe) - Ferritic	Number	Heat treatment [a]	Tensile strength R_m [MPa] min	Yield strength $R_{p0,2}$ [MPa] min	Elongation A [%] min		σ_r		$\sigma_{1\%}$	400°C	800°C	1000°C	At 20°C	At 500°C (800°C)	
							100h	1000 h	1000 0						
GX40CrNiSi22-10 (γ-Fe)	1.4826	No	450	230	8	200	-	-	46 10	17.2	18.3	18.8	14	(25.4)	950
GX40CrNiSi25-20 (γ-Fe)	1.4848	No	450	220	8	170	100 47	80 28	65 17	17	18	19	14.6	(25)	1100
GX40CrNiSiNb24-24 (γ-Fe)	1.4855	No	450	220	4	-	170 60	125 45	80 22	16.8	18	18.5	14	(24.5)	1050
X6CrNiNb18-10 (γ-Fe)	1.4550	No	510 – 740 b)	205 b)	35b)	230 b)	-	-	-	-	-	-	-	-	925 [c]
X10CrAlSi25 (α-Fe)	1.4762	+A	520 - 720	280	10 - 15	223	-	17 3.6	4.7 1.0	11.5	12.0	13.5	17	23	1150 [e]
X9CrNiSiNCe21-11-2 (γ-Fe)	1.4835	+AT	650 - 850	310	25 [d]	210	-	105 24	45 10	18.0	19.0	19.5	15	21	1150
X15CrNiSi25-21 (γ-Fe) (HK30)	1.4841	+AT	550 - 750	230	10 [d]	170	-	90 20	35 4	17.0	18.0	19.0	15	19	1150 [e]
Reference	SiMo51	-	550	450	7	200 - 250	-	-	-	-	-	-	-	-	750

a) + A means: Annealed, + AT means: Solution annealed, b) Metalcor Datasheet c) ASM Specialty Handbook: Heat Resistant Materials, d) A297/A297M-10 Standard Specification for Steel Castings, Iron-Chromium and Iron-Chromium-Nickel, Heat Resistant, for General Application, c) The loss of metal caused by scaling does not exceed 1g/m²·h at T_a, and does not exceed 2g/ m² at Ta+50°C on average for period of 120 h with 4 intermediate cooling

APPENDIX E

Comparison of casting processes advantages and disadvantages

	Green Sand	**Nobake**	**Shell Mold**	**Investment**
Part size: *(Depends on the capacity and material selection of the foundry)*	Weight: 28 g - 408 ton	Weight: 28 g - 408 ton	Weight: 14 g – 100 kg, but better for parts less than 20 kg	Weight: up to 100 kg, but best for parts less than 5 kg
Materials: (*Depends on the capacity and material selection of the foundry)*	Alloy Steel, Carbon Steel, Cast Iron, Stainless Steel, Aluminium, Copper, Magnesium, Nickel	Stainless steel, carbon steel, heat-resistant steel, super alloys, aluminium, ductile iron, gray iron, magnesium alloys	Alloy Steel, Carbon Steel, Cast Iron, Stainless Steel, Aluminium, Copper, Nickel	Alloy Steel, Carbon Steel, Stainless Steel, Aluminium, Copper, Nickel
Advantages:	Can produce very large parts, Can form complex shapes, Many material options, Low tooling and equipment cost, Scrap can be recycled, Short lead time possible	Better surface finish than green sand, consistency, fill in deep or wide molds	Can form complex shapes and fine details, Very good surface finish, High production rate, Low labour cost, Low tooling cost, Little scrap generated, better mechanical properties than sand casting, moderate porosity and inclusions	Can form complex shapes and fine details, Many material options, High strength parts, Very good surface finish and accuracy, Little need for secondary machining, Moderate porosity
Disadvantages:	Poor material strength, High porosity possible, Poor surface finish and tolerance, Secondary machining often required, Low production rate, High labour cost	Cost of resins and binders, speed to produce quantities	High equipment cost	Time-consuming process, High labour cost, High tooling cost, Long lead time possible, Grain growth more pronounced in longer sections, limiting the toughness and fatigue life
Applications:	Engine blocks and manifolds, machine bases, gears, pulleys	Anything that can be cast in a green sand mold can be cast with a chemically bonded mold	Cylinder heads, connecting rods	Turbine blades, armament parts, pipe fittings, lock parts, hand tools, jewelry

APPENDIX F

Machining allowances for steel castings - ISO 8062 [121]

Largest dimension [mm]		**Required machining allowance [mm]** **Note: A minimum of 6 mm RMA required on all cope casting surfaces**					
Over	**Up to and including**	**Required machining allowance grade**					
		E	F	G	H	J	K
-	40	0.4	0.5	0.5	0.7	1	1.4
40	63	0.4	0.5	0.7	1	1.4	2
63	100	0.7	1	1.4	2	2.8	4
100	160	1.1	1.5	2.2	3	4	6
160	250	1.4	2	2.8	4	5.5	8
250	400	1.8	2.5	3.5	5	7	10
400	630	2.2	3	4	6	9	12
630	1000	2.5	3.5	5	7	10	14
1000	1600	2.8	4	5.5	8	11	16
1600	2500	3.2	4.5	6	9	13	18
2500	4000	3.5	5	7	10	14	20
4000	6300	4	5.5	8	11	16	22
6300	10000	4.5	6	9	12	17	24
Sand casting, hand molded → use grade G — K Sand casting, machine molded (and shell) → use grade F — H Investment casting → use grade E							

APPENDIX G

Casting dimensional tolerance grades [121]

Raw casting basic dimensions [mm]		**Total casting tolerance [mm]**											
Over	**Up to & including**	**Casting tolerance grade CT**											
		5	**6**	**7**	**8**	**9**	**10**	**11**	**12**	**13**	**14**	**15**	**16**
-	10	0.36	0.52	0.74	1.0	2.0	2.0	2.8	4.2	--	--	--	--
10	16	0.38	0.54	0.78	1.1	1.6	2.2	3.0	4.4	--	--	--	--
16	25	0.42	0.58	0.82	1.2	1.7	2.4	3.2	4.6	6.0	8.0	10	12
25	40	0.46	0.64	0.90	1.3	1.8	2.6	3.6	5.0	7.0	9.0	11	14
40	63	0.50	0.70	1.0	1.4	2.0	2.8	4.0	5.6	8.0	10	12	16
63	100	0.56	0.78	1.1	1.6	2.2	.32	4.4	6.0	9.0	11	14	18
100	160	0.62	0.88	1.2	1.8	2.5	3.6	5.0	7.0	10	12	16	20
160	250	0.70	1	1.4	2.0	2.8	4.	5.6	8.0	11	14	18	22
250	400	0.78	1.1	1.6	2.2	3.2	4.4	6.2	9.0	12	16	20	25
400	630	0.90	1.2	1.8	2.6	3.6	5.0	7.0	10	14	18	22	28
630	1000	1.0	1.4	2.0	2.8	4	6.0	8.0	11	16	20	25	32
1000	1600	--	1.6	2.2	3.2	4.6	7.0	9.0	13	18	23	29	37
1600	2500	--	--	2.6	3.8	5.4	8.0	10	15	21	26	33	42
2500	4000	--	--	--	4.0	6.2	9.0	12	17	24	30	38	49
4000	6300	--	--	--	--	7.0	10	14	20	28	35	44	56
6300	10000	--	--	--	--	--	11	16	23	32	40	50	64

APPENDIX H 1

Casting geometrical tolerances grades [121]

Method	**GCTG grade**
Sand cast, hand moulding	6 to 8
Sand cast machine moulding and shell moulding	5 to 7
Investment casting	4 to 6[1]

1 – For investment castings, geometrical tolerances are related with the largest overall dimension: ≤100mm: Grade 4 to 6, >100 ≤400mm: Grade 4 to 8 , >400mm: Grade 4 to 9

Casting Tolerances for straightness in mm [121]

Raw casting basic dimensions [mm]		**Total casting tolerance [mm]**						
Over	**Up to and including**	**Straightness tolerances for geometrical casting tolerance grade (GCTG)**						
		2	**3**	**4**	**5**	**6**	**7**	**8**
--	10	0.08	0.12	0.18	0.27	0.40	0.60	0.90
10	30	0.12	0.18	0.27	0.40	0.60	0.90	1.4
30	100	0.18	0.27	0.40	0.60	0.90	1.4	2.0
100	300	0.27	0.40	0.60	0.90	1.4	2.0	3.0
300	1000	0.40	0.60	0.90	1.4	2.0	3.0	4.5
1000	3000	--	--	--	3.0	4.0	6.0	9.0
3000	6000	--	--	--	6.0	8.0	12	18
6000	10000	--	--	--	12	16	24	36

APPENDIX H 2

Casting tolerances for flatness in mm [31]

Raw casting basic dimensions [mm]		**Total casting tolerance [mm]**						
Over	**Up to and including**	**Flatness tolerances for geometrical casting tolerance grade (GCTG)**						
		2	**3**	**4**	**5**	**6**	**7**	**8**
--	10	0.12	0.18	0.27	0.4	0.6	0.9	1.4
10	30	0.18	0.27	0.4	0.6	0.9	1.4	2.0
30	100	0.27	0.4	0.6	0.9	1.4	2.0	3.0
100	300	0.4	0.6	0.9	1.4	2.0	3.0	4.5
300	1000	0.6	0.9	1.4	2.0	3.0	4.5	7.0
1000	3000	--	--	--	4.0	6.0	9.0	14
3000	6000	--	--	--	8.0	12	18	28
6000	10000	--	--	--	16	24	36	56

APPENDIX H 3

Casting tolerances for roundness, parallelism, perpendicularity and symmetry in mm [31]

Raw casting basic dimensions [mm]		**Total casting tolerance [mm]**						
Over	**Up to and including**	**Tolerances for geometrical casting tolerance grade (GCTG)**						
		2	**3**	**4**	**5**	**6**	**7**	**8**
--	10	0.18	0.27	0.40	0.60	0.90	1.4	2.0
10	30	0.27	0.40	0.60	0.90	1.4	2.0	3.0
30	100	0.40	0.60	0.90	1.4	2.0	3.0	4.5
100	300	0.60	0.90	1.4	2.0	3.0	4.5	7.0
300	1000	0.90	1.4	2.0	3.0	4.5	7.0	10
1000	3000	--	--	--	6.0	9.0	14	20
3000	6000	--	--	--	12	18	28	40
6000	10000	--	--	--	24	36	56	80

APPENDIX H 4

Casting tolerances for coaxiality in mm [31]

Raw casting basic dimensions [mm]		**Total casting tolerance [mm]**						
Over	**Up to and including**	**Tolerances for geometrical casting tolerance grade (GCTG)**						
		2	**3**	**4**	**5**	**6**	**7**	**8**
--	10	0.27	0.40	0.60	0.90	1.4	2.0	3.0
10	30	0.40	0.60	0.90	1.4	2.0	3.0	4.5
30	100	0.60	0.90	1.4	2.0	3.0	4.5	7.0
100	300	0.90	1.4	2.0	3.0	4.5	7.0	10
300	1000	1.4	2.0	3.0	4.5	7.0	10	15
1000	3000	--	--	--	9.0	14	20	30
3000	6000	--	--	--	18	28	40	60
6000	10000	--	--	--	36	56	80	120

APPENDIX I 1

Comparison of case hardness

Process	**Nature of case**	**Process temperature [°C]**	**Typical depth [mm]**	**Case hardness HRC**	**Typical metals**	**Process**
Surface hardening						
Carburizing a) b) (Gas)	Diffused carbon	815 – 980	0.075 – 1.5	Up to 63	Low-carbon steels, low carbon alloy steels	Good control of case depth, suitable for continuous operation, good gas controls required, can be dangerous
Nitriding a) (Gas)	Diffused nitrogen, nitrogen compounds	480 – 590	0.125 – 0.75	50 – 70	Alloy steels, nitriding steels, stainless steels	Hardest cases from nitriding steels, quenching not required, low distortion, process is slow, is usually a batch process
Carbonitriding	Diffusion of nitrogen and carbon	550 - 900	0.075		Steels, stainless steels	Low distortion compared with carburizing, lower risk of embrittlement by grain growth
Induction hardening a) c) d) e)	Alternating current to the coil	870 - 900 (230 - 265 V) (20 – 60 mm/s)	0.72 – 3	37 - 58	Carbon and alloy steels with a carbon content in the range 0.40 - 0.45 %	Hard, highly wear-resistant surface, good bending fatigue strength, fair resistance to seizure, fair dimensional control possible, fair freedom from quench cracking, low-cost steels usually satisfactory, medium capital investment required
Laser hardening f)	Laser beam	900 - 1400	0.1 - 1.5	27 - 60	Ferrous materials including steels and cast iron	Low power densities, laser beam with a round focus makes it possible to produce hardened tracks up to 60 mm wide

(a) ASM International Surface Hardening of Steels: Understanding the Basics (#06952G)
(b) Requires quench from austenitizing temperature
(c) Development of induction surface hardening process for small diameter carbon steel specimens 2009 ISSN 1097-0002
(d) http://www.metlabheattreat.com/induction-flame-hardening.html
(e) Relationship Between Case Depth and Hardness in an Induction Hardened Medium Carbon Steel
(f) http://www.us.trumpf.com

APPENDIX I 2

Comparison of case hardness

Process	**Nature of case**	**Process temperature [°C]**	**Typical depth [mm]**	**Case hardness HRC**	**Typical metals**	**Process**
Bulk heat treatment						
Austempering [a]	Isothermal transformation	790 - 915 Quenching bath 260 - 400	0.1 – 12.5	35 - 55	Ferrous materials including steels and cast iron, ADI	Less distortion and no cracking during quenching, materials gain strength and toughness, more wear resistant,
Aging [b]	Precipitation of carbides	760 - 980	-	Up to 60	Heat resistant Stainless steels	high tensile strengths, restore the equilibrium, greatly reduce the resilience and ductility of alloys
Normalizing [c] [d]	Heat treatment with cooling in air	880 - 980	f)	25 - 32	Austenitized ferrous alloys	Provides uniformity in grain size, gives harder and stronger steel
Quenching [e]	Cooling by air, gases, oil or liquid	880 - 980	-	-	Quenched and tempered steels	Minimizing residual stress and distortion while achieving mechanical properties (hardness, tensile strength, fracture toughness, etc.)
Tempering [c] [e]	Low temperature heat treatment	600 - 750	f)	45 - 65	Quenched and tempered steels	Increases ductility and toughness of a material, tempering generally reduces strength, minimizes cracking, and increases workability, decrease hardness

(a) Austempering of steel, Kenough, John R, The Metal Works Industrial Furnaces
(b) http://www.azom.com/article.aspx?ArticleID=9547
(c) http://www.pennsylvaniasteel.com/heat-treatment.php
(d) EN 10293:2005
(e) http://www.bodycote.com
(f) Depending on wall thickness and alloy

APPENDIX J

Work procedure / Process flow at Scania product development.

Work procedure / Process Flow	**Responsible**
Basis Life expectancy, load cases, interface, design volume, choice of production, construction adaptation. Classification of component (determines the extent of testing / verification)	Design Engineer Purchase
Material choice 1 Selection of materials and material parameters for calculation (aluminium / steel / cast iron)	Design Engineer
Design Volume Geometrically limited by other components	Design Engineer
Topology optimization Topology optimization (also known structure optimization) determines the optimal design and load paths for the current limitation volume and the set load cases. This is done with a simple linear FE model based on the design volume. Important to consider all load cases, even smaller loads as traditional shape optimization would be considered irrelevant. A minimum wall thickness should be included	Calculation Engineer Design Engineer
CAD model 1 Created from topology optimization. Parting line is defined (only cast)	Design Engineer
Castability / Malleability Consider parting line, draft	Design Engineer
Machinability Investigate whether the design is machinable. Clamping surfaces, pilot holes (processing index, machinability index)	Production
Surface treatment Investigate whether the design can / should be surface treated to achieve corrosion protection / finishes, see STD4111	Design Engineer UTMR
Surface hardening Investigate the needs of the design is possible, for example, induction harden	Design Engineer UTMN
Material choice 2 Investigate whether the weight / cost can be saved by choosing a more high-strength / lighter materials.	Purchase Design Engineer
CAD model 2 Update on the basis of castability / malleability / processing / finishing / surface hardening	Design Engineer
Casting simulation / Forge Simulation 1 Form filling and solidification analysis to identify the risk of defects based on the CAD model 2	UTMB
Design and production briefing Go-ahead to develop prototype from design, assembly, processors, surface treatment, purchase. The test assembly of plastic mock-up.	Design Engineer Production Purchase
Shape Optimization Calculation of the CAD model 2 and verification of allowable loads. If necessary, changed the geometry to reduce tension in hotspots.	Calculation Engineer Design Engineer
CAD model 3 Update from shape optimization and casting simulation 1	Design Engineer
Casting simulation 2 (advanced) Gating system, material properties are optimized within / from stressed areas and porosity and slag inclusions minimized.	UTMB
CAD model 4 Update from casting simulation 2	Design Engineer
Milestone 1: Optimized component	Design Engineer
Prototype Investigate the need for prototyping, guided by the classification. Some items may be accepted only from simulation results.	Design Engineer
Casting model for the prototype Take the casting model in series or hand shaping. Consultation with the purchase. At least 10 weeks of delivery. Ensure that the machining allowances on the surfaces to be machined.	Foundry Purchase
Casting / Forging of prototype	Foundry/Forge
Machining of prototype	Production
Surface hardening of prototype	Production
Surface treatment & painting of prototype	Production
Milestone 2: Prototype made	Design Engineer
Materials Investigations (castings, see e.g. STD4100)	UTMB
Approval of the prototype alternatively recasting / reforging Clearance from casting defect investigation and geometry measurement.	Design Engineer
Testing of the prototype Testing the design loads	Strength test
Milestone 3: Prototype tested / verified	Design Engineer
Approval: Yes / No	Design Engineer

APPENDIX K

Microstructure of SiMo51 in the as-cast state

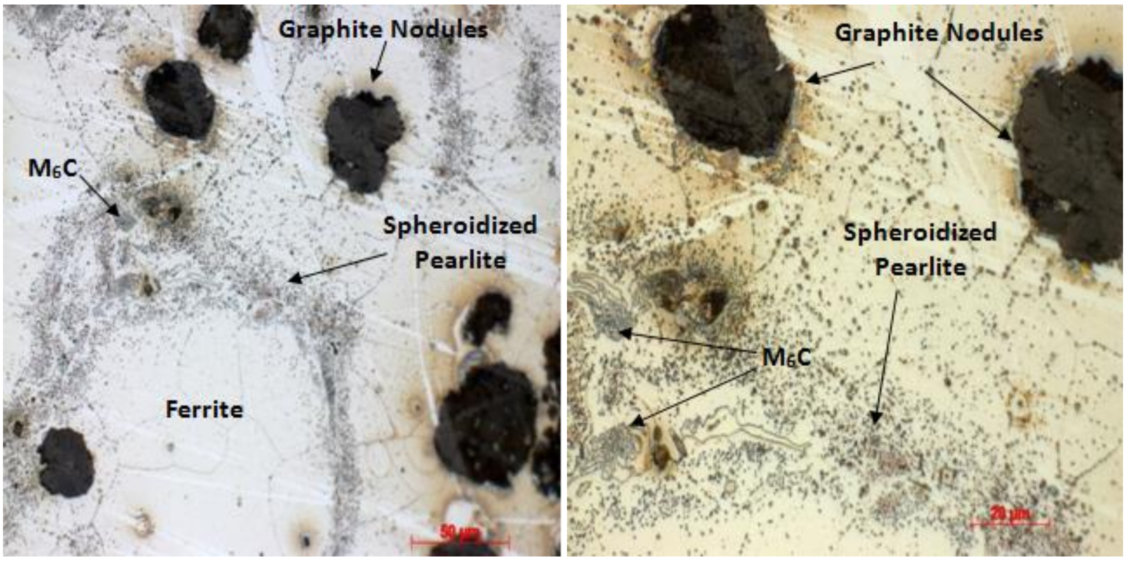

To the left: Microstructure of SiMo51 sample in the as-cast state composed by graphite nodules surrounded by a ferritic matrix, M6C carbides and intercellular spheroidized pearlite. Objective - 50X; Nital 2% etch. To the right: Microstructure obtained in the same sample as to the left with higher magnification. Objective 100X; Nital 2% etch.

APPENDIX L 1

X-ray microanalysis performed in the matrix near grain boundary carbides (sample ST/1.5 + WQ)

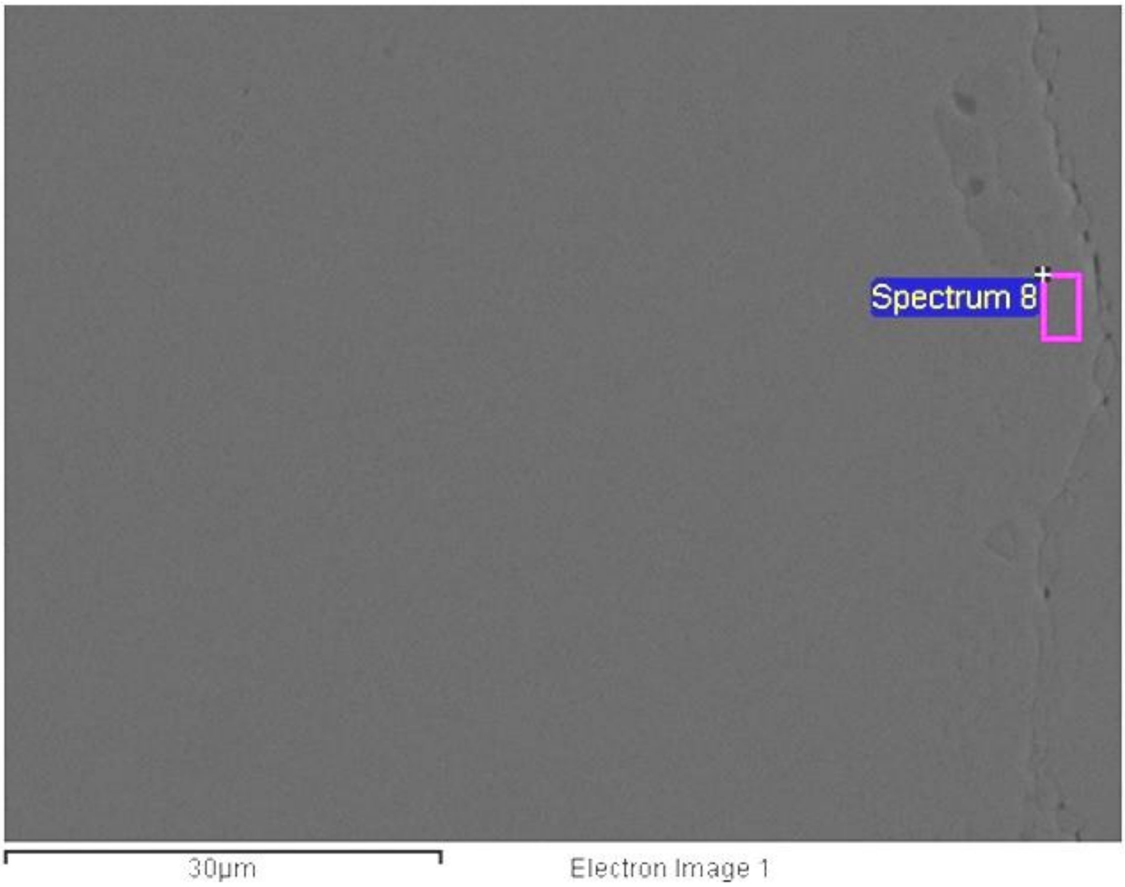

Element	Weight%	Atomic%
Si K	1.58	3.06
Cr K	26.33	27.57
Mn K	1.00	0.99
Fe K	52.23	50.90
Ni K	18.87	17.49
Totals	100.00	

APPENDIX L 2

X-ray microanalysis performed in the matrix far from carbides (sample ST/1.5 + WQ)

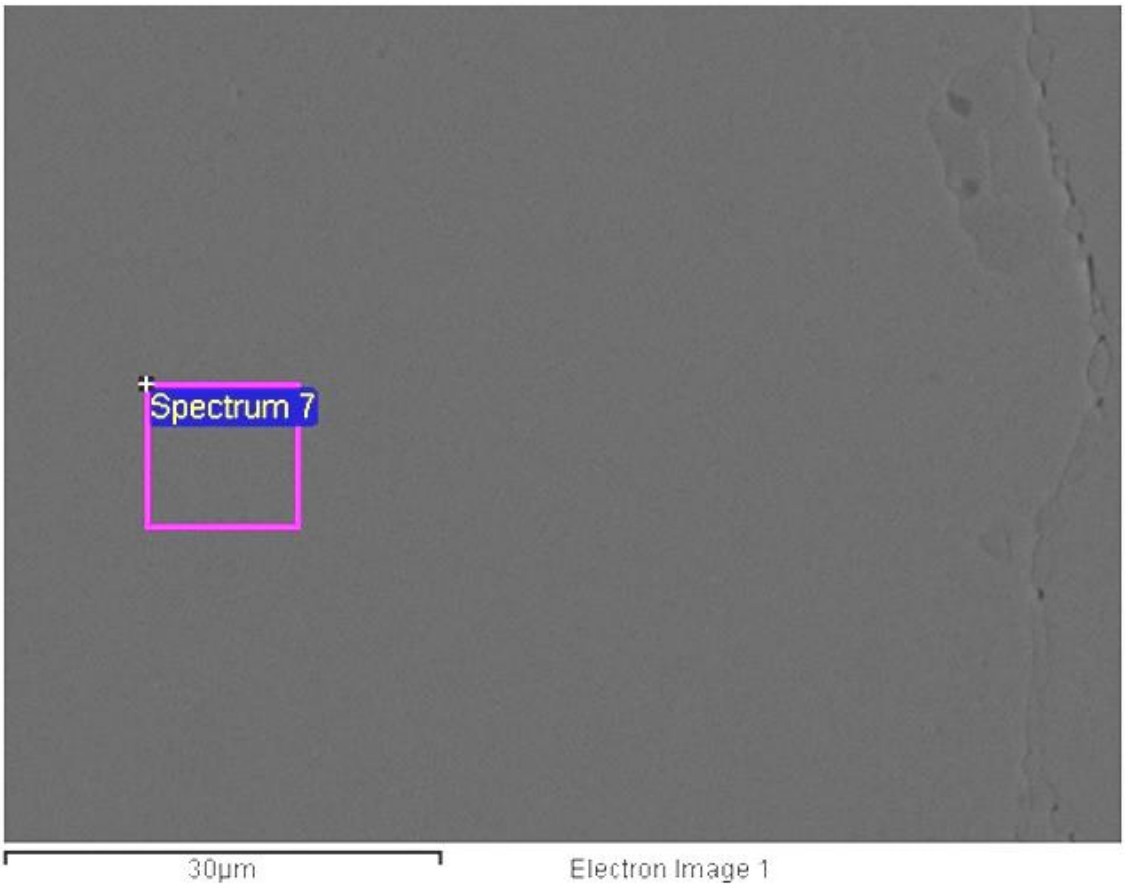

Element	Weight%	Atomic%
Si K	1.58	3.07
Cr K	24.52	25.70
Mn K	1.17	1.16
Fe K	53.63	52.34
Ni K	19.09	17.73
Totals	100.00	

APPENDIX L 3

X-ray microanalysis performed on the as-cast sample for middle surface

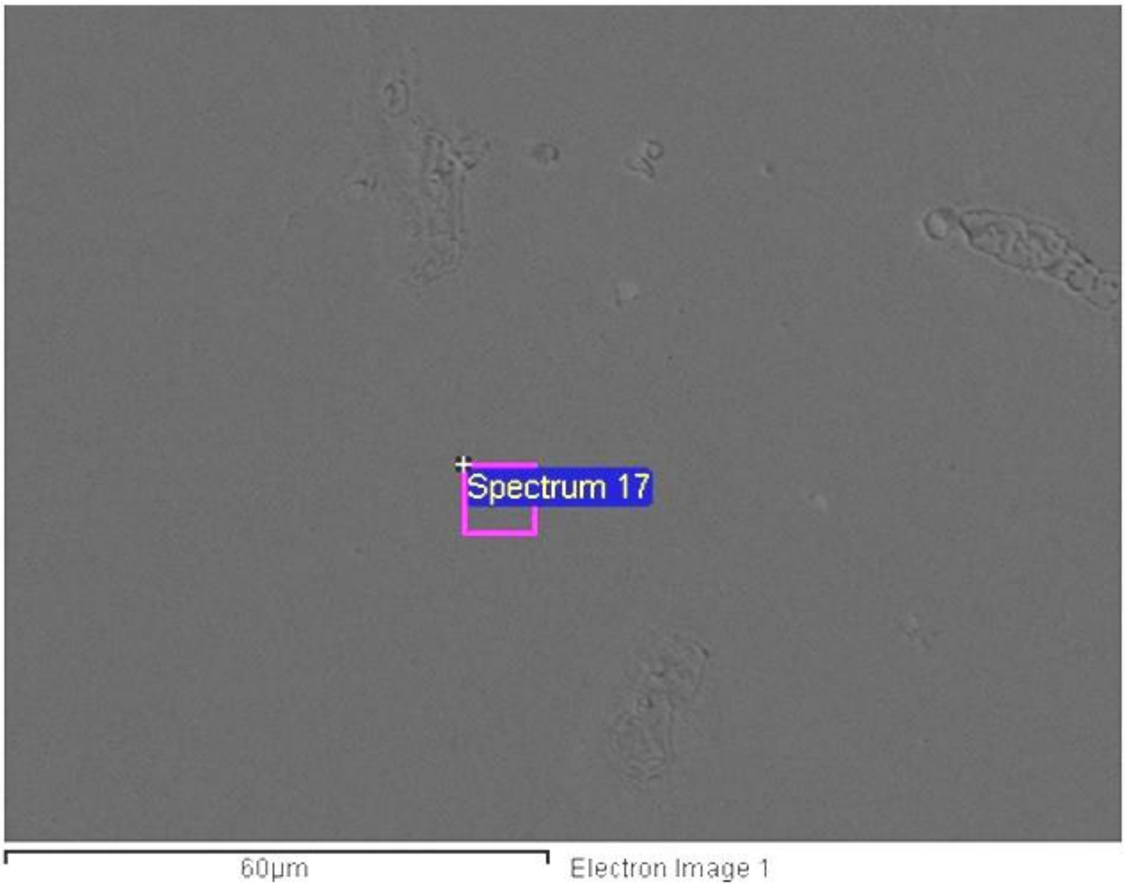

Element	Weight%	Atomic%
Si K	1.26	2.45
Cr K	23.06	24.27
Mn K	1.07	1.07
Fe K	55.88	54.76
Ni K	18.73	17.46
Totals	100.00	

APPENDIX L 4

X-ray microanalysis performed on the as-cast sample for outside surface

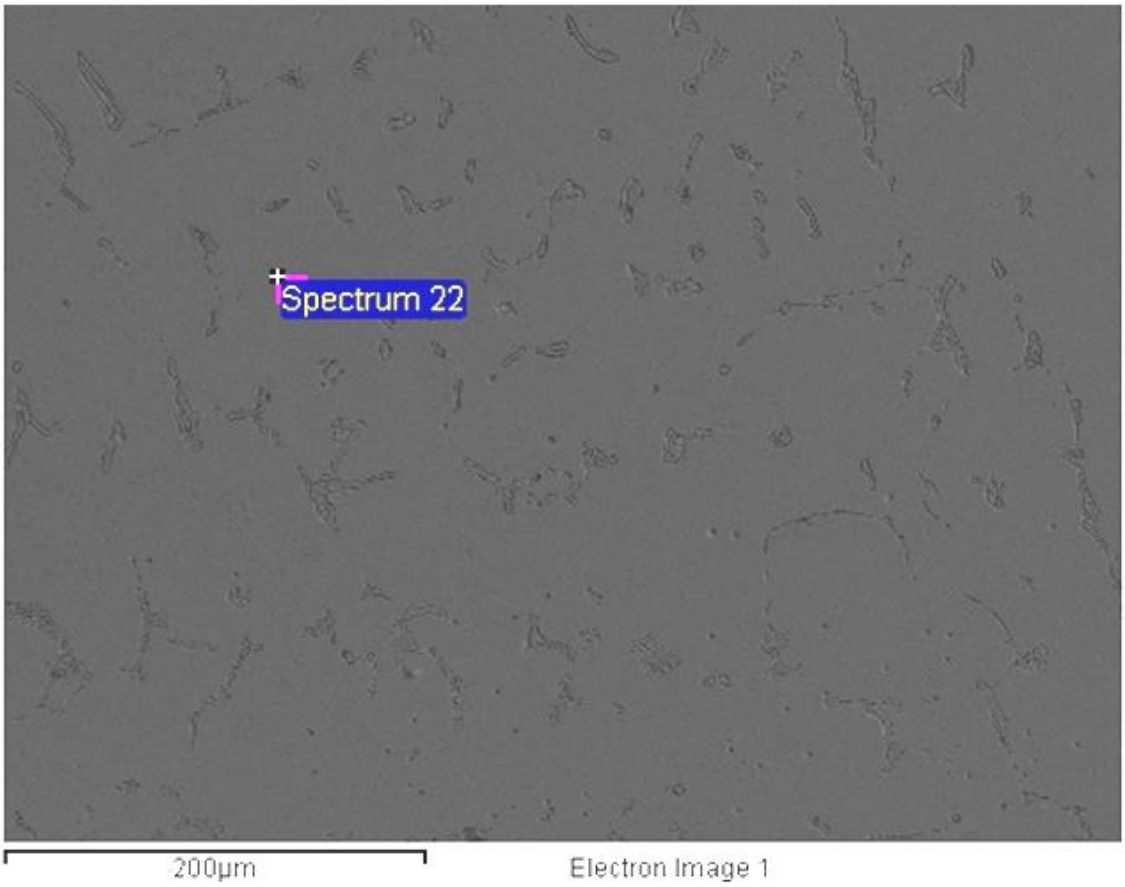

Element	Weight%	Atomic%
Si K	1.59	3.08
Cr K	24.05	25.22
Mn K	1.04	1.03
Fe K	53.92	52.64
Ni K	19.41	18.03
Totals	100.00	